buildings

MDPI

Review

Alkali-Activated Materials and CDW for the Development of Sustainable Building Materials: A Review with a Special Focus on Their Mechanical Properties

Luca Baldazzi, Andrea Saccani and Stefania Manzi *

Department of Civil, Chemical, Environmental and Materials Engineering, University of Bologna, Via Terracini 28, 40131 Bologna, Italy; luca.baldazzi4@unibo.it (L.B.); andrea.saccani@unibo.it (A.S.)
* Correspondence: stefania.manzi4@unibo.it

Abstract

Alkali-activated materials (AAMs) or geopolymers have been considered for many years as a sustainable substitution for the traditional ordinary Portland cement (OPC) binder. However, their production needs energy consumption and creates carbon emissions. Since construction and demolition waste (CDW) can become precursors for manufacturing alkali-activated materials, their use as substitutes for traditional AAM (such as metakaolin, blast furnace slag, and fly ash) can solve both the problem of their disposal and the problem of sustainability. Furthermore, CDW can also be used as aggregate replacement, avoiding the exploitation of natural river sand and gravel. A new circular economy could be created based on CDW recycling, creating a new eco-friendly building practice. Unfortunately, this process is quite difficult owing to several variables that should be taken into consideration, such as the possibility of separating and sorting the CDW, the great variability of CDW composition, the cost of the mechanical and thermal treatment, the different parameters that compose an alkali-activated mix-design, and public opinion still being skeptical about the use of recycled materials in the construction sector. This review tries to describe all these aspects, summarizing the results of the most interesting studies performed on this subject. Today, thanks to a comprehensive protocol, the use of building information modeling (BIM) software and machine learning models, a large-scale reuse of CDW in the building industry appears more feasible.

Keywords: alkali-activated materials; construction and demolition waste; geopolymers; mechanical properties; sustainable building materials

Academic Editor: Baofeng Pan

Received: 30 November 2025
Revised: 25 December 2025
Accepted: 1 January 2026
Published: 11 January 2026

1. Methodology of the Review

This review is focused on sustainable composite materials prepared with alkali-activated materials (AAMs) and construction and demolition waste (CDW). The aim is to define the parameters that most influence their mechanical properties and durability. To achieve this goal, a comprehensive literature search was conducted to identify peer-reviewed papers relevant to AAM-CDW composites using the Scopus database, covering publications from 2012 to 2025. The keywords selected were "alkali-activated materials", "geopolymers", "construction and demolition waste", "CDW", "mechanical properties", and "durability". The query was performed on the title, the abstract, and the keywords of the papers. The language selected was English, and the papers were limited to "Article", "Review", and "Conference Paper". For this review, a tailored procedure was developed

that shares some similarities with the PRISMA (Preferred Reporting Items for Systematic Reviews and Meta-Analysis) framework. Starting from the records retrieved by the Scopus database (274), a subset of papers was subsequently excluded for failing to meet the predefined inclusion criteria. The main criteria were the use of AAM as a precursor (not only ordinary Portland cement binder), the use of CDW without other additions (fibers, filler, biomass), and applications in building construction (no pollutants and heavy metals adsorbents, and no soil stabilization purpose). After applying the exclusion criteria, 199 articles were selected. Figure 1 provides a flow diagram of the methodology applied in this study.

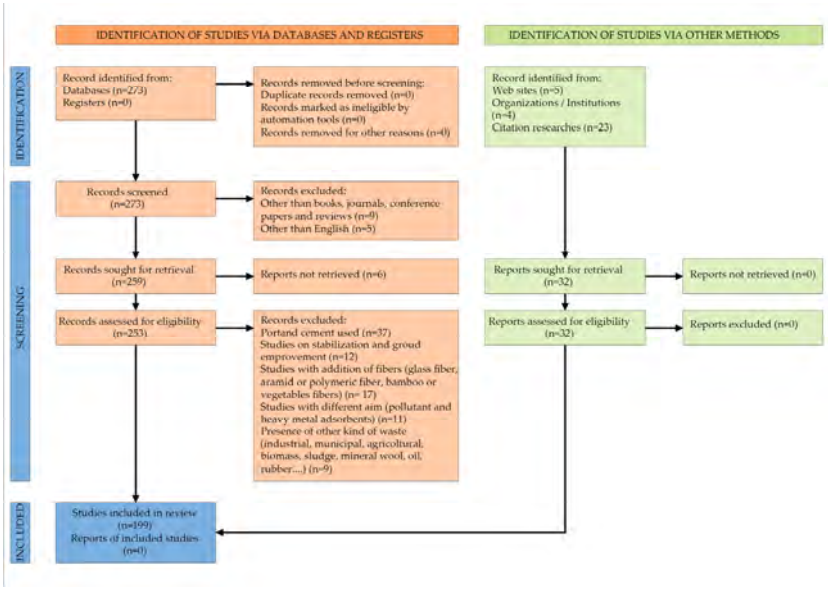

Figure 1. Flow diagram of the methodology applied in this study.

A bibliometric analysis was conducted using the VOSviewer 1.6.20 software to find the cluster of words most present in the literature. The network map obtained with a minimum of two occurrences per keyword is shown in Figure 2. Thirty-three keywords satisfied this criterion, and the analysis revealed that the main clusters were related to ingredients (geopolymer, construction and demolition waste, alkali-activated, bricks, concrete, and waste), mechanical properties (compressive strength), and durability. Among these, "CDW", "geopolymer", and "alkali-activated" were the most frequently occurring keywords.

These words reflect the production process of AAM with CDW, as summarized in Figure 3. Construction and demolition waste can be used both as a precursor and an aggregate. In Sections 3–5, the use of CDW as a precursor is described, analyzing the ingredients (Section 3), the mix-design (Section 4), and the properties of the composites (Section 5), respectively. The use of CDW as an aggregate for AAM is summarized in Sections 6 and 7. Durability properties are finally reported in Section 8. New explanatory tables, specifically designed for this review, summarize and compare the values of mechanical properties reported in the literature, organized by type of CDW and arranged chronologically from the earliest to the most recent studies. To enhance clarity, the table results are consistently color-coded according to the type of CDW used: concrete in green, brick in red, ceramic in pink, and a mix of CDW in yellow. Furthermore, all tables employ consistent abbreviations, symbols, and color codes, the meanings of which are summarized in Table 1.

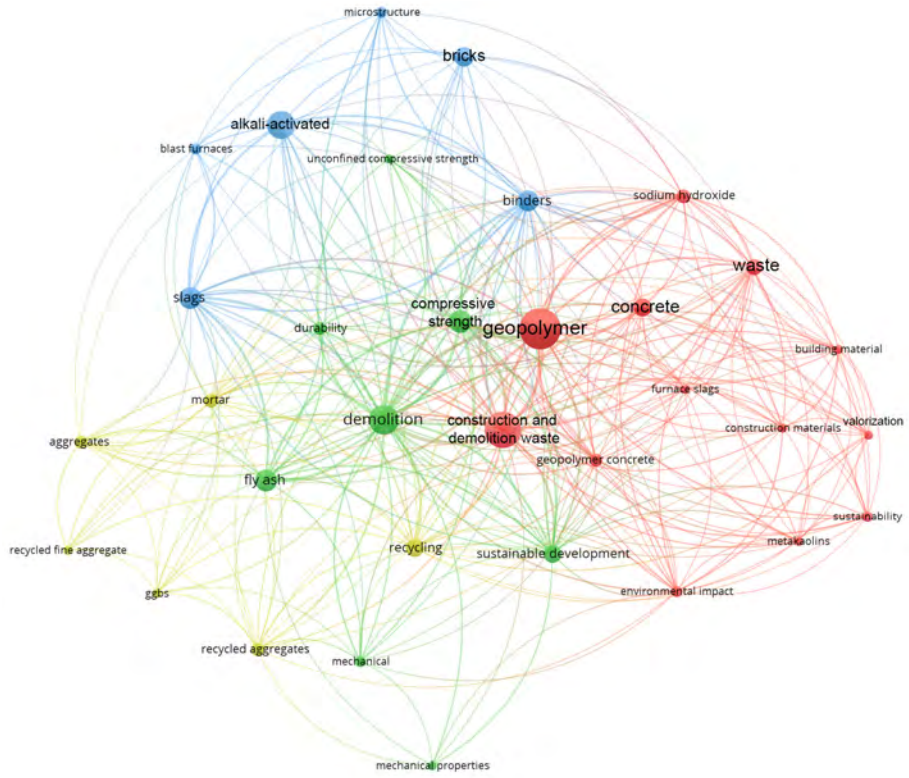

Figure 2. The overlay visualization for "Alkali-Activated Materials with Construction and Demolition Waste". The words "geopolymer", "alkali-activated" and "demolition" are associated with the red, blue and green clusters, respectively. Each line represents a connection between two words. The red cluster shows strong connections to the other ones through the terms "construction and demolition waste" and "compressive strength". The green cluster also includes many words related to the material properties, such as mechanical properties and sustainability.

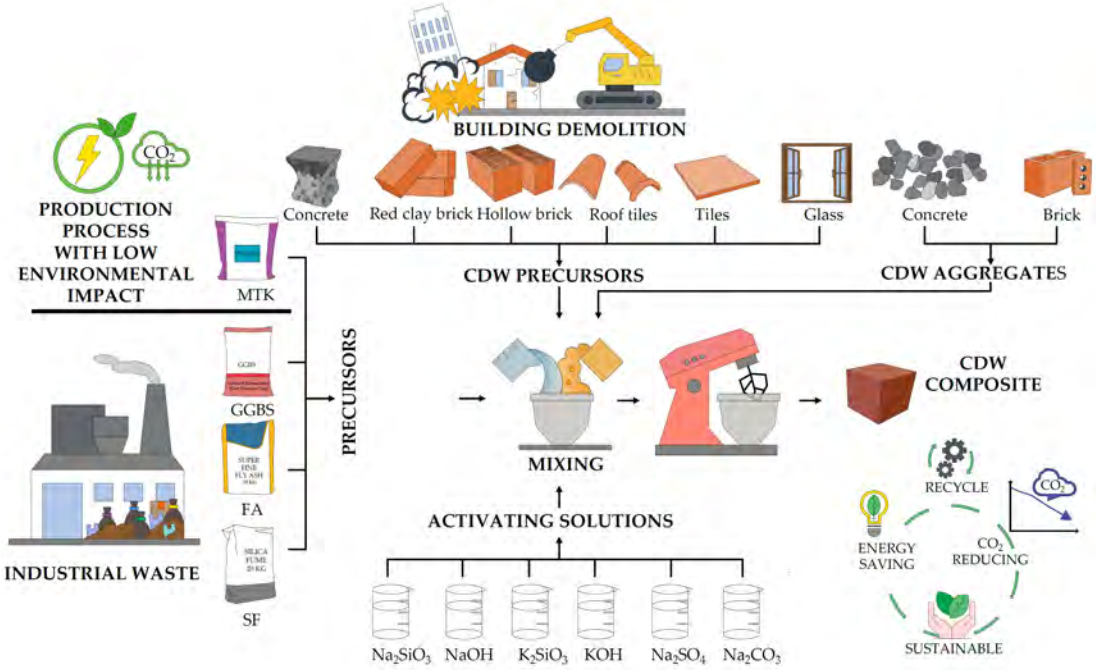

Figure 3. Preparation of alkali-activated composites with CDW.

Table 1. Legend for the abbreviations, symbols, and color codes used in all tables.

Group	Symbol	Meaning
Mixture	P	Paste
	M	Mortar
	C	Concrete
Precursor	OPC	Ordinary Portland cement
	MTK	Metakaolin
	FA	Fly ash
	GGBS	Ground granulated blast-furnace slag
	SF	Silica fume
	RM	Red mud
	GY	Gypsum
	✔	Used
Waste precursor/ Waste aggregate	Waste Prec.	Waste precursor
	Cw	Concrete waste
	Rcb	Red clay brick
	Hb	Hollow brick
	Rt	Roof tile
	Ti	Ceramic tile
	Gl	Glass waste
	Gp	Geopolymer waste
Waste treatment	Thermal	Thermal treatment for CDW
	Carbon.	Carbonation treatment of CDW
Percentage of waste	W%	Percentage of waste present
Aggregate type	Agg.	Aggregate type
	NS	Natural quartz sand
	RA	Recycled CDW aggregate
Aggregate size	Mix	Mix of various CDW aggregates
	FM	Fineness modulus
	NSP	Not specified
Curing temperature	T (°C)	Temperature of curing
Mix Design	Prec.	Precursor
	AS	Activating solution
	Mol.	Molarity
	L/B	Liquid-to-binder ratio
	Na_2O (%)	Percentage of Na_2O
	Agg.	Aggregate type
	B/A	Binder-to-aggregate ratio
Aggregate	Cw %	Percentage of concrete waste aggregate
	Rcb %	Percentage of red clay brick aggregate
	Ti %	Percentage of ceramic aggregate
	Mix %	Percentage of a mix of various CDW aggregates
	Gp %	Percentage of geopolymer concrete waste aggregate
	NS %	Percentage of natural sand

Table 1. *Cont.*

Group	Symbol	Meaning
Test performed	Flow	Flow table test—consistency
	σc—σf	Compressive and flexural strength test
	SEM-EDX	Scanning electron microscope energy dispersive X-ray spectroscopy
	XRD	X-ray diffraction
	FTIR	Fourier-transform infrared spectroscopy
	TGA	Thermogravimetry
	DSC	Differential scanning calorimetry
	DSC	Pe.Abs
	MIP	Mercury intrusion porosimetry
	BET	Brauner–Emmet–Teller instrument
	Dur.	Durability tests
	✓	Tests performed
Ticks	✓	Concrete waste
	✓	Brick waste
	✓	Ceramic waste
	✓	Ceramic waste
	✓	Geopolymer waste
	✓	Mix of various CDWs
Cell colors		Obtained with concrete CDW
		Obtained with brick CDW
		Obtained with tile CDW
		Obtained with a mix of CDW
		Obtained with geopolymer waste
		CDW analyzed separately

2. Environmental Impact of OPC and CDW

Ordinary Portland cement (OPC) is the most used binder to create concrete, thanks to its low cost and its easy funding of raw materials. In 2024, the global production of concrete was equal to 14 billion m^3, and an increase to 20 billion m^3 is expected for 2050 (corresponding to 4.4 Gt) [1,2]. The energy consumption of the cement industry is equal to 15% of the total industrial sector, and the thermal energy consumption is equal to 3.4 GJ/t of clinker produced [3]. In Table 2 [1,4–8] the values of CO_2 emission due to cement production are reported for different countries and different years. The cement industry represents 5–7% of the total anthropogenic CO_2 emissions [9–11]. OPC concrete also shows the problem of its disposal after demolition. Currently, its main uses are site elevation or foundation, downcycling for road pavements and subgrades, or as a cover layer for landfill, all of which are serious concerns for the environment. To reduce this impact, different manufacturing processes were introduced as the possibility of producing blended cement with natural pozzolans or recycling the waste cement kiln dust. According to Huntzinger [12], the substitution of pozzolans for clinker effectively reduces the environmental impact process by 21.6%. Instead, recycling waste cement kiln dust into the kiln process has no effect on the overall impact score. Only the manufacturing processes based on carbon sequestration in the waste cement kiln dust have a lower (but small) overall impact score than the traditional one (−5%) [12]. A CO_2 reduction near 0.35–0.77 tons for each ton produced could

be achieved by replacing OPC with recycled cement, and a reduction near 0.186 tons is expected by replacing OPC concrete with recycled concrete, reaching the impressive value of 1.4–3.08 Gt of CO_2 sequestrated each year.

Luo [13] studied a concrete cycle model in order to obtain new recycled cement, concrete, and aggregate: after the demolition of the old structure, the concrete is subjected to a carbonation treatment to obtain carbon sequestration, and the old cement paste is also thermally activated (near 650 °C) to become a precursor for the new recycled cement. The aggregates of the old structure can be reused as they are (direct replacement is possible only for 30%) or they can be treated (removal of the attached cement paste, carbon sequestration, or surface coating). In particular, the carbonation process increases the bond between aggregates and the matrix and increases the capacity to desorb moisture, improving concrete curing.

Table 2. Data on cement CO_2 emission.

Amount	Country	Year	Reference
0.54 t/t of cement	World	2015	IEA [4]
0.58 t/t of cement	World	2022	WEF [1]
0.58 t/t of cement	World	2022	IEA [4]
0.45 t/t of cement	World	2030	IEA [4]
0.72 billion t (Gt)	World	2000	Tiseo [5]
1.50 billion t (Gt)	World	2018	Andrew [6]
2.50 billion t (Gt)	World	2020	Marmier [7]
1.56 billion t (Gt)	World	2023	Tiseo [5]
39.71 million tons (Mt)	USA	2023	OurWorld [8]
110 million tons (Mt)	EU (27)	2022	Marmier [7]
10.60 million tons (Mt)	Germany	2023	OurWorld [8]
38.27 million tons (Mt)	Turkey	2023	OurWorld [8]
800 million tons (Mt)	China	2014	Andrew [6]
718.02 million tons (Mt)	China	2023	OurWorld [8]
177.23 million tons (Mt)	India	2023	OurWorld [8]
0.42 t/t of cement	World	2050	WEF [1]

The construction sector depletes more raw materials than any other industrial sector. Construction and demolition waste (CDW) mainly consists of different materials, such as concrete, bricks, tiles, plaster, wood, glass, steel, copper, and plastic. In 2022, the total waste generated by the construction sector in the EU amounted to 848 million tons [14]. To produce concrete, each year, 32–50 million tons of natural sand and gravel are extracted [15]. Furthermore, it must be considered that in the near future, there will be a lack of virgin/natural aggregates and that in the longer term, cement use in Europe could be uncertain. The increase in concrete production of the last decades is also connected to the global growth of the population, in particular in the new megalopolis of China (e.g., urbanization here is expected to pass from 59% in 2010–2018 to 70% in 2050 [16]), India, and South Africa. With urbanization, the composition of CDW changes. For example, in 2020, China produced CDW mainly from rural buildings made with wood and bricks. Brick and concrete structures formed 49% of the total CDW production. Instead, with urbanization, buildings with steel and concrete are expected to become the main contributors (for 2100, it is expected a 67% of CDW) [17]. Zhang [16] studied the correlation between urbanization and the production of CDW (in particular in China), proposing new policies to sustain urban and economic environments. For these reasons, every year, 30 billion tons of concrete are produced [18], and an increase in cement production of nearly 50% is expected for 2050 [19]. Some values related to concrete production are summarized in Table 3 [13,14,16,20–27]. As can be observed, China is currently the largest producer of concrete waste, followed by Europe and the USA on equal terms.

Table 3. Production of concrete waste.

Country	Amount (Mt)	Year	Reference
Europe	857	2010	Luo [13]
Europe	830	2012	Khan [20]
Europe	800	2018	Wang [21]
Europe	834	2018	Moschen-Schimek [22]
Europe	857 *	2022	Eurostat [14]
France	247	2012	Eurostat [23]
Italy	39	2012	Eurostat [23]
Germany	201	2012	Eurostat [23]
UK	77	2010	Luo [13]
USA	569	2017	Ilcan [24]
USA	600	2018	Luo [13]
USA	700	2018	Wang [21]
Colombia	22	2020	Villaquirán-Caicedo [25]
China	1800	2017	Xiao [26]
East China	1327	2018	Zhang [16]
China	3210	2021	Luo [13]
China	2600	2022	Ma [27]
China	2300	2022	Wang [21]
South Korea	24	2021	Luo [13]
Australia	5.6	2009	Luo [13]

* = value calculated as the product of the total amount of waste produced multiplied by the percentage of CDW.

The production of OPC concrete creates problems not only connected to the emission of CO_2, NO_x and SO_2 in atmosphere (5–8% impact for the greenhouse effect [20,28]) but also to the consumption of natural stones from rivers and mines (1.5 tons of raw rocks for each ton of OPC [18]) and to the consumption of large amounts of energy to heat the raw rocks at high temperatures (near to 1400 °C). This amount is considered equal to 40% of the total amount of energy consumed during the manufacturing process [20]. Considering the end of the service life of concrete, it can be used in different ways, as recycled aggregate for subgrade cushion, cement stabilized crushed stone, filler wall [13], or road base pavement layer (see Jimenéz [29] for applications in Spain, or Otasowie for reuse in South Africa [30]), or it is disposed of in landfills.

The presence of hazardous materials such as asbestos (normally present as roof tiles in the constructions built during the 1960s and 1980s) makes their reuse very difficult owing to the prohibitive costs of decontamination. For these cases, incineration and landfilling are still adopted [21]. CDW can release also other harmful substances that can affect the environment during their management (handling, incineration, leakage, and crashing), as dust containing carcinogenic species produced during crushing, PM10 during dismantling or sorting, fine particles (Ba, Ca, Cr, and metals) leached in the landfill, gypsum released in the ground that can change the pH of soils, and water pollutants caused by CDW disposal that can contaminate not only rivers and ponds but also the soils, the aquatic life and the animals that drink the water [31].

The demand for green building materials is quickly increasing [32]. The first association to deal with CDW was the Federal Quality Association for Recycled Building Materials, established in Berlin in 1984. Nowadays, it has become the headquarters European Quality Association for Recycling (the main EU organization of quality association) [33]. The EU Commission Communication of 21 December 2005 about "Thematic Strategy on the prevention and recycling of waste" [34] can be considered as the beginning to improve the management of wastes and energy resources, as the EU directive 2008/98 "Waste Framework Directive" [35] specifies more goals for reuse, recycling, and recovery of wastes [32]. For example, it imposed the goal to increase the recovery rate of CDW to 70% in terms of weight by 2020. Moschen-Schimek [22] studied whether this goal was achieved in different

countries, finding that many problems still exist, such as non-unified methods of data collection, different waste coding systems, non-homogeneous meaning for "backfilling", and completeness of collected data.

To achieve the goal of 100% reduction in carbon emissions by 2050, it is necessary to develop strategies for the reduction in greenhouse gases even in the construction sector. For this reason, Directive 2018/851/EU establishes that CDW must be properly separated and treated to remove hazardous substances and recycle them. In this way, CDW becomes a resource that can be a part of a circular economy model [36].

Yi [37], comparing different approaches to the process of waste management, found that the establishment of a carbon tax and economic incentives are effective measures to reduce carbon emissions, as happened in European countries such as Sweden, Germany, Britain, France, and Eastern countries such as Japan and Australia. Also, Cudecka-Purina [38] agrees that a comprehensive policy framework where CDW sorting and recycling are mandatory with financial incentives as support for the industry is always more and more important. Ma [27] analyzed the importance of creating a circular economy model with CDW and the role of different private (customers, designers, contractors) and public (government) stakeholders. For instance, China introduced CDW in the "14th Five-Year Plan on the development of circular economy". According to Wang [21], this circular economy model should be broadly applicable and widely recognized with a universally applicable evaluation model. Saad [39] tested the importance of a circular economy in Canada, finding that the reclamation of building materials decreases transportation and disposal costs, and increases the creation of new businesses and job opportunities in the local economy. Some strategies must be carried out: improving secondary material quality, giving incentives for their use and for waste recovery, creating standards for secondary materials, and the use of advanced technologies for sorting and recycling [27,39]. Similar conclusions are achieved by Martin [40], who studied the UK context. In the UK, the main problems in the implementation of the CDW circular economy are: inadequate policies, bureaucratic delays, and higher costs. In particular, Saad [39] has developed a framework composed of four parts to evaluate the possibility of deconstructing a building and to reuse its materials or components; these stages are technical feasibility assessment, budget and timeframe consideration, heritage value consideration, and final decision.

Table 4 [13,23,27,37,40,41] reports the percentage of CDW recycling for different countries around the world. Lins [42] created a framework based on building information modeling (BIM) software and simulation tools to manage the entire building life from the design to the final deconstruction and reuse of materials. This approach is based on the 3Rs (reduction, reuse, and recycling). New technologies, such as artificial intelligence software and blockchain systems, can increase the reuse of CDW thanks to the possibility of tracking the material flow [38]. Currently, there are already studies on how to calculate the quantity of CDW produced thanks to artificial intelligence modeling techniques [43]. In this way, it is possible to optimize resource allocation and minimize waste generation. Reduction is the most effective method to reduce the production of CDW. It consists of a proper design of the building at a very early stage of the project, avoiding unexpected changes in the building design and improper procurement and handling of materials. Reuse is the possibility to give a second life to the materials without changing their function or structure; it takes no additional time or energy consumption, but it is necessary to perform good sorting during selective demolition (deconstruction). Recycling involves four additional phases (separation, collection, processing, and marketing), and the products obtained depend on the quality and nature of the original material, e.g., concrete can be crushed and recycled as aggregate for new concrete [31]. In Figure 4, a sustainable cycle for CDW is proposed.

Table 4. Percentage of recycling of construction and demolition waste.

Country	CDW Recycling (%)	Year	Reference
Europe	89	2020	Caro [41]
Europe	90	2022	Ma [27]
Europe	89	2024	Caro [41]
Germany	68	2012	Eurostat [23]
Germany	90	2020	Luo [13]
Italy	76	2012	Eurostat [23]
UK	38	2018	Martin [40]
UK	80	2020	Luo [13]
USA	70	2020	Luo [13]
USA	76	2022	Ma [27]
China	13	2020	Luo [13]
China	10	2022	Ma [27]
China	40	2022	Yi [37]
Japan and South Korea	95	2024	Yi [37]

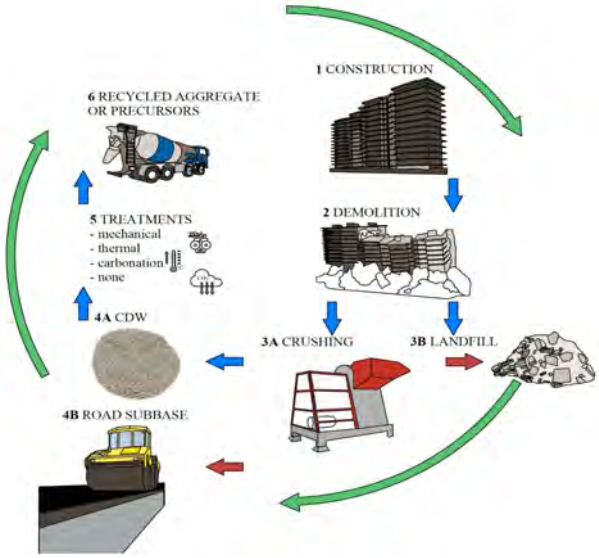

Figure 4. Construction and demolition waste cycle in the building industry. The green arrows represent the recycling process, the blue arrow represents an individual process phase, whereas the red arrow indicates a stage at which CDW exits the recycling process described in this review.

For all these reasons, in recent years, more and more research has focused on the development of new recipes based on alkali-activated materials (replacing OPC) and CDW (replacing natural aggregate or as precursors of the alkali-activated materials). Another possibility to recycle CDW is the development of new lightweight aggregates [44]. Starting from ground CDW (<100 μm), fly ash (FA) and ground granulated blast furnace slag (GGBS), it is possible to add SiC (an expansive agent to create the porous structure) to obtain after palletization in a tilting disk and a heating process (110 °C for 24 h in oven followed by a sintering program in muffle) new recycled aggregate.

Unfortunately, CDW has a great heterogeneity that causes a remarkable variability in the physical and mechanical properties of the pastes and mortars produced with it. Nowadays, this aspect is the most challenging aspect of the recycling of CDW [15]. This problem of heterogeneity was considered even by the Italian Standard that gives the possibility to create new structural concrete with recycled aggregates (up to 30%) only if these ones are almost completely made with old concrete (90%) [15].

Tam [33] found that there are some barriers to the use of recycled aggregate as recycled products are still regarded as suspicious, the price should be lower than the natural

aggregate, the quality of the recycled aggregate should be improved with better selection and sorting, the lower quality concrete should be used as road base aggregate, the concrete factory and the recycled concrete factory should be close to each other to reduce the cost of transportation.

3. Alkali-Activated Materials with CDW as Precursor and Mechanical Properties

3.1. Characteristics of Alkali-Activated Binders

Since the European Green Deal [45], and the construction sector was selected as determining for the transition to a sustainable economy [22], researchers are increasingly testing new eco-friendly binders as partial or complete replacement for OPC, such as fly ash, ground granulated blast furnace slag, and metakaolin (MTK). Alkali-activated materials are now widely used thanks to their good performances in terms of durability and mechanical properties, e.g., the pavement construction of Brisbane West Wellcamp Airport is one of the greatest applications of these materials in industrial-scale applications (>40,000 m^3) [26]. Alkali-activated materials (discovered by Davidovits in 1978) are similar to zeolites but with an amorphous structure. They are created by the co-polymerization of alumino-silicate species originating from the dissolution of Si and Al in the source material at high pH value and in the presence of soluble alkali silicate [46]. In particular, alkali-activated materials have a higher amount of CaO (0–30%) and a lower amount of Na_2O and K_2O (4–10%) compared to geopolymers (respectively, 0–5% CaO and 10–20% Na_2O and K_2O) [47]. For this reason, alkali-activated materials create more C-S-H when activated than geopolymer (which gives more N-A-S-H as a hydration product). Any materials with Si-Al can become an alkali-activated material, including CDW. In particular, in the papers present in the literature, CDW are associated mainly with other precursors as blast furnace slag (high calcium content), or fly ash and metakaolin (low calcium content). The main hydration product of an alkali-activated binder is C-S-H gel (for high-calcium raw materials as slags) or N-A-S-H gel (for low-calcium raw materials). In the process of geopolymerization, the SiO_2/Al_2O_3 ratio and Na_2O/SiO_2 ratio can be used to modulate the composition of the materials. In general, a higher amount of Si gives more C-A-S-H gel, whereas Al rules the network formation of the matrix [18].

To create geopolymeric mortars and concrete, the precursors (100% CDW or a mix among CDW, metakaolin, fly ash, or GGBS) must be activated using a solution (generally composed of NaOH or KOH) and silicates. The molarity of the solution can vary between 6M and 10M. In general, a higher molarity results in higher compressive strength. The curing temperature can vary, and for higher temperatures, the time of curing is lower. The increase in temperature, creating a denser matrix, gives higher strength values. The single parameters will be specifically analyzed in Section 4.6.

3.2. Chemical and Mineralogical Characterization of CDW

CDW is generally collected from the landfill or directly from the demolition site. Later the CDW is cleaned, dried, and ground to obtain a very fine powder. In several studies, CDW was used as an alkali-activated precursor without previously selecting the demolition material. The quality of CDW can thus be very variable, and it depends on various factors, such as the concrete age, the impurities present, the recycling method, and the apparatus used to sort and grind the waste [48]. Construction and demolition waste can be initially sorted according to the different kinds of materials present (concrete, bricks, tiles, glass, ceramic) or used unsorted, but in this case, it is not possible to create a specific mix-design since the percentage of the single waste is unknown. Since the composition of CDW is very important for the characteristics of the final product, CDW must be studied by performing chemical composition test and X-ray diffraction analysis to find

the mineralogical composition. Table S1 [24,25,49–94] and Figure 5A,B [24,25,50–55,57–79,84–94] summarize the chemical composition of CDW present in the literature according to the type of waste present: concrete waste in the first part of Table S1 [24,49–67], bricks and ceramics in the second part [24,49,51,52,54,57,60,64–66,68–86], glass waste, and mixes of various waste in the last part of Table S1 [24,25,52,54,60,73,76,77,80,87–94], respectively. Figure 5B summarizes the area in the ternary diagram where CDWs are present according to their main material. Concrete CDW (green symbols in Figure 5A) and mixes of various CDWs (yellow symbols in Figure 5A) have the greatest variability; instead, waste glass powders are very homogeneous (70% of SiO_2 and 13% of Na_2O, 10% CaO [24,51,53,59,72,75,76,79]). Bricks and ceramics (respectively, red and pink symbols in Figure 5A) are almost superimposable (70% of SiO_2 and 20% of Al_2O_3, 10%CaO). Concrete and mix CDW have a lower amount of Al_2O_3 (left side of the ternary diagram in Figure 5B) than brick and ceramic CDW (right side of the ternary diagram). Concrete powders also have more SiO_2 and CaO. The molar ratios of oxides (SiO_2, CaO, and Al_2O_3) are also generally used to study the composition of the precursor. SiO_2 is the main source of reactive oxide. According to Vasquez [50], the optimum Si/Al ratio for alkali-activated materials should be close to 10.

Table 5 [23–51,55,57,59–61,63,64,66–72,76–79,82–84,87–91,94–96] summarizes the minerals detected in CDW with the X-ray diffraction technique present in the literature. Concrete waste is mainly composed of quartz, C-S-H gel, un-hydrated calcium silicate, and feldspar coming from the aggregate as albite and microcline. It is possible to detect minerals as some alumino-silicate (muscovite and anorthite), unreacted cement powder (alite and belite), products of sulfate attack (gypsum and ettringite) [97]. Geopolymeric products with CDW powders can have different characteristics according to the type of powder (recycled OPC paste, mortar, or concrete). The first one has more C-S-H gel, which benefits the microstructure, calcium hydroxide, and some unreacted cement calcium silicate, which refines the pore size and enhances the microstructure of the final product. The second one has a small amount of hydration products and a high amount of quartz coming from natural sand. Finally, the third one has the highest content of quartz and calcium carbonate (being almost inert, they affect the microstructure) coming from old concrete sand and gravel, so the final geopolymer will have less amount of C-(N)-A-S-H [98,99]. Comparing the mechanical properties of alkali-activated mortars with 100% paste, mortar or concrete waste as precursor it is possible to observe that for replacement of GGBS inferior to 50% there is no great difference among the three different types of waste but for a 100% substitution the best performance is achieved using cement paste as precursor (+182% compared to mortar waste and + 213% compared to concrete waste) [95]. The replacement of FA with paste powders increases the mechanical strength after 28 days (+26%). On the contrary, the use of mortar or concrete powder decreases the strength (−44% and −52%, respectively) [98]. The addition of both mortar and concrete powder increases the average pore diameter, and some distinctive cracks can be observed in the final product. In particular, the beneficial effect of using cement paste powder as a precursor can be explained by the presence of unreacted calcium silicate, C-S-H gels, and calcium hydroxide that can be easily re-polymerized under alkali-activation conditions in new C-(N)-A-S-H gels. Instead, the presence of inert quartz and calcite in the mortar and in the concrete waste decreases the compressive strength to −52% for 100% replacement of concrete powder since these fractions do not participate in the alkali-activated reaction. Furthermore, the high calcium present in concrete powder acts as an inactive filler and slows down the dissolution process because the precursor particles become covered by Ca-rich products, resulting in a general decrease in the strength development [98].

Table 5. Minerals detected in CDW precursor using XRD.

Author	Year	CDW	Minerals Detected with XRD																										
			Q	C	D	Po	Al	Mc	Ms	An	Hm	Pr	I	Mu	Lz	Sa	Cl	W	Or	T	Cr	Di	Ph	Pl	E	A	B	F	Sp	Am
Zaharaki [51]	2016	concrete	•	•			•					•																		
Robayo-Salazar [52]	2017	concrete	•			•	•			•																				
Ren [53]	2020	concrete	•	•																						•	•			
Huo [55]	2021	concrete	•	•					•																					
Ilcan [24]	2022	concrete	•	•					•													•						•		
Liu [95]	2022	concrete	•	•	•	•																				•	•			•
Mahmoodi [57]	2022	concrete	•	•			•		•	•		•		•																
Boros [59]	2023	concrete	•	•		•				•																•				
Cardoza [96]	2023	concrete	•	•			•																		•					
Ozcelikci [60]	2023	concrete	•	•																										
Sasui [61]	2023	concrete	•	•		•				•															•	•				•
Zhang [63]	2023	concrete	•	•																										•
Cantero [64]	2024	concrete	•	•					•															•		•	•			
Kul [66]	2024	concrete	•	•																										
Sasui [67]	2024	concrete	•	•		•			•	•															•					•
Reig [68]	2013	brick	•	•			•			•						•														
Robayo-Salazar [69]	2016	brick	•						•		•													•						
Zaharaki [51]	2016	brick	•	•								•																		
Robayo-Salazar [52]	2017	brick	•				•			•	•																			
Fort [70]	2018	brick	•				•	•			•		•	•								•								
Tuyan [71]	2018	brick	•						•																					
Hwang [72]	2019	brick	•				•			•	•																			
Ulugöl [76]	2021	brick	•				•							•																•
Ilcan [24]	2022	brick	•											•							•	•								
Liang [78]	2022	brick	•					•					•																		
Mahmoodi [57]	2022	brick	•				•		•			•		•																
Cardoza [96]	2023	brick	•	•			•		•		•										•									
Giannopoulou [79]	2023	brick	•				•				•			•								•								•
Ozcelikci [60]	2023	brick	•																		•	•								
Cantero [64]	2024	brick	•	•									•																	
de Castro Carvalho [82]	2024	brick	•							•	•																			
Kul [66]	2024	brick	•											•								•								
Maaze [83]	2024	brick	•				•			•									•											
Rakhimova [84]	2015	ceramic	•				•				•										•									•
Hwang [72]	2019	ceramic	•				•			•																				
Ilcan [24]	2022	ceramic	•											•								•								
Mahmoodi [57]	2022	ceramic	•				•		•			•		•																
Giannopoulou [79]	2023	ceramic	•				•				•			•															•	
Ozcelikci [60]	2023	ceramic	•												•						•	•								
Cantero [64]	2024	ceramic	•																					•						
Robayo-Salazaar [52]	2017	glass																												•
Ulugöl [76]	2021	glass																												•
Ilcan [24]	2022	glass																												•
Ozcelikci [60]	2023	glass																												•
Bassani [87]	2019	mix	•	•	•		•		•		•				•		•	•		•										
Robayo-Salazar [88]	2020	mix	•	•																				•						
Villaquirán [25]	2021	mix	•	•			•																•							
Moreno-Maroto [89]	2022	mix	•	•	•																			•						
Tan [90]	2022	mix	•	•			•																							•
Tan [91]	2022	mix	•	•													•	•		•										•
Tefa [94]	2025	mix	•				•		•								•			•										

mix = mix of various CDWs; Q = quartz; C = calcite; D = dolomite; Po = portlandite; Al = albite; Mc = microcline; Ms = muscovite; An = anorthite; Hm = hematite; Pr = pirssonite; I = illite; Mu = mullite; Lz = lizardite; Sa = sanidine; Cl = clinochlore; W = wavellite; Or = orthoclase; T = thaumasite; Cr = crisobalite; Di = diopside; Ph = phillipsite; Pl = plagioclase; E = ettringite; A = alite; B = belite; F = foshagite; Sp = spinel; Am = amorphous phase; • = present.

For brick waste, mullite, muscovite, and albite are minerals usually present (Table 5). The presence of mullite depends on the type of clay used and the fire temperature. Bricks also have Fe_2O_3 coming from hematite created during the sintering process of bricks. Waste from ceramic materials acts as a source of aluminosilicates, while waste from concrete gives silica and calcium. An increase in the latter allows for obtaining products with greater compressive strength, which can be estimated in advance with a formula based on the Si/Al and Ca/Si ratios [100]. Komnitsas [49] tested both ceramic and concrete waste as precursors, finding that tiles and bricks are generally better geopolymerized than concrete (13 MPa), achieving compressive strength values of 49.5 MPa (tiles) and 57.8 MPa (bricks). The good performance of brick is due to the high level of SiO_2 and Al_2O_3, and a smaller grain size distribution. Cardoza [96] tested a binder made from concrete and brick waste coming from a landfill in Medellin (Colombia). The results show better performance for the brick-based binder (33.1 MPa versus 19.6 MPa for the concrete-based binder, both cured at room temperature) owing to its greater pozzolanic reactivity. Quartz and amorphous-vitreous phases in the brick powder promote a pozzolanic effect; instead, the aluminum oxide helps the formation of ettringite, improving the early mechanical properties of the product with brick waste [97]. Geopolymers obtained from brick achieve low values of strength at the early stage but high values later; on the contrary, geopolymers obtained from concrete have high values at the beginning, but they increase the strength slowly later on [101]. Ulugöl [76] tested pastes made by only one kind of CDW (red clay bricks, roof tile, hollow brick, and glass), activated with different NaOH concentrations (10–12–15%) and cured at different temperatures (from 50 °C to 125 °C). Comparing his results, the best precursor among the ones tested was hollow brick as opposed to glass waste, which resulted in the worst one. Hollow brick had the best performance, even if it was the coarsest precursor, and it showed distinctive crystalline peaks under X-rays, demonstrating that the chemical composition of the precursor is more important than the physical properties to achieve high values of strength [76]. Comparing geopolymers mortars with CDW coming from wastes of roof tile, hollow brick and red clay brick used as precursors, the best results of compressive strength (>60 MPa) are achieved with roof tile waste and fine concrete recycled aggregate (0.85–0.10 mm) with an aggregate to binder ratio of 0.45, a 15 M solution of NaOH and a curing temperature of 105–115 °C [81].

Glass wastes are composed solely of amorphous phases (Table 5). In contrast, the mix of CDW is composed of minerals derived from concrete waste (quartz, calcite, dolomite, albite) with plagioclase, phillipsite, thaumasite, wavellite, clinochlore, and muscovite. The use of sorted, separated CDW gives the possibility to select a correct mix-design, changing the amount of concrete, bricks, and glass. Instead, using an unsorted CDW, this possibility is precluded. The heterogeneity of CDW appeared to be a challenging problem, as the mechanical strengths obtained were very different. Kul obtained values of compressive strength in the range 34.7–68.0 MPa, but thanks to a process of optimization, this range was reduced to 54.5–68.0 MPa. The main factors affecting the results were the Si/Al ratio and the fineness. Increasing the fineness, higher values of strength are expected, but only with a balanced Si/Al ratio, a substantial improvement can be achieved [66].

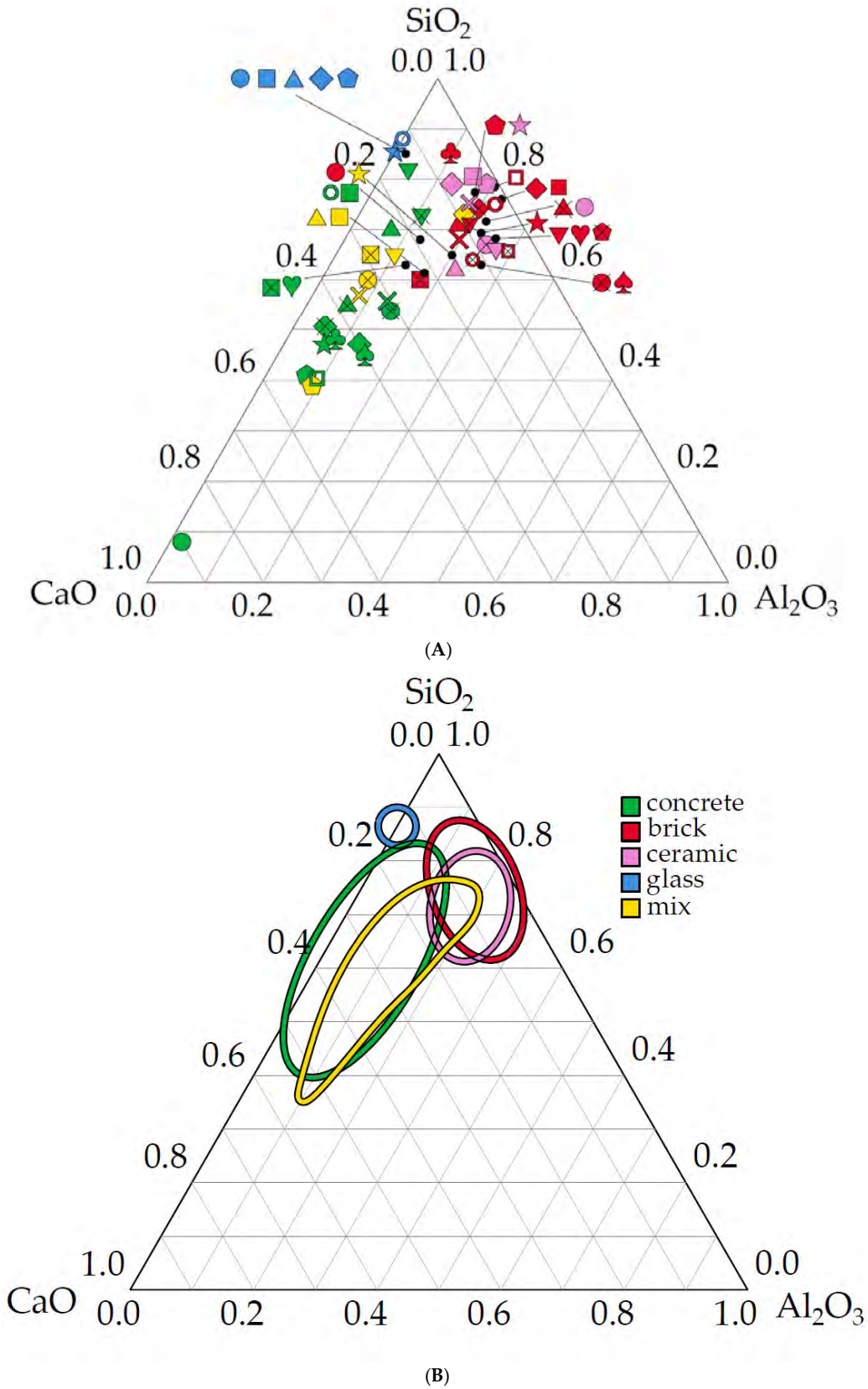

Figure 5. (**A**) Ternary diagram of some CDW precursors in the literature; (**B**) summary of the CDWs considered according to their material.

Legend of Figure 5A

CDW Type	Symbol	Author	Year	CDW Type	Symbol	Author	Year
concrete		Vásquez [50]	2016	brick		Reig [68]	2013
concrete		Zaharaki [51]	2016	brick		Robayo-Salazar [69]	2016
concrete		Robayo-Salazar [52]	2017	brick		Zaharaki [51]	2016
concrete		Ren [53]	2020	brick		Robayo-Salazar [52]	2017
concrete		Akduman [54]	2021	brick		Fort [70]	2018
concrete		Huo [55]	2021	brick		Tuyan [71]	2018
concrete		Ilcan [24]	2022	brick		Hwang [72]	2019
concrete		Mahmoodi [57]	2022	brick		Kioupis [73]	2020
concrete		Wang [58]	2022	brick		Wong [74]	2020
concrete		Boros [59]	2023	brick		Akduman [54]	2021
concrete		Ozcelikci [60]	2023	brick		Migunthanna [75]	2021
concrete		Sasui [61]	2023	brick		Ulugöl [76]	2021
concrete		Wan [62]	2023	brick		Aldemir [77]	2022
concrete		Zhang [63]	2023	brick		Ilcan [24]	2022
concrete		Cantero [64]	2024	brick		Liang [78]	2022
concrete		Ilcan [65]	2024	brick		Mahmoodi [57]	2022
concrete		Kul [66]	2024	brick		Giannopoulou [79]	2023
concrete		Sasui [67]	2024	brick		Kul [81]	2023
ceramic		Rakhimova [84]	2015	brick		Cantero [64]	2024
ceramic		Hwang [72]	2019	brick		de Castro Carvalho [82]	2024
ceramic		Samadi [85]	2020	brick		Ilcan [65]	2024
ceramic		Mahmoodi [57]	2022	mix		Bassani [87]	2019
ceramic		Erol [86]	2023	mix		Robayo-Salazar [88]	2020
ceramic		Giannopoulou [79]	2023	mix		Villaquirán [25]	2021
ceramic		Ozcelikci [60]	2023	mix		Moreno-Maroto [89]	2022
ceramic		Cantero [64]	2024	mix		Tan [90]	2022
glass		Robayo-Salazar [69]	2016	mix		Tan [91]	2022
glass		Kioupis [73]	2020	mix		Valencia-Saavedra [92]	2023
glass		Akduman [54]	2021	mix		Roy [93]	2024
glass		Ulugöl [76]	2021	mix		Tefa [94]	2025
glass		Aldemir [77]	2022				
glass		Ilcan [24]	2022				
glass		Ozcelikci [60]	2023				

3.3. Grinding Process and Particle Size Determination

The debris (composed of bricks, roof and floor tiles, glass, and concrete) is generally ground in a jaw crusher to a size of 2–4.75 mm and then further pulverized using a ball mill. The particle size of the precursor after the milling process is very important since it can affect the final values of strength [21,102,103]. Table 6 [24,49–57,60,61,64–66,68,69,72,73,75–79,81–83,96,104] summarizes the characteristics of the grinding process and the final particle size of CDW present in the literature. Almost all the studies performed used a two-step process composed of a first part where a coarse CDW is produced using a jaw crusher or a hammer mill, and a second step with ball milling to obtain powders less than 170 μm. Even the grinding time is an important factor (grinding time column in Table 6) that must be considered. The grinding time can vary from 40 min [68], 1 h [24,54,55,60,66,76,77] to 2 h [64] or more (5 h in [25,82], 9 h in [89]). Longer

times improve strengths (with a denser microstructure) and decrease the total porosity [105], but excessive grinding times increase the production cost and the agglomeration of the material with a consequent reduction in strength [103]. Fineness influences the reactivity since higher values increase the specific surface area and, consequently, the reactivity of the CDW [97,106]. A longer milling duration (not exceeding 2h) improves the reactivity of CDW, promoting the formation of silica gel [90]. The optimal time of grinding also depends on the type of apparatus and on the characteristics of CDW [97], but considering energy consumption, a ball milling of 60 min resulted in the optimum timing [106]. Kul [66] tested different kinds of CDW (composed of concrete, roof tile, glass, hollow, and clay brick) collected in five different locations in Turkey. In the last column of Table 6, the particle size of CDW after the milling process is reported. These values are measured by performing a laser diffraction granulometry. Comparing the values of volume mean diameter D(4, 3), it can be observed that all the CDW have very similar values in the range 20–30 µm.

Table 6. Characteristics of grinding process and final particle size of CDW precursor.

Author	Year	Material	Treatment	Grinding Time	Particle Size
Komnitsas [49]	2015	concrete	Bico pulverizer Type UA Fritsch-Bico pulverizer		190–400 µm
Vásquez [50]	2016	concrete	Hammer mill and ball mill		D(4, 3) 24.73 µm
Zaharaki [51]	2016	concrete	Bico pulverizer Type UA Fritsch-Bico pulverizer		<190 µm
Robayo-Salazar [52]	2017	concrete	Hammer mill and ball mill		D(4, 3) 24.73 µm
Ren [53]	2020	concrete			0.075–2.36 mm <0.075 mm
Akduman [54]	2021	concrete	Pre-crusher and grinder	1 h	<100 µm
Huo [55]	2021	concrete	Jaw crusher, mesh sieve, and ball mill	1 h ball mill	<75 µm
Aldemir [77]	2022	concrete	Jaw crusher and scale ball mill	1 h	<100 µm
Ilcan [24]	2022	concrete	Jaw crusher and ball mill	1 h ball mill	<140 µm
Liang [56]	2022	concrete	Pulverisette 4 high-energy ball mill 400 rpm	4 h ball mill	D(50) 0.76 µm
Mahmoodi [57]	2022	concrete	Size crusher and ball mill		D(50) 15.1 µm
Cardoza [96]	2023	concrete	Jaw crusher and ball mill	4 h jaw crusher	D(50) 30 µm
Ozcelikci [60]	2023	concrete	Jaw crusher and ball mill	1 h ball mill	D(4, 3) 24.90 µm
Sasui [61]	2023	concrete	Daihan scientific digital ball mill	1 h 30 min	<75 µm
Cantero [64]	2024	concrete	Jaw crusher, roll crusher, and ball grinding	2 h ball mill	<175 µm
Ilcan [65]	2024	concrete	Crusher and ball mill		<100 µm
Kul [66]	2024	concrete	Crushing–milling process	1 h ball mill	50% < 15 µm
Xi [104]	2024	concrete	Jaw crusher, disk mill, and heating to 750 °C for 3 h	3 h disk mill	<150 µm
Reig [68]	2013	brick	Porcelain ball mill with alumina milling	40 min	20.9 µm
Komnitsas [49]	2015	brick	Bico pulverizer Type UA Fritsch-Bico pulverizer	-	140–350 µm
Robayo-Salazar [69]	2016	brick	Ball mill	-	D(4, 3) 24.25 µm
Zaharaki [51]	2016	brick	Bico pulverizer Type UA Fritsch-Bico pulverizer	-	<140 µm
Robayo-Salazar [52]	2017	brick	Hammer mill and ball mill	-	D(4, 3) 24.25 µm
Hwang [72]	2019	brick	Not specified	-	D(50) 10.32 µm
Kioupis [73]	2020	brick	Pro-pilot plant ball mill	-	D(50) 13.70 µm
Akduman [54]	2021	brick	Pre-crusher and grinder	1 h	<100 µm
Migunthanna [75]	2021	brick	Ball mill grinder	-	<150 µm
Ulugöl [76]	2021	brick	Hammer mill and ball mill (2 times)	1 h ball mill	D(4, 3) 16.40 µm
Aldemir [77]	2022	brick	Jaw crusher and scale ball mill	1 h	<100 µm
Ilcan [24]	2022	brick	Jaw crusher and ball mill	1 h ball mill	<80 µm
Liang [78]	2022	brick	QM3SP04 planetary ball milling	-	<100 µm
Mahmoodi [57]	2022	brick	Size crusher and ball mill	-	D(50) 19.9 µm
Cardoza [96]	2023	brick	Jaw crusher and ball mill	1 h jaw crusher	D(50) 5 µm
Giannopoulou [79]	2023	brick	Jaw crusher and ball mill	-	D(50) 35.35 µm
Kul [81]	2023	brick	Jaw crusher, ball mill with steel ball	1 h ball mill	D(50) 8.50 µm
Ozcelikci [60]	2023	brick	Jaw crusher, ball mill	1 h ball mill	D(4, 3) 18.00 µm
Cantero [64]	2024	brick	Jaw crusher, roll crusher, and ball grinding	2 h ball mill	<175 µm
de Castro Carvalho [82]	2024	brick	10 L ball mill with 45 alumina balls	5 h	D(50) 30.69 µm
Ilcan [65]	2024	brick	Crusher and ball mill	-	<70 µm
Kul [66]	2024	brick	Crushing–milling process	1 h ball mill	50% < 15 µm
Maaze [83]	2024	brick	Chip off the adhered mortar, wash with 0.1 M NaOH, dry for 24 h, and jaw crusher	-	D(50) 31.34 µm
Ulugöl [76]	2021	roof tiles	Hammer mill and ball mill (2 times)	1 h ball mill	D(4, 3) 44.40 µm
Kul [81]	2023	roof tiles	Jaw crusher and ball mill with steel ball	1 h ball mill	D(50) 4.75 µm
Ozcelikci [60]	2023	roof tiles	Jaw crusher and ball mill	1 h ball mill	D(4, 3) 10.30 µm
Komnitsas [49]	2015	tiles	Bico pulverizer Type UA Fritsch-Bico pulverizer	-	140–477 µm
Zaharaki [51]	2016	tiles	Bico pulverizer Type UA Fritsch-Bico pulverizer	-	<140 µm
Hwang [72]	2019	ceramic	Not specified	-	D(50) 25.34 µm
Akduman [54]	2021	tiles	Pre-crusher and grinder	1 h	<100 µm
Aldemir [77]	2022	tiles	Jaw crusher and scale ball mill	1 h	<100 µm
Mahmoodi [57]	2022	tiles	Size crusher and ball mill	-	D(50) 15.5 µm
Giannopoulou [79]	2023	ceramic	Jaw crusher and ball mill	-	D(50) 48.34 µm
Cantero [64]	2024	tiles	Jaw crusher, roll crusher, and ball grinding	2 h ball mill	<175 µm
Robayo-Salazar [52]	2017	glass	Hammer mill, ball mill	-	D(4, 3) 43.12 µm
Akduman [54]	2021	glass	Pre-crusher and grinder	1 h	<100 µm
Ulugöl [76]	2021	glass	Hammer mill and ball mill (2 times)	1h ball mill	D(4, 3) 111.90 µm
Aldemir [77]	2022	glass	Jaw crusher and scale ball mill	1 h	<100 µm
Ilcan [24]	2022	glass	Jaw crusher and ball mill	1 h ball mill	<140 µm
Ozcelikci [60]	2023	glass	Jaw crusher, ball mill	1 h ball mill	D(4, 3) 33.40 µm
Kul [66]	2024	glass	Crushing–milling process	1 h ball mill	40% < 15 µm
Robayo-Salazar [88]	2020	mix	Hammer mill, ball mill	-	D(4, 3) 92.1 µm
Villaquirán [25]	2021	mix	Hammer mill and ball mill	5 h ball mill	D(4, 3) 25.60 µm D(50) 29.00 µm
Moreno-Maroto [89]	2022	mix	Retsch Model BB200 Mangan jaw crusher, Royal Triumph brand hammer mill, ball mill Ceramic Instruments SRL	2.5–9 h	D(50) 27.40 µm D(50) 33.40 µm
Tan [90]	2022	mix	Jaw crusher, ball mill with alumina balls	1–4 h	10–80 µm
Tan [91]	2022	mix	Jaw crusher, ball mill	-	D(50) 10.80 µm
Valencia-Saavedra [92]	2023	mix	-	-	D(4,3) 75 µm
Tefa [94]	2025	mix	-	-	<63 µm

D(4, 3) = volume mean diameter; D(50) = median grain diameter.

3.4. Thermal Treatments

Three different processes to activate the CDW precursor can be performed. The most effective one is the thermal activation at 800 °C, followed by the chemical activation using a $Ca(OH)_2$ + $CaSO_4$ solution, and finally the mechanical activation performed with a grinding apparatus for 75 min [107]. The first two processes are more feasible because they produce more nucleation points for the following hydration products. Xu [108] tested powder obtained from scrap concrete as the only precursor for geopolymeric pastes with different activation parameters (heating temperature and grinding time). The best performance was achieved at 750 °C with 10 min of grinding. In particular, increasing the temperature of calcination (until 750 °C), the compressive strength increased (27 MPa), but for higher temperatures, there is a slight decrease (22 MPa at 950 °C). The decrease in compressive strength for calcination temperatures higher than 800 °C is confirmed even by Zhang [63] due to the many microcracks occurring at extremely high temperatures. A denser microstructure without C-S-H formation can be found in the range 300–600 °C [109], and the formation of new components appears at 900 °C (calcium silicate, larnite, and the transition of α-SiO_2 connected to the decrease in crystalline quartz [103]). A direct proportion was observed between the temperature of calcination and density (2.73 g/cm^3 for 600 °C and 2.81 g/cm^3 for 800 °C) and an inverse proportion with BET surface area (5 m^2/g for 600 °C and 1.9 m^2/g for 800 °C) [67]. The 10% replacement of treated concrete powder gives compressive strength values similar to the reference sample [109]. The thermal treatment at temperatures near 700–800 °C can also increase the activity index of the CDW with values between 70 and 90% [21,103,106,110,111]. Lower temperatures cannot convert the kaolinite phase into metakaolinite and fail to break the chemical bonds in the in situ waste. Instead, higher temperatures can induce a re-crystallization that reduces the release of active silica-alumina components [21]. Tan [100], by first washing the CDW and drying it at only 50 °C, obtained 7-day compressive strength values of up to 29.7 MPa.

3.5. Carbonation of CDW Precursor

Another treatment that can be performed on CDW before its use as a precursor is the carbonation process, where alkali Ca and Mg react with CO_2 to form carbonates. This process can happen directly with a chemical reaction in a gas–solid system (CO_2 curing, flow-through carbonation, and pressurized carbonation) or into an aqueous one (the solid material is submerged in a bulk liquid with CO_2 injected) [103]. The indirect process of carbonation uses acid and basic substances to dissolve the powder and extract calcium ions that are later exposed to CO_2 to precipitate calcium carbonate [103]. Zhang [63] compared carbonation treatment (vacuum pressure reactor at 25 °C, 0.4 MPa for 3–24 h) and thermal activation (from 200 °C to 800 °C for 150 min), finding that calcination temperature at 600 °C gives higher compressive strength than carbonated concrete waste. In particular, for carbonated samples, the compressive strength after 28 days was nearly 52 MPa, and the slump and the setting time were higher than the thermally treated ones.

4. Mix-Design and Mechanical Properties of CDW with Alkali-Activated Materials

4.1. Mixing Concrete Waste with Other Reactive Precursors

Concrete CDW precursor can also be mixed with other more reactive ones, such as metakaolin, fly ash, silica fume, and ground granulated blast-furnace slag, to increase the compressive strength and durability of the final product. The replacement of traditional alkali-activated materials (e.g., FA and GGBS) with paste, mortar or concrete waste powders decreases the fluidity of the mixture, but increases also the drying shrinkage, compressive strength (only for paste powder substitution, optimum 50% replacement of metakaolin or

100% replacement of FA) and durability due to a reduction in water and chloride entrance in the mortar (−43% of chloride diffusion for 75% of substitution with paste powder) [99].

Comparing different mortars with concrete waste powder associated with three different reactive materials (GGBS, FA, and metakaolin), the greatest strength improvement can be achieved with 1/3 part of GGBS and 2/3 of concrete waste powder (47 MPa); instead, metakaolin and fly ash reached, respectively, 35 MPa and only 15 MPa [59]. This combination gave the best strength values due to the type of gels (N-A-S-(H) and C-(A)-S-H) and the amount of reaction products formed during the alkali-activation process [112]. Ren [53] created new recycled concrete blocks using GGBS with concrete waste powder (20–60% of replacement) and the same crushed concrete (0.075–2.36 mm) as aggregate to replace river sand. The results showed that the 20% GGBS replacement gave the highest compressive strength, 46 MPa (+13% after 28 days), due to the reactivity and filler effect of CDW that refines the microstructure, decreasing also the water absorption and increasing the apparent density, as confirmed by SEM results. The higher percentage of replacement decreases the strength (e.g., 60% of CDW achieves only 28 MPa) due to a lower reactivity of CDW compared to GGBS [53]. Ahmari [113] tested CDW coming from ground concrete with the addition of fly ash activated by a 5–10 M NaOH and Na_2SiO_3 solution, finding that the optimum amount of ground concrete waste is 50%.

4.2. Mixing Brick Waste with Other Reactive Precursors

Pastes with bricks and ceramic waste powder with FA and GGBS have the optimal mix-design in terms of compressive strength (near 65 MPa), composed of brick powder (60%), blast furnace slag (30%), and fly ash (10%). The lowest value (near 35 MPa) was instead obtained with ceramic powder (60%), blast furnace slag (10%), and fly ash (30%). Pastes produced with brick powder had better mechanical strength and a denser matrix. The reason was found in the finer particle size and higher CaO content of brick powder [72]. For pastes with fly ash as precursors, the addition of recycled brick powder reduced flowability, while its effect on sorptivity was minimal (mainly influenced by NaOH concentration). In contrast, for compressive strength, the highest value (44.2 MPa after 28 days) is achieved with 10% of replacement of brick powder, Na_2SiO_3/NaOH ratio equal to 2.5, and a 10 M NaOH solution [74]. Instead, pastes with GGBS, FA, and red brick powder (from 10 to 40% of replacement) have the highest compressive strength value after 28 days, near 73.2 MPa for the following recipe: 50% of GGBS, 30% of FA, and 20% of red brick powder [78]. Pavement base construction made again with waste brick powder, FA, and slag has compressive strength after 7 and 28 days of 62 and 82 MPa, respectively [75]. A new original application was found by Capasso [114], who produced pastes with waste brick powder and FA activated by Na_2SiO_3 and a 10 M NaOH solution, useful for the restoration of buildings. These pastes show values of open porosity and capillary absorption similar (or even smaller) to the historical mortar values. Indeed, to avoid original material loss, a repair mortar should have a hardness value similar to that of the brick but lower than that of the existing mortar.

4.3. Mixing Concrete and Brick Waste with Other Reactive Precursors

Sometimes, CDW is not sorted due to the high cost of this operation. Comparing pastes with mixed CDW (red clay bricks, ceramic wall tiles, and concrete), a good mix-design for mechanical strength was found with 20% of bricks, 40% of tiles, 40% of concrete, and a Na_2O/SiO_2 molar ratio equal to 0.18 [57]. Adding metakaolin, ground granulated slag, and fly ash to the CDW precursor, the best results (85 MPa of compressive strength) are achieved with 7% of bricks, 24% of tiles, 24% of concrete, and 45% of GGBS. The best performances are obtained with the addition of GGBS instead of FA and metakaolin, thanks to the larger

supply of amorphous phase present in the GGBS and to the presence of Ca^{2+} cations that act as additional nucleation and deposition sites for C-A-S-H gel. The mix-design with the addition of metakaolin gives a lower increase in strength due to the formation of more Al-O-Si metastable bonds at an early stage, with an increase in the release of silica from CDW and metakaolin, which causes an excess of silanol compounds. Concerning the fly ash, a delay in the pozzolanic reaction can be observed with a longer time of maturation of metastable gels at environmental temperature. For fly ash, an unbalanced concentration of silica, calcium, and alumina ions can be the cause of the low percentages of improvement in strength [57].

For pastes obtained mixing CDW (mortars and concrete at 40%, bricks and tiles at 25%, stone materials at 16% and ceramics at 15%) with GGBS activated with sodium silicate and NaOH, a direct proportionality was found between the amount of GGBS and compressive strength, reaching values of 58.2 MPa for pastes cured for 7 days at 65 °C and with a 50% of replacement and a ratio SiO_2/Na_2O equal to 1.56 [115]. Instead, after 28 days of curing at room temperature, these values of compressive strength were observed: 45 MPa for 50% of CDW and 50% of GGBS, 30 MPa for 70% of CDW and 30% of GGBS, 15–20 MPa for 80% of CDW and 20% of GGBS, and <10 MPa for 100% of CDW. For pastes with GGBS, the morphology of the products of hydration was more compact than the ones made only with CDW. The main product of the reaction was C-(N)-A-S-H gel, detected even in [116,117].

Zaharaki [51] tested different mixes made of CDW (concrete, bricks, and tiles) and industrial wastes (ferronickel slag and red mud). The pastes were cured at 80 °C for 24 h and later stored for 7 days at room temperature. For ferronickel slag and CDW mixes, the increase in molarity from 8 to 10 also increased the compressive strength. Its maximum value was reached around 76 MPa for specimens with lower percentages of concrete waste (10–15%). Increasing the amount of concrete waste (30%) decreased the value of strength below 60 MPa. Even for red mud and ferronickel slag specimens, the optimum NaOH molarity is 10 M, but here the compressive strength decreased for higher amount of red mud (40 MPa for slag/red mud ratio equal to 1:1 compared to 65 MPa for slag/red mud ratio equal to 9:1), since red mud cannot be activated alone (2.5 MPa for 100% red mud sample) [51].

4.4. Mixing CDW with Alkali-Activated Materials and OPC

The addition of OPC to CDW precursor and/or alkali-activated binders is linked to the need to have high strength. These precursors are generally named as binary systems. The improvement in mechanical properties can depends on the amount of OPC, for example, a binary system CDW + 30% OPC can achieve 33 MPa cured at room temperature [50], a binary system bricks CDW + 20% OPC can achieve 100 MPa cured at room temperature and using a solution made of NaOH and Na_2SiO_3, and a binary system concrete CDW + 20% OPC can achieve 35 MPa cured at room temperature and using a solution made of NaOH and Na_2SiO_3 [52]. Lower values were obtained without OPC addition (54.8 MPa for brick powder and 25.6 MPa for concrete powder). With similar recipes (CDW used as precursor composed of concrete, ceramics and masonry activated by Na_2SiO_3 and NaOH with the addition of 10% of OPC and CDW used as aggregate too) new eco-friendly bricks and blocks were produced with the following values of compressive strength after 28 days: 22.6 MPa for solid blocks (11.6% water absorption), 19.8 MPa for hollow blocks (11.6% water absorption) and 4.2 MPa for interlocking concrete paver units (10.1% water absorption) [118]. Except for the paver units, the other two products satisfy the local standard for use in earthquake-resistant houses. Mortars and concretes with CDW + 10% OPC as precursors, activated by NaOH and Na_2SiO_3, and crushed CDW as aggregate, showed values of compressive strength of 33.9 MPa for concrete and 34.6 MPa for mortars after

28 days [88]. Changing the activating solution with sodium sulfate, the mortars prepared with fly ash and 30% of OPC with CDW as fine aggregate gave a strength value of 32 MPa after 28 days, and the ones prepared with CDW both as precursor and aggregate with 30% of OPC gave a value of 25 MPa. For fly ash-based concretes, 22 MPa was reached, and 18 MPa for CDW-based concrete [92]. As in [118], these recipes were used to obtain new alkali-activated brick and blocks classified as high-class structural unit (with fly ash as precursor) and high-class structural unit (with CDW as precursor). The optimum amount of Na_2O in the system should be in the range 4–6%, and even in this case, there is a direct proportion between the curing temperature and the increase in the mechanical strength (with 70 °C, +70% of compressive strength [50]).

The addition of 20% OPC in bricks CDW increased the compressive strength until 102.6 MPa after 28 days for pastes cured at 25 °C and activated with Na_2SiO_3 and NaOH (80 MPa for 10% OPC, and 54 MPa for 0% OPC) [69]. Changing the activating solutions (Na_2SO_4, Na_2CO_3, Na_2OH, and Na_2SiO_3 with NaOH), the worst performances are obtained with Na_2CO_3 (15 MPa with 20% OPC), followed by Na_2SO_4 (20 MPa with 20% OPC) and NaOH (42 MPa with 10% OPC) [119]. The highest value of compressive strength is obtained with 20% of OPC and Na_2SiO_3 with NaOH as activating solution, as confirmed also in [69]. Comparing binary systems with a traditional OPC binder with ceramic waste power (coming from waste tiles) as precursor and the same ceramic waste as aggregate it is possible to observe an increase in compressive strength after 28 days with the addition of 40% ceramic waste powder as precursor (+7% compared to reference sample with 100% of OPC, equal to 55.7 MPa) [85]. This behavior can be explained by the pozzolanic effect of the powder (reactive silica reacts with calcium hydroxide generated from OPC hydration, increasing the amount of C-S-H gel formed). However, an additional increase in ceramic powder (>60%) decreased the strength (38.8 MPa). These values are similar to the binary alkali-activated system, confirming the possibility of activating brick waste also with an activating solution.

4.5. Role of Activating Solution

The concrete CDW powder obtained is activated by solutions containing NaOH, KOH, $Ca(OH)_2$, sodium silicate (Na_2SiO_3), sodium sulfate (Na_2SO_4), or sodium carbonate (Na_2CO_3) [25]. In general, the maximum amount of NaOH does not exceed 12 wt%, and the molarity is usually in the range 4–9 M, with a direct proportion between molarity and final strength [113,120–123]. Low alkali concentration values cannot break the Al-O and Si-O bonds, while higher molarities can create residual unreacted alkali concentrations that decrease the mechanical strength and a rapid formation of surface products inhibiting the dissolution of active components [21]. Furthermore, Na_2SiO_3 increases the mechanical strength, generating soluble silica species that promote the geopolymer matrix, providing a strong connection between the gel and the non-reacting particles [123–125]. Huo [55], testing geopolymers made only with concrete waste powder, found that the dissolution of Si^{4+} and Al^{3+} present in the waste powder was affected by the alkali content and the dissolution time. In particular, by increasing the alkali and Na_2SiO_3 content with the liquid activator to solid powder ratio, the compressive strength after 7 days increases too (best performance with 14 mol/L NaOH, Na_2SiO_3/NaOH ratio equal to 1.5, and liquid to mass ratio equal to 0.4). There is also a direct proportion between the Si/Al ratio and the geopolymerization reaction, and an inverse proportion between the first one and with initial and final setting time [126]. Comparing pastes prepared with 100% of concrete waste powder activated with different concentrations of NaOH and KOH (from 4 M to 12 M), the highest values of compressive strength are reached with an 8 M solution, both with NaOH and KOH activators [61]. Between the two different solutions, the first one had the best performance (5.9 MPa for NaOH solution versus 4.5 MPa for KOH solution after

28 days). In particular, NaOH solution had an increase in strength even after 14 days due to its greater dissolution of the minerals in concrete waste powder. Na^+ ions are also smaller than K^+ ions, improving the interaction between cations and ions and between Na^+ ions and silicate monomers. Comparing NaOH and Na_2SO_4 as activating solution, for pastes obtained with CDW and 10–20% of OPC, the sodium sulfate activator for concentrations of 0.4%, 0.8% and 1.4% of Na_2O increased the strength after 28 days, respectively, by 9%, 19% and 23% compared to those with NaOH with the same Na_2O concentration. Using sodium sulfate, the presence of ettringite was discovered too [25].

Brick waste powders are activated in the same way as concrete waste powders; even in this case, an increase in the molarity of the activating solution achieves an improvement in compressive strength. A higher-concentration NaOH solution dissolves the brick CDW precursors better, liberating substances used to form SiO_4 and AlO_4 tetrahedral units and activating the polymerization. But, continuing to increase the concentration of the solution, an electrostatic shielding will lower the activity of ions, preventing the dissolution of the precursors [76]. Using red brick powder as precursor to create new pastes and mortars activated with Na_2SiO_3 and NaOH it is possible to achieve 30 MPa of compressive strength after 7 days of curing at 65 °C with a molarity of 7.0, a SiO_2/Na_2O ratio equal to 1.6, a binder to sand ratio equal to 1:3. The compressive strength increased with an increase in sodium silicate (but reducing setting time) and with a decrease in the water/binder ratio [68]. On the contrary, Fořt found an inverse proportion between the amount of Na_2SiO_3 and the compressive strength (range 42–10 MPa), connected to a higher presence of large pores (>100 μm) in the samples with more sodium silicate [70]. Compressive and flexural strength also increased with a higher amount of silicate modulus of the liquid activator (i.e., decreasing alkalinity), which could be explained by a better incorporation of crystalline remainders of ceramic particles in the matrix [127]. The optimum alkali activator concentration corresponds to the following parameters: SiO_2/Na_2O ratio of 1.6, a Na_2O content of 10% by weight of the binder, and a binder to sand ratio equal to 1:2.75. With these values, the compressive strength after 5 days of curing at 90 °C is equal to 36.2 MPa [71]. Na_2SO_4 and Na_2CO_3 have a low potential for activating brick wastes [52,119].

4.6. Role of Curing Temperature

Different conditions of temperature and humidity can be applied: environmental temperature, high temperature, or water ponding [121]. In general, low-Ca precursors are particularly sensitive and require temperatures in the range of 40–120 °C to reach sufficient strength [18]. Samples can be cured generally in sealed plastic bags (wet curing) or in plastic bags not sealed (dry curing). Huo [55] tested both ways, finding the best products with the sealed bags (+40.6% of compressive strength after 7 days). Among different temperatures and times of curing (from 20 °C to 90 °C for temperatures and from 4 to 48 h for time), the highest compressive strength (14.32 MPa) is achieved after 7 days for pastes stored at 70 °C for 24 h. There is generally a direct proportion between the temperature of curing, the curing time, and the compressive strength until an upper limit, because if the temperature continues to rise, the strength growth begins to weaken (owing to a reduction in the humidity of the reaction system). Mahmoodi [112] compared different geopolymeric pastes with concrete waste powder as precursor at different initial curing conditions (50 °C, 75 °C, and 100 °C for 24 h). The results confirmed the direct proportion between strength and curing temperature; in particular, the best results are achieved at 100 °C of curing with SiO_2/Al_2O_3 equal to 12.9, H_2O/Na_2O equal to 11.5, and Na_2O equal to 7.91%. Separated CDWs (singular concrete, asphalt, brick, and tile) used for road pavement subbase products cured at 80 °C for 48 h have high values of strength, but also the unseparated fraction cured at 40 °C has performance compatible with road

pavement products [87,123,128]. Comparing pastes obtained with a single type of waste, the bricks and tiles mix showed the best results with compressive strength near 30 MPa for curing at 80 °C, whilst recycled concrete obtained the best result for curing around 40 °C with a compressive strength near 17–20 MPa [128]. An increase in temperature generally gives higher values of compressive strength [71,127]. The increase in compressive strength for higher temperatures is connected to the acceleration of initial dissolution of amorphous phases in the CDW precursor and to the increased activity of hydroxide ions of the alkaline solution. During this process, the formation of zeolites and calcite improves the matrix-aggregate composite effect and the pore structure, too [127]. Since this process is very fast for higher temperatures, the compressive strength will be higher, too. The reaction products obtained are sodium-aluminosilicate hydrate gels with zeolite-like structure or sodium silicate gels when glass waste is used as a precursor [76]. Rakhimova also tested the steam curing (4 h preset, 3 h of heating, 6 h at 90–95 °C, 3 h of cooling [84]).

5. Properties of Alkali-Activated Materials with CDW as Precursor

5.1. Workability

The addition of CDW replacement generally decreases the slump of the mixes due to the porosity of the CDW that absorbs water from the mix (in particular, this decrease is significant in FA-based mixes beyond 20% replacement [129]). Thermal treatments on the CDW precursor can reduce slump, too [63]. Generally, concrete waste powder has a lower particle fraction and lower water absorption than brick waste powder [130]. The addition of CDW increases the setting time due to the lower reactivity of the CDW than the standard precursor [63]. The use of brick powder gives a mixture with a higher slump compared to concrete powder due to the lower surface area and water demand of bricks (103–105% for bricks and 110–114% for concrete at the same fineness) [111]. Workability can be affected by the aluminosilicate source, the alkaline liquid concentration, and the ratio of silicate to hydroxide. The addition of precursors such as silica fume, fly ash, and blast furnace slag to the CDW produced an increase in the flowability of the mixtures, a greater open time performance, an improvement in mechanical strength, an improvement in workability, and a guaranteed environmental burden slightly higher than 100% CDW samples [80]. CDW with a high Na/Si ratio can increase the flow of the mixtures and decrease the setting time due to the higher amount of OH^- ions that can break the Si-O-Al and Si-O-Si bonds of the precursors, giving more workability. Increasing the molarity of the solution, a more viscous mixture is obtained with a lower flowability [130]. The use of CDW with high concentrations of alkali or a high SiO_2/Al_2O_3 ratio can give an early setting time. In the first case, owing to a rapid dissolution of precursors, and in the second one, owing to an accelerated interaction between aluminate and silicate that increases polycondensation [126]. Higher content of Na_2O in the CDW can initiate the quicker dissolution of silico-aluminates, creating a rapid coagulation stage [131].

5.2. Insulating Properties

The high porosity and small pore size of metakaolin-CDW pastes make them suitable for creating insulating and thermal-acoustic panels for greenhouse buildings or for the restoration of ancient buildings to prevent damage to the existing original materials [132]. Mortars with concrete waste powder and more reactive materials (GGBS, fly ash, and metakaolin) prepared for thermal insulation applications have a thermal conductivity for foamed geopolymer equal to 0.049 W/mK, which is similar to that of the insulating products actually in commerce [59]. Brick powder coming from the demolition of buildings and from batches rejected by industry, activated with sodium silicate and NaOH, was

also used as a precursor to create a geopolymeric layer with a compressive strength near 37 MPa for an insulating wall package with a reduction in the heat flow of about 66% [133].

5.3. Mechanical Properties

Tables 7–9 [25,49–83,86–90,93–96,98,99,112,118,129,131,134–137] summarize and compare the mix-designs tested in the literature for CDW precursors. In Table 7, papers with concrete waste precursors are reported. Brick waste precursor and ceramic waste precursor are recapitulated in Table 8. Instead, in Table 9 are summarized the papers where a mix of various CDWs is used as precursors altogether or studied separately. As previously explained in Section 1, each type of CDW is associated with a different colored tick (green for concrete, red for bricks, pink for tiles, and blue for glass). The value of the percentage of waste replacement is colored using the same correspondence of colors when the same CDW is used. If a mix of different CDW types was used, the box is colored in yellow; instead, if different CDW types were analyzed separately, the box is colored in lilac. In the charts are also indicated the types of the precursor (MTK, FA, GGBS, SF, or red mud) and if a binary system was tested (with a black tick in the OPC box). The "waste precursor" section specifies the type of CDW tested, including the type of bricks used (red clay brick, hollow brick, or roof tile). In the "activating solution" part, the type of silicate, the type and molarity of the hydroxide are specified. At the bottom of the chart, the presence of natural or recycled CDW aggregate is indicated. If an alkali-activated mortar or concrete were tested, the ticks are colored according to the type of CDW used, using the same color match previously described. Analyzing Tables 7–9, it can be observed from the literature that pastes and mortars are mainly tested, whereas alkali-activated concrete wastes are scarcely studied. Other precursors, in addition to CDW ones, are mainly used to increase the mechanical properties of the composites. Among the different types of CDW, bricks and concrete are the most used ones, instead glass waste is scarcely used. Sodium silicate and sodium hydroxide can be considered as the main activating solutions with a molarity in the range 4–18 M. The temperature of curing varies from the environmental temperature until 100 °C. In Tables 10–12 [25,49–56,58–60,62–83,86–90,93,95,96,98,99,118,129,131,135–137], the mix-design of the composite that achieved the highest value of compressive strength for each paper is analyzed. In particular, papers with concrete waste used as a precursor are reported in Table 10, bricks and ceramic precursors are collected in Table 11, and the use of a combination of different types of precursors is reported in Table 12. As explained in Section 1, the same color match used for Tables 7–9 is used (green for concrete waste, red for brick waste, pink for tile waste, and blue for glass waste). If the value of compressive strength is reached using a mix of different CDW, the box is colored in yellow. As can be observed in Tables 10–12, the values of compressive strength are included in the range 10–100 MPa. This great variability is affected by many parameters, as described in the previous paragraphs of Sections 2–4. However, it is possible to observe that, increasing the amount of CDW precursor (until 100% CDW), the compressive strength decreases, and generally the binary system with OPC gives better performances (80–100 MPa). Particular attention should be paid to the papers of Komnitsas [49] and Reig [137] that reached an impressive value of compressive strength near 60 MPa for 100% tile waste composites. Among the different types of CDW, brick precursors generally achieve the highest performance. Mixing different CDW gives a great variability in the compressive strength values since a range of 10–85 MPa is obtained. For this reason, when it is not possible to sort the CDW, a proper mix-design is necessary. Cardoza [96] and Cantero [64] tested separately different types of CDW (lilac box), confirming that bricks precursor gives higher performance than concrete waste precursors. Since the alkali-activating solution is almost constant for all the

papers, the parameter to compare is the molarity. The highest performances are reached with higher molarity; in particular, the optimum amount is close to 10 M.

Table 7. Main types of alkali-activated composites with concrete powders used as precursors present in the literature.

	Author	Vasquez [50]	Ren [53]	Huo [55]	Mahmoodi [112]	Liang [56]	Liu [98]	Liu [95]	Sharma [129]	Wang [58]	Wang [134]	Boros [59]	Liu [99]	Sasui [61]	Wan [62]	Zhang [63]	Liu [135]	Sasui [67]	Elhadi [136]
	Year	2016	2020	2021	2021	2022	2022	2022	2022	2022	2022	2023	2023	2023	2023	2023	2024	2024	2025
Mixture	P	✓		✓	✓	✓					✓			✓		✓		✓	
	M						✓	✓	✓	✓		✓	✓		✓		✓		✓
	C		✓																
Precursor	OPC	✓																	
	MTK	✓			✓							✓	✓						✓
	FA				✓	✓	✓		✓		✓	✓				✓			
	GGBS		✓		✓	✓		✓		✓	✓	✓			✓	✓		✓	
	SF																		✓
	RM																		
Waste Prec.	Cw	✓	✓	✓	✓	✓	✓	✓	✓	✓	✓	✓	✓	✓	✓	✓	✓	✓	✓
Waste Treatment	Thermal															✓	✓	✓	
	Carbon.															✓			
W%	from	70	20		55	0	0	0	10	10	50	0	25		0	10		0	50
	to	100	60	100	85	8	100	100	50	100	90	100	100	100	40	40	100	50	100
Activating Solution	Na_2SiO_3	✓	✓	✓	✓	✓	✓	✓	✓	✓	✓	✓	✓			✓	✓		
	NaOH	✓	✓	✓	✓	✓	✓	✓	✓	✓		✓	✓	✓	✓	✓	✓	✓	
	KOH													✓					
	$Ca(OH)_2$																		
	Na_2O																		✓
	Na_2CO_3																		
Mol.	from			6										4					
	to			18			1.4	1.4	12					12				8	1.3
Agg.	NS		✓				✓	✓	✓	✓			✓		✓		✓	✓	✓
	RA		✓									✓							
T (°C)	from	25		20	25				23					50					
	to	70	25	90	100	23	20	20	60	20	20	23	20	70	20	23	23	22	

Table 8. Main types of alkali-activated composites with brick and tile powders used as precursors present in the literature.

	Author	Reig [68]	Robayo-Salazar [69]	Robayo-Salazar [52]	Fort [70]	Tuyan [71]	Kioupis [73]	Wong [74]	Migunthanna [75]	Liang [78]	Kul [81]	deCastro Carvalho [82]	Maaze [83]	Reig [137]	Erol [86]
	Year	2013	2016	2017	2018	2018	2020	2020	2021	2022	2023	2024	2024	2017	2023
Mixture	P		✓	✓	✓		✓	✓	✓	✓		✓			
	M	✓		✓		✓					✓		✓	✓	✓
	C														
Precursor	OPC		✓	✓											
	MTK														
	FA							✓	✓	✓					✓
	GGBS								✓	✓		✓			✓
	SF														
	RM														
Waste Precursor	Cw														
	Rcb	✓	✓	✓	✓	✓	✓	✓	✓	✓	✓	✓	✓		
	Hb										✓	✓	✓		
	Rt										✓	✓			
	Ti													✓	✓
	Gl						✓								
W%	from		70	70				10	20	10		25			35
	to	100	90	90	100	100	100	20	80	40	100	75	100	100	45
Activating Solution	Na_2SiO_3	✓	✓	✓	✓	✓	✓	✓	✓	✓		✓	✓	✓	✓
	NaOH	✓	✓	✓	✓	✓	✓	✓		✓	✓	✓	✓	✓	✓
	KOH														
	$Ca(OH)_2$													✓	
	Na_2O			✓											
	Na_2CO_3			✓											
Mol.	from	2.5						6			10		8		8
	to	10						10		1.5	19		12		16
Agg.	NS	✓		✓		✓							✓	✓	✓
	RA										✓			✓	
T (°C)	from		25			50					105		40	20	
	to	65	70	25	20	100	80	25	25	20	125	23	60	65	23

Table 9. Main types of alkali-activated composites with a mix of various CDW powders used as precursors present in the literature.

	Author	Zaharaki [51]	Bassani [87]	Robayo-Salazar [88]	Akduman [54]	Mahmoodi [131]	Villaquirán-Caicedo [25]	Aldemir [77]	Mahmoodi [57]	Moreno-Maroto [89]	Robayo-Salazar [118]	Tan [90]	Ilcan [80]	Ozcelikci [60]	Ilcan [65]	Kul [66]	Roy [93]	Tefa [94]	Komnitsas [49]	Robayo-Salazar [52]	Hwang [72]	Ulugol [76]	Cardoza [96]	Giannopoulou [79]	Cantero [64]
	Year	2016	2019	2020	2021	2021	2021	2022	2022	2022	2022	2022	2023	2023	2024	2024	2024	2025	2015	2017	2019	2021	2023	2023	2024
Mixture	P	✓	✓	✓		✓	✓		✓	✓		✓	✓			✓			✓	✓	✓	✓	✓	✓	
	M										✓			✓	✓		✓	✓		✓					✓
	C			✓	✓			✓			✓						✓								
Precursor	OPC			✓			✓	✓		✓	✓									✓					
	MTK					✓			✓																
	FA				✓	✓		✓	✓				✓												✓
	GGBS	✓			✓	✓		✓	✓				✓	✓	✓		✓				✓				
	SF												✓		✓						✓				
	RM	✓																							
Waste Precursor	Cw	✓	✓	✓	✓	✓	✓	✓	✓	✓	✓	✓		✓	✓	✓	✓	✓	✓				✓		✓
	Rcb	✓	✓	✓	✓	✓	✓	✓	✓	✓	✓	✓	✓	✓	✓	✓	✓	✓	✓	✓	✓	✓	✓	✓	✓
	Hb				✓			✓		✓			✓	✓		✓						✓			
	Rt				✓		✓	✓		✓			✓	✓								✓			
	Ti	✓	✓	✓					✓		✓	✓						✓	✓	✓	✓			✓	✓
	Gl				✓			✓				✓	✓	✓		✓				✓		✓			
W%	from	50				65	80		65	80			80	80	70		0			70					
	to	100	100	90	80	100	90	80	100	100	90	100	100	100	100	100	20	100	100	90	60	100	100	100	100
Activating Solution	Na_2SiO_3	✓	✓	✓	✓	✓	✓	✓	✓	✓	✓	✓		✓			✓	✓	✓	✓	✓		✓	✓	✓
	NaOH	✓	✓	✓	✓	✓	✓	✓	✓	✓	✓	✓	✓	✓	✓	✓	✓		✓	✓	✓	✓	✓		✓
	KOH																							✓	
	$Ca(OH)_2$				✓			✓					✓	✓											
	Na_2SO_4						✓																		
	Na_2O																								
Mol.	from	8	1.5				6	8		6				6	4		3		8			12			
	to	12	4		8		10	8		12			6	10	8	15	6		14		10	18	8	8	
Agg.	NS																✓			✓					✓
	RA			✓	✓			✓			✓			✓	✓		✓	✓							
T (°C)	from					25			25	25									60	25		50			25
	to	80	25	25	23	100	25	23	100	90	90	50	23	23	23	115	23	20	90	70	25	125	25	50	100

Table 10. Mix-design with concrete CDW as precursor developed to achieve the maximum compressive strength and tests performed.

		Author	Vasquez [50]	Ren [53]	Huo [54]	Mahmoodi [131]	Liang [56]	Liu [98]	Liu [95]	Sharma [129]	Wang [58]	Wang [134]	Boros [59]	Liu [99]	Sasui [61]	Wan [62]	Zhang [63]	Liu [135]	Sasui [67]	Elhadi [136]
		Year	2016	2020	2021	2021	2022	2022	2022	2022	2022	2022	2023	2023	2023	2023	2023	2024	2024	2025
Mix-Design		Prec.	10% MTK,90% Cw	80% GGBS, 20% Cw	100% Cw	45% GGBS, 55% Cw	47% GGBS, 47% FA, 6% Cw	50% FA, 50% Cw paste	50% GGBS, 50% Cw	70% FA, 30% Cw	70% GGBS, 30% Cw	50% GGBS, 50% Cw	100% Cw	50% MTK, 50% Cw	100% Cw	90% GGBS, 10% Cw	45% GGBS 45% FA 10% Cw treated at 600 °C	100% Cw paste treated at 600 °C	50% GGBS50% Cw treated at 700 °C	50%MTK, 50%Cw
		AS	Na_2SiO_3 NaOH	Na_2SiO_3 NaOH	Na_2SiO_3 NaOH	Na_2SiO_3 NaOH	Na_2SiO_3 NaOH	Na_2SiO_3 NaOH	Na_2SiO_3 NaOH	Na_2SiO_3 NaOH	Na_2SiO_3 NaOH	Na_2SiO_3	Na_2SiO_3 NaOH	Na_2SiO_3 NaOH	NaOH	NaOH	Na_2SiO_3 NaOH	Na_2SiO_3 NaOH	NaOH	Na_2O
		Mol.			14			1.4	1.4	1.2					8				8	2
		L/B		0.60	0.40	0.30	0.45	0.35	0.35	0.35	0.5		0.40		0.4	0.5	0.5	0.45	0.4	0.30
		Na_2O (%)	6	10		5		6	6					10		9		10		
		Agg.		RA				NS	NS	NS	NS		RA	NS		NS		NS		NS
		B/A		0.25				0.50	0.50	0.33	0.67		0.50	1.00		0.33		1.00		
		T (°C)	25	25	70	25	23	20	20	60	20	20	23	20	25	20	53	23	22	
		σc max	46	46	14	82	83	33	80	27	45	85	12	55	6	30	54	45	25	85
Tests Performed		Flow				✓				✓		✓				✓	✓			
		σc–σf	✓	✓	✓	✓	✓	✓	✓	✓	✓	✓	✓	✓	✓	✓	✓	✓	✓	✓
		SEM EDX	✓	✓	✓	✓	✓	✓	✓	✓	✓	✓	✓	✓	✓	✓	✓	✓	✓	✓
		XRD	✓	✓	✓	✓	✓	✓	✓	✓	✓	✓	✓		✓	✓	✓	✓	✓	✓
		FTIR	✓			✓			✓		✓	✓		✓	✓		✓	✓	✓	✓
		TGA DSC					✓	✓			✓			✓		✓		✓	✓	
		Pe.Abs.		✓					✓	✓			✓	✓				✓		
		Density											✓					✓	✓	
		MIP BET					✓	✓	✓		✓			✓			✓	✓	✓	
		Dur.						✓						✓				✓		

Table 11. Mix-design with brick and tile CDW as precursor developed to achieve the maximum compressive strength and tests performed.

	Author	Reig [68]	Robayo-Salazar [69]	Robayo-Salazar [52]	Fort [70]	Tuyan [71]	Hwang [72]	Kioupis [73]	Wong [74]	Migunthanna [75]	Ulugol [76]	Liang [78]	Cardoza [96]	Kul [81]	Cantero [64]	de Castro Carvalho [82]	Maaze [83]	Komnitsas [49]	Reig [137]	Erol [86]	Giannopoulou [79]
	Year	2013	2016	2017	2018	2018	2019	2020	2020	2021	2021	2022	2023	2023	2024	2024	2024	2015	2017	2023	2023
Mix-Design	Prec.	100% Rcb	80% Rcb, 20% OPC	80% Rcb, 20% OPC	100% Rcb	100% Rcb	60% Rcb, 10% FA, 30% GGBS	100% Rcb	10% Rcb, 90% FA	40% Rcb, 60% GGBS	100% Hb	20% Rcb, 30% FA, 50% GGBS	40% Rcb, 60% activating solution	100% Rt	100% Rt	25% Rcb, 75% GGBS	100% Rcb	100% Ti	100% Ti	15%Ti, 50% GGBS, 35% FA	100% Ti
	AS	Na_2SiO_3 NaOH	Na_2SiO_3 NaOH	Na_2SiO_3 NaOH	Na_2SiO_3 NaOH	Na_2SiO_3 NaOH	Na_2SiO_3 NaOH	Na_2SiO_3 NaOH	Na_2SiO_3 NaOH	Na_2SiO_3	NaOH	Na_2SiO_3 NaOH	Na_2SiO_3 NaOH	NaOH	Na_2SiO_3 NaOH	Na_2SiO_3 NaOH	Na_2SiO_3 NaOH	Na_2SiO_3 NaOH	Na_2SiO_3 NaOH $Ca(OH)_2$	Na_2SiO_3 NaOH	Na_2SiO_3 KOH
	Mol.						10		10		15	2	8	10			12	10	10	16	8
	L/B	0.30	0.23	0.23	0.50	0.46	0.45	0.20		0.35	0.35	0.40	1.50		0.60	0.40		0.40	0.50	0.50	0.30
	Na_2O (%)	7				10					12				12	7					
	Agg.	NS				NS								RA	NS		NS		RA	NS	
	B/A	0.5				0.36								2.22			1		0.33	0.44	
	T (°C)	65	25	25	20	90	25	80	25	25	115	20	25	115	70	23	50	80	65	23	50
	σc max	50	102	100	42	36	65	43	44	82	45	74	32	65	12	69	17	58	53	63	37
Tests Performed	Flow						✓		✓						✓	✓				✓	
	σc–σf	✓	✓	✓	✓	✓	✓	✓	✓	✓	✓	✓	✓	✓	✓	✓	✓	✓	✓	✓	✓
	SEM EDX	✓	✓	✓	✓	✓	✓	✓	✓	✓	✓	✓	✓	✓	✓	✓	✓	✓	✓	✓	✓
	XRD	✓	✓	✓	✓	✓	✓	✓	✓	✓	✓	✓	✓	✓	✓	✓		✓	✓	✓	✓
	FTIR	✓	✓			✓	✓	✓							✓	✓		✓			✓
	TGA DSC	✓				✓					✓					✓					
	Pe.Abs.								✓				✓		✓				✓		
	Density														✓				✓		✓
	MIP BET	✓			✓																
	Dur.																✓			✓	✓

In the lowest part of Tables 10–12, the tests performed in each paper are reported and compared. CDW is mainly characterized by the X-ray diffraction technique (XRD), Fourier-Transform Infrared spectroscopy (FTIR), and chemical composition analysis. XRD, FTIR, TGA and DSC tecniques are also performed on the final composite materials to detect the presence of calcium aluminium silicates and carbonates. Their presence is further confirmed by SEM-EDX analysis, which also allows observation of other important elements such as pores, unreacted particles, matrix homogeneity, and the microcraks. As can be observed, the mechanical properties are deeply analyzed, while workability and durability tests are scarcely performed. This last aspect should be better investigated in future studies to ensure the possibility of offering new CDW and alkali-activated products in the market. Different

aggressive environmental conditions should be tested too (as sulfate attack, chloride ion penetration, freeze–thaw cycles, and salt spray test).

Table 12. Mix-design with a mix of various CDW as precursor developed to achieve the maximum compressive strength and tests performed.

	Author	Year	Prec.	AS	Mol.	L/B	Na_2O (%)	Agg.	B/A	T (°C)	σc max	Flow	σc–σf	SEM EDX	XRD	FTIR	TGA DSC	Pe.Abs.	Density	MIP BET	Dur.
Mix-Design	Zaharaki [51]	2016	10% Cw, 20% Rcb, 20% Tl, 50% GGBS	Na_2SiO_3 NaOH	10					80	76		✓	✓	✓	✓	✓				
	Bassani [87]	2019	100% CDW	Na_2SiO_3 NaOH	4	0.40				25	13	✓	✓	✓	✓	✓			✓		
	Robayo-Salazar [88]	2020	90% CDW, 10% OPC	Na_2SiO_3 NaOH		0.40		RA	0.40	25	44	✓	✓	✓	✓						
	Akduman [54]	2021	24% Rt, 14% Rcb, 19% Hb, 10% Gl, 9% Cw, 19% GGBS, 5% FA	Na_2SiO_3 NaOH $Ca(OH)_2$	8	0.55		RA	1.00	23	37		✓								
	Mahmoodi [131]	2022	35% Cw, 25% Rcb, 45% GGBS	Na_2SiO_3 NaOH		0.30				25	106	✓	✓	✓	✓	✓					
	Villaquirán-Caicedo [25]	2021	5%Na_2SO_4 22% OPC, 78% CDW	Na_2SO_4						25	14		✓	✓	✓	✓	✓		✓		
	Aldemir [77]	2022	25% Rt, 20% Rcb, 15% Hb, 10% Gl, 10% Cw, 15% GGBS, 5% FA	Na_2SiO_3 NaOH $Ca(OH)_2$	8	0.35		RA	1.00	23	37		✓								
	Mahmoodi [57]	2022	24% Cw, 7% Rcb, 24% Tl, 45% GGBS	Na_2SiO_3 NaOH		0.30				90	85	✓	✓	✓	✓	✓					
	Moreno-Maroto [89]	2022	20% OPC, 80% CDW	Na_2SiO_3 NaOH		0.30				25	15		✓	✓	✓	✓			✓		✓
	Robayo-Salazar [118]	2022	30% Cw, 30% Rcb, 30% Tl, 10% OPC	Na_2SiO_3 NaOH		0.40		RA	1.00	25	32		✓	✓				✓			
	Tan [90]	2022	100% CDW	Na_2SiO_3 NaOH		0.40				50	38		✓	✓	✓	✓					
	Ilcan [80]	2023	24% Hb, 24% Rcb, 24% Tl, 20% SF, 8% Gl	NaOH $Ca(OH)_2$	6					23	30	✓	✓								
	Ozcelikci [60]	2023	18% Hb, 14% Rcb, 24% Rt, 16% Cw, 20% GGBS, 8% Gl	Na_2SiO_3NaOHCa(OH)$_2$	6	0.70		RA	2.80	23	52		✓	✓	✓		✓	✓		✓	
	Ilcan [65]	2024	55% Rcb, 15% Cw, 25% GGBS, 5% SF	NaOH	5	0.40		RA	1.00	23	25	✓	✓	✓				✓			✓
	Kul [66]	2024	40% Hb, 20% Rcb, 20% Rt, 5% Cw, 25% GGBS, 15% Gl	NaOH	15					115	68	✓	✓	✓	✓	✓					
	Roy [93]	2024	85% OPC, 15% CDW	Na_2SiO_3NaOH	6	0.45		RA	0.30	23	35	✓	✓	✓				✓			

The high value of mechanical strength at early ages of alkali-activated products is due to the fast rate of hydration for elevated pHs (even faster for samples cured at high temperature) and to the homogeneous interface transition zone (ITZ) created. Also, a higher molar concentration of sodium hydroxide solution (around 10 M) gives higher compressive strength. Thanks to the higher pH value, there is an extended breakage of the glassy chain at the surface of the raw material, increasing the reaction between internal Si and Al and the creation of gel phases [138]. Generally, the drying and autogenous shrinkage for these products is greater than that of OPC concrete, but it can be easily reduced by adding some shrinkage-reducing additives or fibers into the matrix [139,140].

The results obtained as best compressive strength values for each paper (reported in Tables 10–12) were divided and cross-referenced with the main parameters that influence the mechanical properties (Figures S1–S3) [25,49–55,57–82,86,88–90,93,95,96,98,112,118,129,131,134–136]. In particular, Figure S1 reports the values of compressive strength compared to the percentage of replacement. Comparing the values obtained for 100% CDW precursor, brick and tile wastes achieve the best results. Concrete waste shows high values for a lower amount of replacement (near 50%) and only in association with GGBS (poor results are obtained with FA). Figure S2 shows the influence of fineness on the strength, confirming that most of the articles used ground granulated blast-furnace slag waste with a diameter inferior to 60 µm. Bricks and tiles are generally easier to grind and can achieve a higher fineness compared to concrete waste (green symbols). The influence of the curing temperature on compressive strength is reported in Figure S3. As can be observed, almost all the studies cured the samples at room temperature, obtaining a great variability in the results. To better analyze the influence of these parameters, however, it is necessary to compare recipes in which only one parameter is changed while leaving the others constant. Therefore, additional explanatory charts were created in which the entire mix-designs with the related strength values are reported (Figure 6A–D) [49,52,53,57,69,71,75,76,78,82,93,112,129,131,134]. The mechanical properties of alkali-activated materials can vary considerably. In Figure 6A, the influence of the percentage of CDW present is summarized, and the type of the other precursor (FA, GGBS, or MTK) is described according to the style of the line, as shown in the legend. As can be observed, there is an inverse proportion between the compressive strength achieved after 28 days of curing and the percentage of CDW precursor. CDW precursor is generally less performing than traditional FA or GGBS. For some studies, there is a small increase in the mechanical properties for percentages of replacement near 20–40% (Ren [53], Migunthanna [75], Liang [78], Sharma [129]), in particular for brick waste. In Figure 6B, the role of the fineness of the precursor on the mechanical properties is shown. Fineness increases reactivity (as previously explained in paragraph 3.3) since finer particles have more active nucleation sites able to interact with the activating solution. This improves the formation of new bonds and subsequently the compressive strength [49]. For concrete waste, the role of fineness appears less relevant since high values of compressive strength are not achieved (green line in Figure 6B). In Figure 6C, the role of the Si/Al ratio is described. The chemical composition of brick and tile waste has a higher amount of SiO_2 and Al_2O_3 than concrete powder (as confirmed by Table S1 and Figure 5A), which has more CaO. The higher amount of Si and Al ions facilitates a greater formation of Si-O-Si and Si-O-Al bonds. Instead, the presence of Ca^{2+} ions leads to a consumption of stabilizing Na^{+} ions. This causes an accelerated condensation and a flash setting that causes a decrease in compressive strength. For this reason, bricks and tiles work better as precursors than concrete, as confirmed by Figure 6C, where brick precursors drawn in red are generally higher than the concrete precursor in green. A mix of different precursors is in the middle. In Figure 6D, the role of the curing temperature on compressive strength after 28 days is summarized. Elevated temperatures and prolonged times generally assure great performances. This is caused by an accelerated

geopolymerization (ion transportation and reaction kinetics). A denser matrix is generated, and mechanical properties are improved. Observing Figure 6D, it is possible to see that an optimal curing temperature is close to 100 °C. For higher temperatures, the formation of microcracks and excessive evaporation damage the composite products.

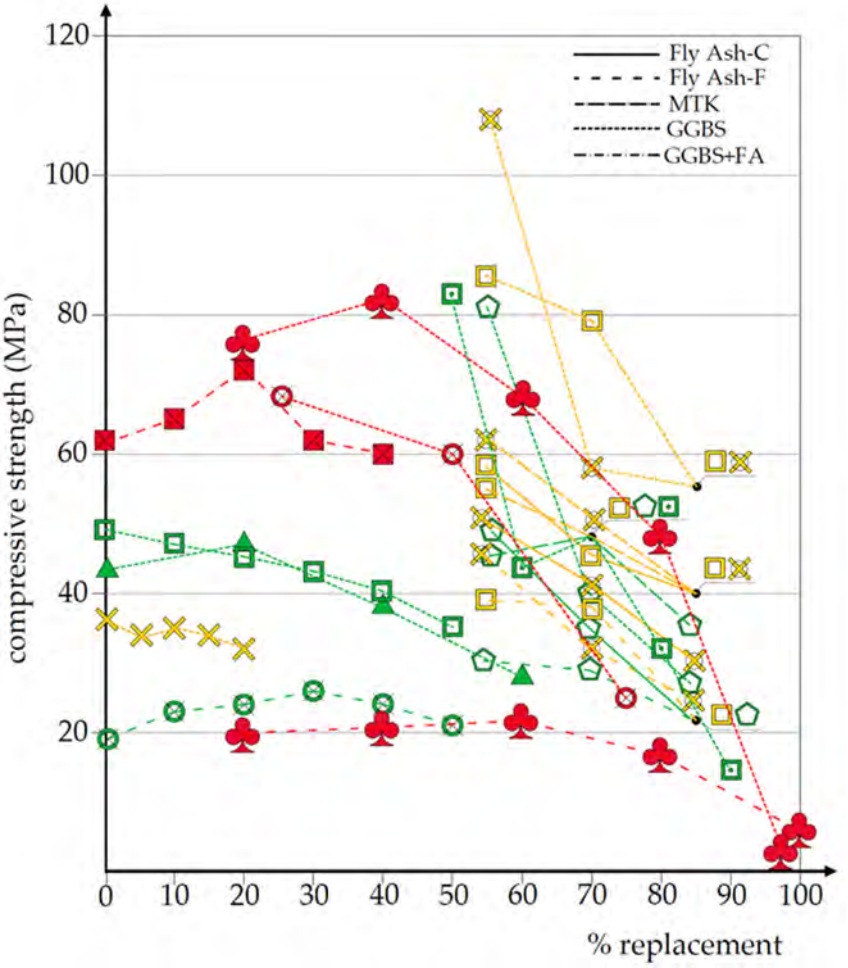

(**A**)

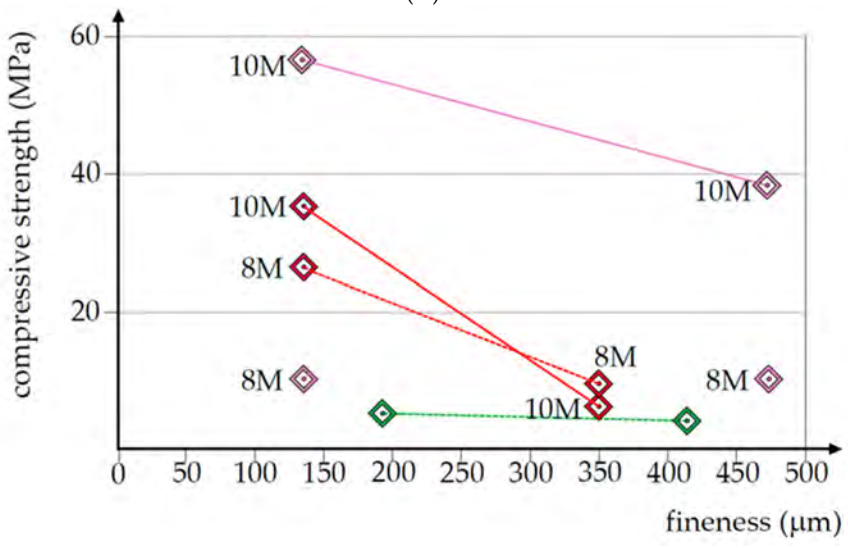

(**B**)

Figure 6. *Cont.*

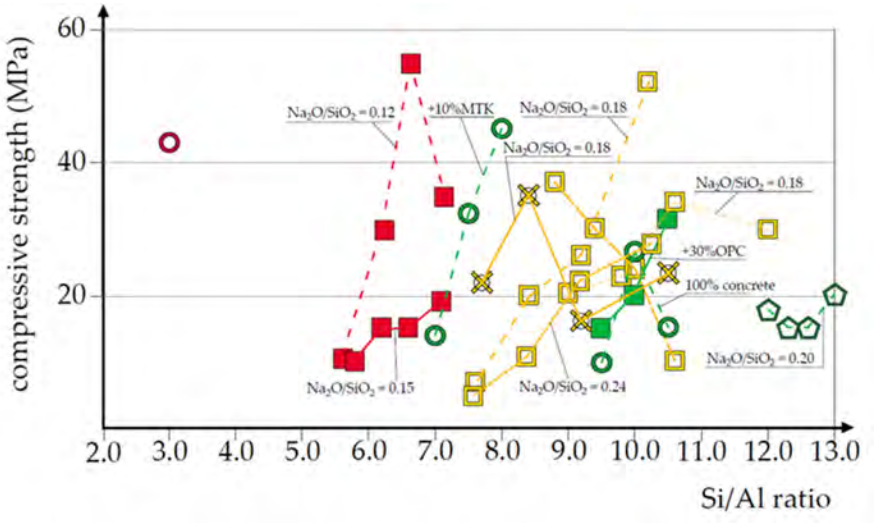

(**C**)

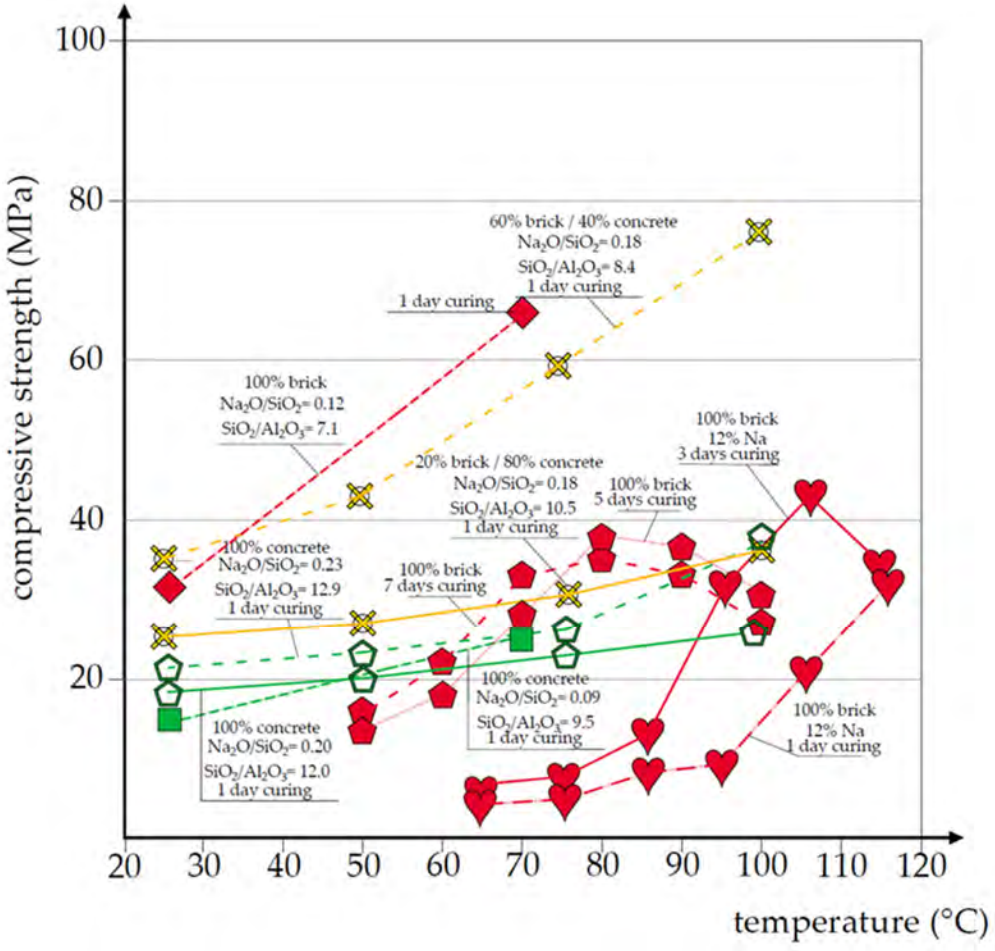

(**D**)

Figure 6. (**A**) Effect of the percentage of replacement on the compressive strength. (**B**) Effect of the fineness on the compressive strength. (**C**) Effect of the Si/Al ratio on the compressive strength. (**D**) Effect of the curing temperature on the compressive strength.

Legend of Figure 6A–D							
CDW Type	Symbol	Author	Year	CDW Type	Symbol	Author	Year
concrete		Komnitsas [49]	2015	brick		Robayo-Salazar [52]	2017
concrete		Robayo-Salazar [52]	2017	brick		Tuyan [71]	2018
concrete		Ren [53]	2020	brick		Migunthanna [75]	2021
concrete		Mahmoodi [112]	2021	brick		Ulugöl [76]	2021
concrete		Sharma [129]	2022	brick		Liang [78]	2022
concrete		Wang [134]	2022	brick		de Castro Carvalho [82]	2024
ceramic		Komnitsas [49]	2015	mix		Mahmoodi [131]	2022
brick		Komnitsas [49]	2015	mix		Mahmoodi [57]	2022
brick		Robayo-Salazar [69]	2016	mix		Roy [93]	2024

5.4. Thermal Stability at High Temperature

Mortars and concretes with alkali-activated binders generally have a higher stability than OPC ones, in particular below 300 °C. For mortars with GGBS (50%), low-calcium FA (35–45%) and ceramic waste powder (5–15%) activated by sodium silicate and a NaOH solution with natural sand and crushed limestone as aggregates, the addition of ceramic waste powder has both a filling and a pozzolanic effect (compressive strength after 28 days near to 63 MPa for 15% of ceramic powder and 16 M solution). Samples exposed to 300 °C temperature improved their compressive strength results by 7% due to greater geopolymerization. Instead, for temperatures in the range 600–900 °C, all properties decreased (respectively, −70% and −85%) due to the initial free water evaporation, followed by the dehydration of the gel, and the increase in the final vapor pressure [86]. Changing NaOH in the activating solution with KOH in pastes with brick and ceramic waste powder used as precursors, a good thermal stability is found until 1050 °C (25 MPa of compressive strength for brick-based geopolymer and 37 MPa for ceramic tile geopolymer) [79]. In particular, the cracks formed at 800 °C disappeared at 1050 °C thanks to self-healing phenomena that are related to the sintering of the geopolymeric gel phase, making them suitable materials for fire-resistant applications. The thermal stability of pastes made with metakaolin and CDW as precursors is close to 650 °C. For higher temperatures (750 °C), an expansion was observed due to the formation of gases trapped in the matrix, whilst at 1000 °C, dense struts and macropores are formed with geopolymeric matrix sintering [132].

6. Alkali-Activated Materials with CDW as Aggregate and Mechanical Properties

6.1. General Parameters

CDW can also replace the natural aggregate in a mortar or a concrete structure. Even for these applications, the CDW can be composed of old concrete structures, bricks, asphalt, and tiles [141]. In Table 13 [19,53,142–145], the chemical composition of CDW aggregates present in the literature is reported. In particular, Zhu [145] tested the possibility of reusing old geopolymeric samples as aggregate to create new recycled geopolymeric composites. As can be observed in Table 13, the CDW aggregate has almost the same chemical composition as the CDW precursor observed in Table S1 and Figure 5A. In Table 14 [19,137,143,144,146–148], the minerals detected in the CDW aggregate using the X-ray diffraction technique are reported. The CDW aggregate made by concrete waste is composed of quartz, calcite, portlandite, amorphous C-S-H, feldspars (albite, microcline), and a product of sulfate attack (gypsum and ettringite). Brick and ceramic waste are mainly composed of quartz, calcite, and muscovite. Other minerals, such as microcline, anorthite, hematite, diopside, mullite, and dolomite, can

be detected too. In Table 15 [19,53,88,93,94,118,137,142,143,146,149–154], Los Angeles abrasion loss, specific gravity, fineness modulus, and particle size of the CDW aggregate are reported. The Los Angeles (LA) abrasion test is generally performed for construction aggregate to analyze its resistance to abrasion and degradation. Concrete CDW has an LA abrasion loss in the range 28–43%, and brick CDW in the range 31–42%. Comparing these values with those of natural aggregate (near 25% [154], CDW values are generally lower than natural aggregates. Concrete CDW also has a higher specific gravity than brick CDW. Concerning the particle size (last column of Table 15), it is possible to use the coarse fraction (4.5–25.4 mm, FM6) directly and the fine fraction (<2–4 mm, FM2-3) without grinding or heating them, with a reduction in cost and environmental burden. The quality of the final product is strictly connected with the physical and chemical properties of the CDW. For example, if the CDW is composed mainly of concrete, the type of cement, water-to-cement ratio, age of concrete, and quality of the natural aggregate will affect the quality of the final CDW and the compressive strength of the recycled concrete. Concrete powders can also be granulated to create new lightweight aggregates, e.g., Kursala [155]. Adding 30% of ladle slag reached a crushing strength of 127 N for aggregates cured in a humidity chamber (20 °C and 100% relative humidity). This granulating process is composed of different steps. First of all, concrete waste is crushed into smaller pieces (2–16 mm), and later they are sieved. Pieces inferior to 4.75 mm are dried and ground using a vibrator disk mill for 2 min. The ladle slags are added with the concrete powder into a granulator with a rotating drum that agglomerates the powders in the shape of small balls (5–8 mm).

Table 13. Chemical composition of CDW aggregate present in the literature.

Author	Year	CDW	Chemical Component (wt%)													
			SiO_2	Al_2O_3	Fe_2O_3	MgO	CaO	K_2O	Na_2O	P_2O_5	SO_3	TiO_2	MnO	ZnO	LOI	Ot
Bui [142]	2018	concrete	62.56	12.52	5.82	1.83	12.01	1.30	2.69	–	–	0.62	0.12	–	–	–
Panizza [143]	2018	concrete	38.03	5.01	1.80	12.21	39.88	1.06	0.74	0.07	–	0.23	0.06	–	31.3	–
De Rossi [144]	2019	concrete	75.40	19.73	0.93	0.64	10.37	0.99	0.13	–	0.46	0.17	–	–	6.48	–
De Rossi [144]	2019	concrete	69.51	0.75	1.07	0.75	15.41	0.99	0.14	–	0.71	0.20	–	–	6.35	–
Ren [53]	2020	concrete	64.81	7.77	1.59	1.54	19.14	2.94	1.76	–	–	0.45	–	–	–	–
Pawluczuk [19]	2021	concrete	24.39	5.86	1.87	2.31	27.56	1.09	0.34	0.28	1.47	0.31	0.06	–	–	0.10
Panizza [143]	2018	brick	63.00	15.14	5.03	3.22	8.52	2.57	1.00	0.11	-	0.79	0.08	–	6.66	-
De Rossi [144]	2019	brick	58.253	19.73	6.45	2.44	3.29	4.16	0.28	–	0.11	0.78	–	–	3.87	–
Zhu [145]	2020	geopolymer	32.60	20.50	3.10	–	2.00	–	9.00	–	–	0.78	–	–	29.6	0.30

Table 14. Minerals detected in CDW aggregate using XRD.

Author	Year	CDW	Minerals Detected with XRD																			
			Q	C	D	Po	Al	Mc	Ms	An	Hm	Hr	Ba	Mu	Mi	Fe	Cl	Di	Ph	G	E	A	B	Am
Nuaklong [146]	2016	concrete	•	•	•	•																		
Panizza [143]	2018	concrete	•	•	•		•	•	•	•							•			•	•			•
Pawluczuk [19]	2021	concrete	•	•	•	•	•					•									•			
Panizza [143]	2018	brick	•	•	•		•	•	•	•	•							•		•				•
De Rossi [144]	2019	brick	•	•					•															
El-Seidy [147]	2024	brick	•						•															
Reig [137]	2017	ceramic	•				•							•				•						
El-Seidy [147]	2024	geopolymer	•	•																				
Volpintesta [148]	2023	mix	•	•									•		•	•								•

mix = mix of various CDWs; Q = quartz; C = calcite; D = dolomite; Po = portlandite; Al = albite; Mc = microcline; Ms = muscovite; An = anorthite; Hm = hematite; Hr = hatrurite; Ba = bassanite; Mu = mullite; Mi = micas; Fe = feldspars; Cl = clinochlore; Di = diopside; Ph = phillipsite; G = gypsum; E = ettringite; A = alite; B = belite; Am = amorphous phase; • = present.

As studied by Thomas [156], it is not possible to recycle concrete an infinite number of times. The analysis with computerized axial tomography shows that in the 5th generation of recycled concrete, the coarse natural fraction of the recycled aggregate turns to sand, creating a product much more similar to mortar than concrete. In addition, a great number of fissures due to shrinkage appear. Concerning physical properties, a loss of density and an increase in the closed porosity in multi-recycled aggregates were observed. Chemical analysis also revealed that multi-recycled aggregates have a higher amount of Al and Fe. These two aspects (the loss of density and the increase in Al and Fe) are a consequence of the increase in the volume of the adhered mortar between the natural aggregate and the paste.

Table 15. Properties of CDW aggregates.

Author	Year	CDW	Los Angeles Abrasion Loss (%)	Specific Gravity	FM	Particle Size (mm)
Sata [149]	2013	concrete	43.3	2.53		4.5–9.5
Nuaklong [146]	2016	concrete	38.0	2.32	6.0	4.5–9.5
Bui [142]	2018	concrete		2.62	2.55	<12.5
Nuaklong [150]	2018	concrete	38.8	2.30	6.0	4.5–9.5
Panizza [143]	2018	concrete				< 2
Nuaklong [151]	2019	concrete		2.63	3.06	<4
Xie [152]	2019	concrete		2.27	2.7	5–20
Ren [53]	2020	concrete		2.27	2.2	0.075–2.36
Wang [153]	2020	concrete		2.27		2–20
Pawluczuk [19]	2021	concrete		2.50–2.53		4–8 8–16
Robayo-Salazar [118]	2022	concrete	28.2	2.32		<25.4
Sata [149]	2013	brick	42.4	2.02		4.5–9.5
Reig [137]	2017	brick			2.86–4.94	2–4
Panizza [143]	2018	brick				< 2
Roy [93]	2024	brick	31.4		2.42	<2
Ojha [154]	2020	mix	34	2.50	6.7	<20
Robayo-Salazar [88]	2020	mix	33.65	2.32		<25.4
Robayo-Salazar [88]	2020	mix		2.03	3.04	<4.76
Robayo-Salazar [118]	2022	mix		2.20	3.17	<4.76
Tefa [94]	2025	mix		2.59		<25

FM = Fineness modulus.

6.2. Mechanical, Thermal, and Chemical Treatments

Mechanical and thermal treatments can be performed to remove the hydrated cement from the surface of the aggregate (old adhered mortar). The main treatments applied to CDW aggregates are reported in Table 16 [19,53,88,93,94,118,137,142,143,146,149,150,152,154,157–159]. The main mechanical treatments are: presoaking in water (also with ultrasonic bath, this method removes only small amount of mortar), autogenous cleaning (crushing milling with balls inside as for Los Angeles abrasion test, but this process can create micro-cracks on the aggregate), steel ball milling, impact crushing (impact roller crusher with forced air fan), eccentric shaft rotor (circular eccentric cylinders) and screw abrading mill (two cones that scrub and abrade). Thermal treatments are performed both with high temperature (<500 °C) or low temperature (using freeze–thaw cycles to remove the adhered mortar), with or without the addition of microwaves or using electro-hydraulic pulse/sonic discharge (for big concrete chunks) [160]. Acid treatments (with sulfuric acid, hydrochloric acid, phosphoric acid, acetic acid) have problems with environmental pollution [161]. Instead recent chemical treatments tested are: the use of solutions to remove the adhered mortar (HCl, H_2SO_4, $C_2H_4O_2$ and CH_3COOH [162]), accelerated carbonation (achieving a densification of the microstructure from 2.45 to 2.51 g/cm^3) [162], coating the surface (e.g., with pozzolanic materials, OPC, fly ash [163], silica gel, silane-based polymers or lithium silicate coating [164]), bacterial bio-deposition (S. pasteurii bacteria to precipitate $CaCO_3$) and spraying with nano-silica suspensions [162] or a

combination of them [160,163,165,166]. The combination of thermal and mechanical treatment increases the compressive strength (best performance with heat treatment at 350 °C for 1 h followed by a 15 min mechanical treatment [157]). Pawluczuk [19] tested fly ash mortars and concrete with treated recycled aggregate from concrete waste treated with a thermal and mechanical patented process (PAT229887), summarized in Table 16. The concrete is crushed until 40 mm and later heated at 650 °C for 1 h. The aggregate is finally placed in a Los Angeles drum to separate adhered mortar from aggregate and is then sieved in three fractions (0–4 mm, 4–8 mm, 8–16 mm). Different percentages of natural and recycled aggregate were tested at different curing temperatures and molarities of the activators. The replacement of 100% of natural aggregate with recycled aggregate increased the mechanical strength for 10 M activating solution and 80 °C for 24 h of curing temperature, thanks to the formation of C-S-H and C-A-S-H on the ITZ and to the free lime present on the surface of the recycled aggregate. The final product also showed a decrease in water absorption (-12.6% for 6 M with temperature increase from 40 °C to 80 °C, −18.5% for 10 M with temperature increase from 40 °C to 80 °C). Bui [142] also tested a pre-treatment procedure where recycled aggregates are soaked in a sodium silicate solution for 1 h at 20 °C, dried, and coated with a silica fume and cement (3–7%) layer. With this process, an increase near to 50% of compressive strength was reached. Xie [159] tested different calcination temperatures to improve CDW coming from the renovation of an old highway, finding an improvement at 400 °C for 2 h and 30 min. Shahidan [158] covered concrete aggregate with epoxy resin to reduce water absorption, finding that the compressive strength value is affected even by the dimension of the recycled aggregate. In particular, the size of 10 mm gave the best results (41 MPa versus 33 MPa for 20 mm), also in terms of reduced water absorption (4.5% versus 5.6% for 20 mm). Anyway, these processes are quite expensive, increasing the final product cost, and can be problematic from a sustainability perspective. For this reason, and to reduce the energy consumption of the production process, recycled aggregates are usually only washed, dried, and then crushed (Table 16).

Table 16. Treatments performed on CDW aggregates.

Author	Year	CDW	Treatments
Sata [149]	2013	concrete	crushed and sieved
Al-Bayati [157]	2016	concrete	pre-soaking in a solution HCl and $C_2H_4O_2$ for 24 h at 20 °C
Al-Bayati [157]	2016	concrete	heating at different temperatures (250 °C, 350 °C, 500 °C, 750 °C) for 1 h
Al-Bayati [157]	2016	concrete	thermal heating at 350 °C and mechanical treatment
Nuaklong [146]	2016	concrete	crushed and sieved
Shahidan [158]	2017	concrete	covered with epoxy resin
Bui [142]	2018	concrete	sodium silicate 10% for 1 h at 20 °C, coated in SF
Nuaklong [150]	2018	concrete	crushed and sieved
Panizza [143]	2018	concrete	crushed and sieved
Xie [152]	2019	concrete	manually sorted, cleaning with high-pressure water jet
Ren [53]	2020	concrete	crushed and sieved
Wang [153]	2020	concrete	crushed and sieved
Pawluczuk [19]	2021	concrete	thermal (650 °C, 1 h) and mechanical treatment (Los Angeles drum)
Robayo-Salazar [118]	2022	concrete	crushed and sieved
Xie [159]	2024	old highway CDW	calcination (200 °C 400 °C 600 °C 800 °C) for 2 h 30 min
Xie [159]	2024	old highway CDW	carbonation with pure CO_2 at 400 kPa for 3 h, 6 h, 12 h, 24 h
Sata [149]	2013	brick	crushed and sieved
Reig [137]	2017	brick	crushed and sieved
Panizza [143]	2018	brick	crushed and sieved
Roy [93]	2024	brick	crushed and sieved
Ojha [154]	2020	mix	crushed and sieved
Robayo-Salazar [88]	2020	mix	crushed and sieved
Robayo-Salazar [118]	2022	mix	crushed and sieved
Tefa [94]	2025	mix	crushed and sieved

6.3. Carbonation of CDW Aggregate

As seen in Section 3.5, concrete-based CDW can be carbonated to increase the amount of calcium carbonate. The main methods are gas–solid (CO_2 curing, flow-through, pressurized carbonation) and liquid-solid carbonation (more effective) [167]. It is also possible to treat CDW aggregate, achieving an increase in the consistency of mortars, in the slump of concrete, in the final compressive strength (+14% and +17%), in the apparent density, and consequently a decrease in water absorption (−38% and −48%) and in the open porosity. This method is also very useful for capturing CO_2 and storing it. Carbonation is an exothermic chemical reaction connected to the diffusion of CO_2 through the matrix pores, with alkaline elements that can be performed in air but also in water, and it may be preceded by some pre-treatments before CO_2 curing [168]. This process should also be considered in terms of additional costs since the impact of energy and work could increase the price of the final carbonated recycled aggregate. The carbonation process with a previous impregnation of the recycled aggregate in a calcium hydroxide emulsion for 60 min can increase the final compressive strength compared to the same carbonation process without impregnation and to coating treatments (with OPC or OPC and FA). Considering the chloride ion penetration, the slurry coating treatment had a higher decrease in ion migration (32–37%) compared to the carbonation process (15–26%) due to an increase in tortuous path [169]. Xie [159] tested different times of exposition to pure CO_2 at 400 kPa to improve the formation of calcite, densifying the old adhered mortar attached to the surface of the aggregate in CDW coming from the renovation of an old highway, finding an improvement for 3–6h. Calcium carbonate can coat the surface of the recycled aggregate also with the bio-deposition technique [170] based on bacteria (Bacillus pseudofirmus) able to induce the precipitation of $CaCO_3$ during respiration.

6.4. Role of the Interfacial Transition Zone

When CDW replaces the natural aggregate, the most significant problem is the formation of the interfacial transition zone (ITZ) between the recycled aggregate and the new cement or alkali-activated paste because, in this area, the old adhered mortar is still present on the surface of CDW, and it can create micro-cracks and fissures. The physical properties of the wastes (e.g., the open porosity and the density) can be a problem, in particular if the wastes are composed of bricks. If CDW has high values of open porosity and low values of density, even the final product will show insufficient values of compressive strength, low durability, and a decrease in workability [171]. To improve the fresh properties of the recycled concrete, it is possible to use additives as superplasticizers.

The ITZ between geopolymer binder and recycled CDW aggregate has lower bond strength for a higher water-to-solid (w/s) ratio for fly ash/recycled aggregate and greater bond strength for OPC/recycled aggregate owing to the more porous microstructure of the geopolymer [172]. Anyway, the geopolymer mortars with recycled aggregate showed a higher bond strength (1.3 MPa for w/s equal to 0.3 and 0.9 MPa for w/s equal to 0.4) compared to natural aggregate (0.6 MPa for w/s equal to 0.3 and 0.8 MPa for w/s equal to 0.4) at the same curing time and water-to-solid ratio. This can be explained by the fact that recycled aggregate absorbs more alkaline solution, leaving a smaller quantity in the geopolymer. Furthermore, this alkaline solution absorbs and dissolves Si, Al, and Ca from the recycled concrete aggregate, giving a beneficial effect to geopolymerization. Comparing the OPC and geopolymer interfacial transition zone, it is possible to observe more cracks in OPC that cause the entrance of sulfates and chlorides, decreasing the durability of the final product. Instead, the matrix of geopolymer is denser than OPC and less microstructurally distinct from the bulk of the binder region [173,174].

6.5. Role of Type of Aggregate

Panizza [143] replaced natural aggregate with recycled concrete and brick waste in mortars with metakaolin and commercial furnace slag as precursors activated with KOH solution. Different parameters were tested in this research: type of waste, curing temperature, waste amount, and dimension of the aggregate. Concerning the waste type, brick aggregates, thanks to their residual pozzolanic reactivity, achieved the best performance despite their higher open porosity. Similar results were achieved by Reig [137], who prepared different recipes using either tile waste as precursor activated with NaOH and sodium silicate, or mixed ceramic wastes (coming from bricks, tiles, and sanitaryware) as aggregate with natural sand (quartz and calcium carbonate). Comparing the values of the aggregates of the same type, the results of compressive strength are: quartz 10 MPa, calcium carbonate 32 MPa, sanitaryware 17 MPa, bricks 26 MPa, and tiles 23 MPa. Since tile waste is very porous, it is necessary to pre-saturate it with water before being mixed as aggregate.

The presence of CDW aggregate (<2mm) decreases the density, but for aggregate dimension ranges 0.5–1.0 mm and 0.5–2.0 mm, the compressive strength is higher than sand-based mortars (respectively, 21 MPa and 40 MPa) [144]. This increase can be explained by chemical reactions between the non-hydrated cement in concrete waste or pozzolanic reactivity in brick waste.

6.6. Role of Percentage of Replacement

In concrete made with metakaolin and GGBS activated by potassium silicate, an inverse proportion is observed between the strength and the recycled aggregate percentage (−20% with 50% of aggregate and −55% with 60% of aggregate) [143]. For 40% and 50% of replacement no great difference is observed between concrete and clay brick waste (near to 90 MPa for 40% and 75–80 MPa for 50%), but with a 60% of replacement pure clay bricks give lower strength loss (−45% equal to 50 MPa instead of −55% equal to 45 MPa). In particular, the replacement with brick waste demands more water than concrete waste (+11%) due to its higher porosity. In terms of particle size distribution, fine aggregates (<0.25 mm) need more water to achieve sufficient workability, increasing the porosity of the final product. Similar conclusions were achieved even when adding fly ash to metakaolin and furnace slag [175]. For fine concrete powder (20% of finer particles are <0.25 mm) composed of calcite and 40% of amorphous OPC paste, the presence of Ca-rich components (due to calcite) reacting with alkaline reagent decreases workability, making it necessary to add water to the mixture. This also reduces the compressive strength and increases the open porosity (60% of CDW aggregate 28.7 MPa–19.0 MPa) [148]. Similar conclusions can be achieved for mortars with metakaolin, fly ash, and NaOH as activating solutions instead of KOH [144].

Metakaolin mortars achieved a compressive strength decrease near to 50% replacing 25% of natural aggregate with concrete waste aggregate [176]. Also for fly ash geopolymer concrete, the increase in CDW aggregate causes a detriment in the mechanical properties, e.g., a replacement of 50% with CDW aggregate has a compressive strength value after 28 days equal to 36.8 MPa; instead, using a lower amount of CDW aggregate (15%), a compressive strength equal to 41.8 MPa is obtained [177]. Even the indirect tensile strength and the elastic modulus show the same behavior: respectively, 3.7 MPa and 14 GPa with 50% of CDW, 4.1 MPa and 20 GPa with 15% CDW. The presence of ITZ, cracks, and fissures during the grinding process affected the properties of the CDW aggregate.

Roy [93] prepared mortars with GGBS and recycled brick powder as precursors and a mix of standard sand and brick waste (<2 mm) as aggregates with different molarities of the NaOH solution (3–4–6 M) and different aggregate replacement. With a 6 M activating solution, a geopolymeric concrete was also prepared by adding coarse brick waste

(4.75–12.5 mm and 12.5–20 mm). For all the molarity, there was an inverse proportion between the percentage of brick aggregate and the compressive strength; in particular, with 40% of replacement, the lowest value was reached. The compressive strength of geopolymer concrete with brick waste was equal to 10.5 MPa, a low value compared to traditional OPC concrete, due to the presence of coarse brick aggregate and also to the low molarity of the activating solution (usually 8–10 M).

A 100% geopolymer concrete was created using CDW both as precursor (mix of bricks, roof tiles, glass, and concrete with size < 100 μm) and aggregate (only concrete waste with maximum grain size 16 mm) to produce reinforced beams. The addition of recycled aggregate gave strength values similar to natural aggregate (near 36 MPa), but the effect on displacement capacities was significant (+30%), as for normalized energy dissipation capacity (−30%). In particular, a secondary ITZ formation was observed in samples with recycled concrete aggregate due to the old adhered mortar that reduced the flexural capacity, postponing the shear crack [54]. For share-span to effective depth ratio equal to 0.50 and 1.0 the failure mechanism of geopolymer concrete with recycled aggregate is similar to OPC concrete with natural aggregate (shear mechanism in a brittle way), instead for share-span to effective depth ratio equal to 1.65 the addition of recycled aggregate caused an increase in shear-dominated failure mechanism compared to the other ones with a mixed shear-flexure cracks [77]. The displacement ductility decreased, too. Instead, both geopolymer and OPC concrete with natural aggregate have similar failure behavior for a share-span to effective depth ratio equal to 1.65 [77].

CDW aggregates were even used to prepare roller-compacted geopolymer concrete [166]. This particular product is drier than traditional concrete, and it must be compacted after placement since it has a slump close to zero; it also has a reduced amount of cement (200 kg/m^3). This geopolymeric version with fly activated by NaOH and CDW aggregate showed compressive strength values near 20–27 MPa.

To test the possibility of reusing a geopolymer concrete in the creation of a new alkali-activated concrete, a first concrete was created with fly ash and GGBS, and river sand and basalt coarse aggregate. After 60 days of curing, concrete samples were crushed to obtain three size fractions of recycled aggregates (4.7–6.7 mm, 6.7–9.5 mm, 9.5–13.2 mm). These aggregates at different percentages (20–50–100%) were reused to create new geopolymeric concrete. An inverse proportion between the amount of geopolymer concrete waste and the compressive strength was found (until −12% for 100% replacement), but the same process repeated for OPC concrete gave lower results (−28% for 100% replacement), making recycled geopolymer concrete a potentially recyclable material for future applications [178].

7. Mix-Design and Mechanical Properties of Alkali-Activated Materials with CDW Aggregate

Table 17 [19,53,54,60,65,77,81,88,93,118,137,143–154,177] summarizes the mix-design tested in the literature when concrete CDW, ceramic CDW, geopolymer waste, and various CDW types are used as aggregate (both with CDW precursors or different types of precursors). As previously described in Section 1, the type of CDW is associated with different colors (green for concrete, red for bricks, pink for tiles, and gray for geopolymer waste). The box of the value of the percentage of aggregate replacement is colored using the same match when only one type of CDW is used. Instead, for a mix of CDW, the box is colored yellow. In the charts are also indicated the types of the precursor (CDW, MTK, FA, GGBS, and SF) and if a binary system was tested (with a black tick in the OPC box). In the "waste aggregate" window, the type of CDW aggregate tested is indicated (concrete, bricks, tiles, and geopolymer waste), and in the "activating solution" window, the type of silicate and the type and the molarity of the hydroxide are specified. Analyzing Table 17,

it is possible to observe that concrete waste is used for almost all the papers analyzed as a natural aggregate replacement. The reason can be found in the high porosity of brick waste, which can affect both the compressive strength and the durability of the composites. The main activating solution is composed of sodium silicate and sodium hydroxide with a molarity range of 8–20 M (but the most used values are 8 M and 10 M). Potassium silicate and potassium hydroxide were used by Panizza [143] and Volpintesta [148], instead of calcium hydroxide, which was tested by Akduman [54], Aldemir [77], and Reig [137] as an alternative to sodium silicate. In the bottom of Table 17, the aggregate size is indicated with the curing temperature. The aggregate size for sand replacement is 2 mm, and for coarse aggregate, seven papers used a maximum diameter in the range 16–25 mm. Comparing curing temperature, the range is 23–80 °C, but the environmental temperature is the most commonly used for curing. Comparing papers where only OPC [142,171] or OPC with FA [179] without activating solution are used as binders, it is possible to observe that the results of compressive strength achieved (near to 60 MPa) are similar to the alkali-activated precursors without OPC (40–80 MPa), confirming that the type of precursor does not affect the result as the percentage of aggregate replacement does.

In Tables 18 and 19 [19,53–60,65,77,81,88,93,118,137,143–154,177], the mix-design of the composite that achieved the highest value of compressive strength for each paper is reported (using the same color match applied for previous Tables). Table 18 reports the recipes with concrete CDW aggregate; instead, Table 19 the recipes with brick CDW aggregate, ceramic CDW aggregate, geopolymer waste aggregate, and a mix of various CDW types. The most used liquid-to-binder ratio is in the range 0.3–0.6, and for the binder-to-aggregate ratio, the most used values are 0.3–0.45. The replacement of natural aggregate with recycled CDW is tested, starting with low percentages (as 40% for Panizza [143]) until higher ones (70–100%). In particular, nine papers tested only recycled aggregate (100% replacement) [54,60,65,77,81,88, 144,149,151]. The curing temperature is another factor that affects the mechanical properties of the final product. Generally, the samples were stored at environmental temperature, but for six papers, higher temperatures were set (60 °C [149–151] and 80 °C [19,152,153]). If the value of compressive strength is reached using a mix of different CDW aggregates, the box is colored in yellow. Kul [81] and Reig [137] tested the possibility of creating a 100% CDW alkali-activated composite, reducing the environmental impact using CDW both as precursor and aggregate (Kul used a brick waste precursor and a concrete waste precursor; instead, Reig used ceramic waste for both uses). The compressive strength values achieved are, respectively, 65 MPa for Kul and 23 MPa for Reig. The value achieved by Kul is very high considering that it is a 100% CDW composite, and other mix-designs with other precursors (as GGBS, FA, or MTK) have lower values. The explanation can be found in the high curing temperature (115 °C), confirming that this parameter has a direct proportionality with the compressive strength achieved. The highest values are obtained by Panizza [143] with MTK and GGBS (88 MPa) and by Xie [152] with GGBS and FA (80 MPa).

Table 17. Main types of alkali-activated composites with CDW aggregates in recent papers.

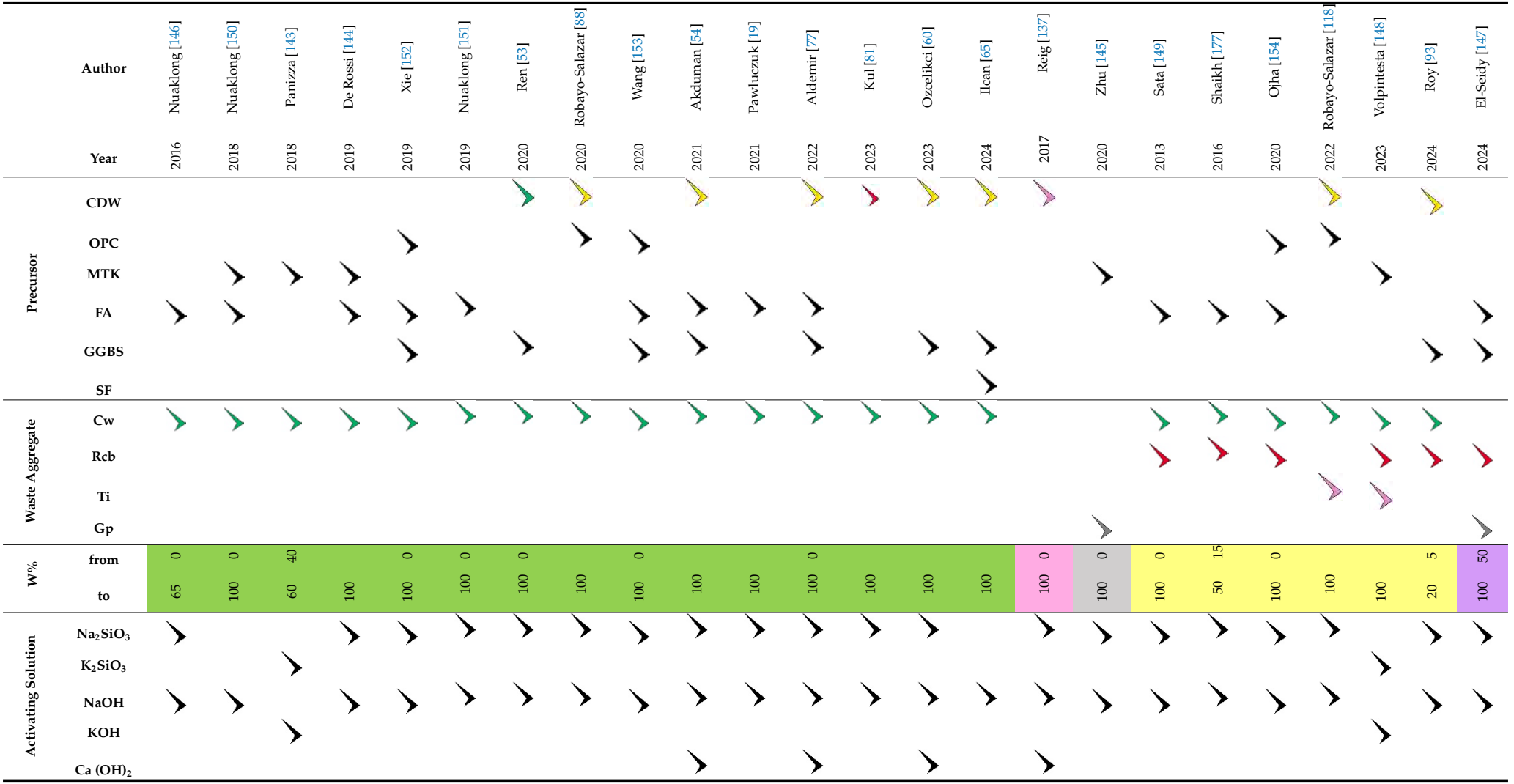

Table 17. *Cont.*

Author	Year	MoI. from	MoI. to	Aggregate size NS	Aggregate size Gp	Aggregate size Mix	Aggregate size Ti	Aggregate size Rcb	Aggregate size Cw	T (°C) from	T (°C) to
Nuaklong [146]	2016	12	16	2.6 MF–6.0 FM	-	-	-	-	6.0 FM 4.5–9.5 mm		23
Nuaklong [150]	2018		12	<−9.5 mm	-	-	-	-	4.5–9.5 mm		60
Panizza [143]	2018		10	-	-	-	-	<2 mm	<2 mm	20	60
De Rossi [144]	2019		10	-	-	-	-	-	0.5–1.0 mm 1.0–2.0 mm		23
Xie [152]	2019		8	5–20 mm	-	-	-	-	2–20 mm		80
Nuaklong [151]	2019		10	-	-	-	-	-	<4 mm		60
Ren [53]	2020			1.6 FM	-	-	-	-	<2.36 mm		25
Robayo-Salazar [88]	2020			-	-	-	-	-	3.04 FM <25 mm		25
Wang [153]	2020		8	2.7 FM 5–20 mm	-	-	-	-	2–20 mm	20	80
Akduman [54]	2021		8	-	-	-	-	-	<16 mm		23
Pawluczuk [19]	2021	6	10	<16 mm	-	-	-	-	<4.8 mm 8–16 mm	40	80
Aldemir [77]	2022		8	<16 mm	-	-	-	-	<16 mm		23
Kul [81]	2023	10	19	-	-	-	-	-	<5 mm	105	125
Ozcelikci [60]	2023	6	10	-	-	-	-	-	<2 mm		23
Ilcan [65]	2024	4	8	-	-	-	-	-	<4.75 mm		23
Reig [137]	2017			<4 mm	-	-	<4 mm	-	-	20	65
Zhu [145]	2020		12	2.59 FM <4.75 mm	2.59 FM <4.75 mm	-	-	-	-		80
Sata [149]	2013	10	20	4.5–9.5 mm	-	-	-	4.5–9.5 mm	4.5–9.5 mm	23	60
Shaikh [177]	2016		8	-	-	NSP	-	-	-		60
Ojha [154]	2020		10	6 3. FM <20 mm	-	6 7. FM <20 mm	-	-	-	23	65
Robayo-Salazar [118]	2022			-	-	-	<4.76 mm	-	<4.76 mm <25 mm		25
Volpintesta [148]	2023			-	-	<−2 mm	-	-	-		20
Roy [93]	2024	3	6	2.32 FM	-	<20 mm	-	2.42 FM	-		23
El-Seidy [147]	2024		10	0–0.5 mm 0.5–1 mm	1–2 mm	-	-	1–2 mm	-		60

Table 18. Mix-design with concrete CDW aggregates developed to achieve the maximum value of compressive strength and the tests performed.

Author	Year	Mix-Design					
		L/B	Mol.	AS	Prec.		
Sata [149]	2013	0.45	20	Na_2SiO_3 $NaOH$	100% FA		
Nuaklong [146]	2016	0.60	12	Na_2SiO_3 $NaOH$	100% FA		
Nuaklong [150]	2018	0.60	12	$NaOH$	80% FA, 20% MTK		
Panizza [143]	2018		10	K_2SiO_3 KOH	50% MTK, 50% GGBS		
De Rossi [144]	2019		10	Na_2SiO_3 $NaOH$	75% FA, 25% MTK		
Nuaklong [151]	2019	0.54	10	Na_2SiO_3 $NaOH$	100% FA		
Xie [152]	2019	0.30	8	Na_2SiO_3 $NaOH$	75% GGBS, 25% FA		
Ren [53]	2020	0.60		Na_2SiO_3 $NaOH$	80% GGBS, 20% Cw		
Robayo-Salazar [88]	2020	0.40		Na_2SiO_3 $NaOH$	10% OPc, 90% CDW		
Wang [153]	2020	0.68	8	Na_2SiO_3 $NaOH$	75% GGBS, 25% FA		
Akduman [54]	2021	0.55	8	Na_2SiO_3 $NaOH, Ca(OH)_2$	24% Rt, 14% Rcb, 19% Hb, 10% Gl, 9% Cw, 19% GGBS, 5% FA		
Pawluczuk [19]	2021	0.60	10	Na_2SiO_3 $NaOH,$	100% FA		
Aldemir [77]	2022	0.35	8	Na_2SiO_3 $NaOH, Ca(OH)_2$	25% Rt, 20% Rcb, 15% Hb, 10% Gl, 10% Cw, 15% GGBS, 5% FA		
Kul [81]	2023		10	$NaOH$	100% Rt		
Ozcelikci [60]	2023	0.70	6	Na_2SiO_3 $NaOH$ $Ca(OH)_2$	18% Hb, 14% Rcb, 24% Rt, 16% Cw, 20% GGBS, 8% Gl		
Ilcan [65]	2024	0.40	5	$NaOH$	55% Rcb, 15% Cw, 25% GGBS, 5% SF		

Table 18. *Cont.*

	Author	Sata [149]	Nuaklong [146]	Nuaklong [150]	Panizza [143]	De Rossi [144]	Nuaklong [151]	Xie [152]	Ren [53]	Robayo-Salazar [88]	Wang [153]	Akduman [54]	Pawluczuk [19]	Aldemir [77]	Kul [81]	Ozcelikci [60]	Ilcan [65]
	Year	2013	2016	2018	2018	2019	2019	2019	2020	2020	2020	2021	2021	2022	2023	2023	2024
Aggregate	Cw %	100	67 (100 coarse)	67	40	100	100	70 (100 coarse)	75	100	70 (100 coarse)	100	55 (100 coarse)	100	100	100	100
	Rcb %	-	-	-	-	-	-	-	-	-	-	-	-	-	-	-	-
	Ti%	-	-	-	-	-	-	-	-	-	-	-	-	-	-	-	-
	Mix %	-	-	-	-	-	-	-	-	-	-	-	-	-	-	-	-
	Gp %	-	-	-	-	-	-	-	-	-	-	-	-	-	-	-	-
	NS %	-	33	33	60	-	-	30	25	-	30	-	45	-	-	-	-
	B/A	0.12	0.30	0.30		0.33	0.40	0.45	0.25	0.40	0.22	1.00	0.20	1.00	2.22	2.80	1.00
	T (°C)	60	23	60	30	23	60	80	25	25	80	23	80	23	115	23	23
	σc max	10	38	45	88	40	47	80	46	44	45	37	60	37	65	52	25

Table 18. *Cont.*

	Author	Sata [149]	Nuaklong [146]	Nuaklong [150]	Panizza [143]	De Rossi [144]	Nuaklong [151]	Xie [152]	Ren [53]	Robayo-Salazar [88]	Wang [153]	Akduman [54]	Pawluczuk [19]	Aldemir [77]	Kul [81]	Ozcelikci [60]	Ilcan [65]
	Year	2013	2016	2018	2018	2019	2019	2019	2020	2020	2020	2021	2021	2022	2023	2023	2024
Tests Performed	Flow		✓	✓		✓	✓	✓		✓							✓
	σc−σf	✓	✓	✓	✓	✓	✓	✓	✓	✓	✓	✓	✓	✓	✓	✓	✓
	SEM EDX			✓		✓	✓	✓	✓	✓	✓		✓		✓	✓	✓
	XRD			✓		✓			✓	✓	✓		✓		✓	✓	
	FTIR																
	TGA DSC												✓			✓	
	Pe. Abs.	✓	✓	✓		✓			✓				✓			✓	✓
	Density	✓	✓			✓	✓										
	MIP BET															✓	
	Dur.	✓	✓	✓			✓	✓					✓			✓	✓

Table 19. Mix-design with various CDW aggregates developed to achieve the maximum value of compressive strength and the tests performed.

	Author	El-Seidy [147]	Roy [93]	Reig [137]	Zhu [145]	Shaikh [177]	Ojha [154]	Robayo-Salazar [118]	Volpintesta [148]	Roy [93]
	Year	2024	2024	2017	2020	2016	2020	2022	2023	2024
Mix-Design	Prec.	60% FA, 25% GGBS, (50% NS, 50% RA)	85% GGBS, 15% CDW	100% Ti	100% MTK	100% FA	100%FA	30% Cw, 30% Rcb, 30% Ti, 10% OPC	60% CDW Aggregate, 40% MTK	85% GGBS, 15% CDW
	AS	Na_2SiO_3 NaOH	Na_2SiO_3 NaOH	Na_2SiO_3 NaOH	Na_2SiO_3 NaOH	Na_2SiO_3 NaOH	Na_2SiO_3 NaOH	Na_2SiO_3 NaOH	K_2SiO_3 KaOH	Na_2SiO_3 NaOH
	Mol.	10	6	10	12	8	10			6
	L/B	0.40		0.45			0.30	0.40		0.40
Aggregate	Cw %	-	-	-	-	-	-	85	-	-
	Rcb %	50	20	-	-	-	-	-	-	11
	Ti%	-	-	100	-	-	-	15	-	-
	Mix %	-		-	-	15	60 (100coarse)	-	100	45
	Gp %	-	-	-	20	-	-	-	-	-
	NS %	50	80	-	80	85	40	-	-	44
	B/A	0.80	0.30	-	0.50	0.33	0.20	1.00	0.67	0.30
	T (°C)	60	23	65	80	60	65	25	70	23
	σc max	61	20	23	59	42	26	32	29	11

Table 19. *Cont.*

	Author	El-Seidy [147]	Roy [93]	Reig [137]	Zhu [145]	Shaikh [177]	Ojha [154]	Robayo-Salazar [118]	Volpintesta [148]	Roy [93]
	Year	2024	2024	2017	2020	2016	2020	2022	2023	2024
Tests Performed	Flow		✓							✓
	σc–σf	✓	✓	✓	✓	✓	✓	✓	✓	✓
	SEM EDX	✓	✓	✓	✓			✓		✓
	XRD	✓	✓	✓	✓				✓	✓
	FTIR				✓					
	TGA DSC									
	Pe. Abs.	✓	✓	✓	✓	✓		✓	✓	✓
	Density			✓						
	MIP BET									
	Dur.	✓				✓				

In the lowest part of Tables 18 and 19, the tests performed in each paper are reported. CDW aggregate is mainly characterized by XRD, FTIR, and chemical composition analysis. Since aggregate composition is one of the main factor affecting the properties of the composites, particularly their mechanical performances, XRD analysis and chemical composition of CDW are performed by almost all the reviewed studies. Fresh state properties (i.e., flow table test) are reported in only 9 out of the 25 analyzed papers. This type of test should be increased, given its importance to the construction sector and the recent introduction of 3D printing technologies. In particular, for this application, fresh state properties are crucial to prevent damage to the equipment and to ensure proper extrusion and deposition of the composite material. SEM-EDX analysis is performed in almost all studies, in particular to analyze the ITZ between the aggregate and the paste and to detect the presence of defects and microcracks that may influence mechanical properties. TGA and DSC analyses are performed on the composites to identify the presence of calcium aluminium silicates and carbonates; however, their use is limited among the considered studies, with only two employing this technique. Indeed, the presence of N-A-S-(H) and C-(A)-S-H phases in the composite materials is predominantly identified through XRD analysis, while only one study [145] additionally used FTIR analysis to confirm their presence. Mercury intrusion porosimetry (MIP) and Brauner–Emmet–Teller analysis are scarcely performed, even if the porosity of the recycled aggregate could affect the durability properties. Durability test on the final composite product should be increased, too. In particular, since CDW aggregates are generally more porous than natual aggregates, tests such as freeze-thaw cyclying and water absortion by capillary are crucial for evaluating the durability and environmental degradation of these materials. Acid attack resistance and chloride ion diffusion are especially important under aggressive exposure conditions. Comparing the different precursors for mortars with the same concrete waste as aggregate, metakaolin gives higher strength than fly ash, owing to the highly reactive surfaces of metakaolin

particles. The addition of metakaolin can also decrease the values of open porosity that are generally high for mortars with CDW as aggregate (−13%) [150].

8. Durability of Alkali-Activated Materials and CDW as Both Precursor and Aggregate

8.1. Comparison with OPC Concrete

In OPC concrete containing recycled fine aggregates coming from waste concrete, by increasing the amount of CDW also the shrinkage, chloride penetration, and permeability generally worsened [174]. An improvement of shrinkage (−14%), porosity (−25%), and chlorine penetration (−25%) can be achieved by replacing only 30% of natural aggregate with CDW, and for a higher curing time, thanks to the formation of more hydration compounds filling the voids of the microstructure [174]. For alkali-activated concrete, better durability properties are expected thanks to a denser matrix. For alkali-activated binders, increasing the molarity of the activating solution and the soluble silicates improves the binding capacity, but the presence of chloride salts can decrease the interfacial bond strength [173]. The treatment method adopted for recycled aggregate can improve the durability of the final product. Comparing five different CDW aggregate treatments (immersion in acetic acid alone or with rubbing, carbonation, immersion in acetic acid followed by carbonation, immersion in lime followed by carbonation) the immersion in lime followed by carbonation and the immersion in acetic acid with rubbing enhances the durability properties (−24% for chloride migration coefficient and only 10% of reduction in compressive strength after acid immersion) [180].

8.2. Open Porosity and Water Absorption

The type of precursor can affect the water absorption value. CDW precursors tend to have higher water demand, which increases the water absorption. The addition of more reactive precursors as GGBS, can improve the results thanks to its higher amount of Ca^{2+} ions available for the formation of C-A-S-H gel [65].

As previously seen (Section 4.5), the increase in the molarity of the activating solution led to a reduced amount of water in the mixture and a facilitated dissolution of the precursors that improves the geopolymerization of the matrix with a denser and more homogeneous structure (lower presence of voids, higher quality, and lower water absorption) [65,146] (Table 20 [60,65,83,93,135,146,151,177]). Among the different activating solutions, the combined use of NaOH and $Ca(OH)_2$ gave the lowest water absorption values. The highest ones are instead reached with NaOH and N_2SiO_3 [60] (Table 20). Water absorption is also increased by using CDW aggregate owing to the higher absorption value of recycled aggregate connected to the presence of cracks produced during the grinding and milling process [65]. In particular, in fly ash-based concrete with 50% of CDW as aggregate, the water absorption measured is 5.9%, and with 15% of CDW, it is 4.8% [177]. For 100% fly ash-based mortar, an increase equal to +30% was measured using only concrete CDW aggregate [151] (9.0% water absorption for 0% CDW and 13.4% water absorption for 100% CDW) (Table 20). Similar behavior was found by Roy [93] using brick waste as aggregate, since the recycled aggregates have higher water absorption than standard sand. In alkali-activated mortars obtained with only brick waste powder as precursor, similar conclusions were achieved by Maaze [83]. Higher molarity, creating a denser matrix, decreases the water absorption. Higher curing temperature, accelerating the polymerization process, creates a more compact matrix with lower permeability values. Higher SiO_2 and lower Na_2O percentages in the solution, forming a more robust network, reduce the water absorption too.

Table 20. Values of water absorption (WA) found in recent papers for pastes and mortars with CDW as precursors and aggregates.

Author	Year	Precursor	CDW Precursor %	Aggregate	CDW Aggregate %	Activators	Mol.	T (°C)	WA (%)
Nuaklong [146]	2016	FA	0	Cw NS	65	$NaSiO_3$ NaOH	8	60	11.2
Nuaklong [146]	2016	FA	0	Cw NS	65	$NaSiO_3$ NaOH	16	60	9.6
Nuaklong [151]	2019	FA	0	Cw	25	$NaSiO_3$ NaOH	10	60	11.1
Nuaklong [151]	2019	FA	0	Cw	100	$NaSiO_3$ NaOH	10	60	13.4
Ozcelikci [60]	2023	Mix GGBS	80	Cw	100	$NaSiO_3$ NaOH	10	23	6
Ozcelikci [60]	2023	Mix GGBS	80	Cw	100	$NaSiO_3$ NaOH $Ca(OH)_2$	10	23	4.5
Ilcan [65]	2024	Rcb Cw	100	Cw	100	NaOH	4	23	9
Ilcan [65]	2024	Rcb Cw	100	Cw	100	NaOH	8	23	4
Ilcan [65]	2024	Rcb Cw GGBS	75	Cw	100	NaOH	5	23	7
Maaze [83]	2024	Rcb	100	NS	-	$NaSiO_3$ NaOH $Ca(OH)_2$	10	60	11
Liu [135]	2024	Cw	100	NS	-	$NaSiO_3$ NaOH	10	20	18
Shaikh [177]	2016	FA	0	Cw Rcb NS	50	$NaSiO_3$ NaOH	8	60	5.9
Roy [93]	2024	Mix GGBS	15	Rcb	100	$KSiO_3$ KOH	6	23	18

FA = fly ash; GGBS = ground granulated blast-furnace slag; waste: Cw = concrete waste; Rcb = red clay brick; Mix = mix of various CDWs; Mol. = molarity; NS = natural sand; T (°C) = temperature of curing; WA = water absorption.

Water absorption can increase over time, too. This effect can be correlated with the increments in pore volume over time (observed even +20%) due to the formation of efflorescence that deteriorated the pore structure or to the drying shrinkage cracks [19,60,181,182].

Liu [135] found that, increasing the temperature of calcination of concrete waste precursor until 800 °C, the water absorption decreased (−52.18% equal to 8.5%). This result can be explained by the presence of CaO and C_2S, which create a denser microstructure.

8.3. Water Absorption by Capillary and Sorptivity

Sorptivity is strictly connected to water absorption; therefore, the same conclusions can be drawn. The increase in molarity of the activating solution gives lower absorption capacity [65] (Table 21 [65,93,146,177]). The same effect is reached with the addition of GGBS (or more reactive precursors). On the contrary, the addition of coarse CDW aggregate [146,177] or a higher amount of CDW precursor can increase the sorptivity, due to the presence of cracks in the coarse aggregate and higher water absorption for fine particles [65]. In particular, in fly ash geopolymer concrete with 50% of CDW as aggregate, the sorptivity measured was 0.033 $mm \cdot s^{-0.5}$, instead with 15% of CDW it was 0.023 $mm \cdot s^{-0.5}$ [177] (Table 21). A higher tortuosity of the pore network resulting from the addition of GGBS can reduce sorptivity. A similar effect can be achieved with the addition of silica fume, which fills the pores and provides a denser structure [65]. GGBS concrete exhibits a higher absorption rate than fly ash concrete, because secondary absorption (controlled by air voids) is higher than that of fly ash-based concrete. The initial absorption, which is controlled by capillary forces, is instead very similar [183]. High values of sorptivity were found by Roy [93], who prepared an alkali-activated concrete using as precursors GGBS with CDW powder and standard sand as aggregate, fine and coarse brick waste. These high values can be explained by the complete

replacement of coarse natural aggregate with brick waste, since other studies in the literature used a lower amount of waste aggregate [177,183] (Table 21).

Table 21. Values of sorptivity (SO) found in recent papers for pastes and mortars with CDW as precursors and aggregates.

Author	Year	Precursor	CDW Precursor %	Aggregate	CDW Aggregate %	Activators	Mol.	T (°C)	SO ($mm \cdot s^{-0.5}$)
Nuaklong [146]	2016	FA	0	Cw NS	65	$NaSiO_3$ NaOH	8	60	0.03
Nuaklong [146]	2016	FA	0	Cw NS	65	$NaSiO_3$ NaOH	16	60	0.02
Ilcan [65]	2024	Rcb Cw	100	Cw	100	NaOH	4	23	1.5
Ilcan [65]	2024	Rcb Cw	100	Cw	100	NaOH	8	23	0.4
Ilcan [65]	2024	Rcb Cw GGBS	75	Cw	100	NaOH	5	23	0.9
Shaikh [177]	2016	FA	0	Cw Rcb NS	50	$NaSiO_3$ NaOH	8	60	0.03
Roy [93]	2024	Mix GGBS	15	Rcb	100	$KSiO_3$ KOH	6	23	0.93

FA = fly ash; GGBS = ground granulated blast-furnace slag; waste: Cw = concrete waste; Rcb = red clay brick; Mix = mix of various CDWs; Mol. = molarity; NS = natural sand; T (°C) = temperature of curing; SO = sorptivity.

8.4. Wet-Dry and Freeze–Thaw Cycling Resistance

During freeze–thaw cycles (−22 °C for 4h, and 20 °C for 8 h in wet conditions) on alkali-activated mortars, cracks formed when the hydraulic pressure exceeded the tensile strength of the matrix, as water increases its volume by about 9%. In particular, after more than 25 cycles, the compressive strength decreased by about 12–17%. In contrast, during wet-dry cycles (+70 °C for 24 h, followed by a water bath at 20 °C for 24 h), the strength of the alkali-activated mortars increased, thanks to an improvement in hydration reaction with the formation of new crystals and gels [184]. To improve both the freeze–thaw and the wet-dry cycling resistance, it is possible to add slag to the alkali-activated composites. This addition can enhance the degree of polymerization, ensuring volumetric stability. The dimension of the recycled aggregate did not change the wet-dry resistance, as the NaOH molarity did. In contrast, for freeze–thaw cycling resistance, mixtures with higher molarity (8M) formed stronger gels that better resist the stresses caused by this kind of cycling [65]. The addition of coarse recycled aggregate can also have a detrimental effect on the final product due to its lower mechanical performance. Tests performed on mortars with concrete and brick waste as precursor (with a possible addition of GGBS and silica fume) and recycled concrete as aggregate show that using only CDW as precursor, a lower durability is expected compared to those with the addition of slag and silica fume. In particular, a high susceptibility to wet-dry cycling (near to 50% of strength loss) and freeze–thaw cycling (near to 24–29% of strength loss) was observed [65]. Instead Erol [86], testing mortars produced with ceramic waste as precursor (5–15%) with FA and GGBS and natural sand as aggregate found that after 100 freeze–thaw cycles the compressive strength loss was close to 23% and the weight loss decreased with the increase in the molarity and the amount of ceramic precursor (due to the fineness of the ceramic powder, making pores more impermeable). The inclusion of slag and silica fume improved durability, in particular, slags assure the maturity of polymerization and a volumetric stability, leading to reduced crack formation and better resistance to deterioration [65]. After 50 freeze–thaw cycles (−22 °C for 4h and 20 °C for 8 h in wet condition), alkali-activated mortars with higher amount of GGBS (30%) showed a lower bond strength loss (30%) compared to the ones with lower amount (10% GGBS loss near to 40%, 20% loss near to 45%). A similar conclusion can be achieved by comparing compressive strength loss (12% for 30% of GGBS) [184]. Silica fume, by reducing permeability and increasing mechanical strength, also improves durability, particularly under freeze–thaw cycles. On the contrary, increasing the size and

amount of recycled concrete aggregates, there is a decrease in the wet-dry and freeze–thaw cycling resistance [65]. During freeze–thaw cycles, an increase in the mass can be observed after an initial decrease, due to the humid environment filling degraded zones (cracks, fissures, and pores) and the occurrence of calcification and peeling on the surface of the sample with the formation of new reaction products [184].

8.5. Chloride Ion Penetration

Alkali-activated concrete exhibits better resistance to acid-sulfate attack and chloride penetration than OPC concrete [185]. However, these properties, including mechanical strength, are influenced by various parameters such as the raw material, curing conditions (temperature and humidity), the molarity of the solution, and the mass ratio of sodium silicate to sodium hydroxide solution (optimal at 2.5) [185]. For metakaolin-based mortar with concrete waste as precursor, the use of cement paste compared to concrete powder decreases the chloride ingress since cement paste has superior alkali-activated activity [98,99]. Chloride ion penetration is higher in alkali-activated concrete with recycled aggregate than in the same concrete with natural aggregate, due to the more accessible pore network of the attached old mortar in concrete waste, in which chloride ions can be transported [186]. For example, in fly ash-based concrete with 50% of CDW as aggregate, a chloride ion penetration of 25.5 mm was observed, whereas with 15% and 30% of CDW, it was 18.6 mm and 21.1 mm, respectively [177]. Comparing these values with the reference sample with natural aggregate, the measured increase in the chloride ion penetration was +67% for 15% of recycled aggregate, +90% for 30% of recycled aggregate, and +130% for 50% of substitution. A high value of molarity of NaOH solution [146] (Table 22 [98,99,135,146,177]) and an increase in Na_2SiO_3/NaOH ratio from 2.0 to 3.0 can reduce chloride ion penetration, owing to a reduction in deboning with the ITZ. The higher amount of dissolved Si and Al due to the higher NaOH concentration can achieve an improvement in the polycondensation and a reduction in porosity and chloride entrance [186]. According to studies performed on alkali-activated composites with a ratio of Na_2SiO_3/NaOH equal to 2.0 and 10–30% of recycled aggregate, during a test with the samples immersed in 3% NaCl solution, the charges measured were 2700 C (for 10% of recycled aggregate) and 3100 C (for 30% of recycled aggregate), respectively. Instead, for the same composites but with different ratios of Na_2SiO_3/NaOH (equal to 3.0), the charges passed for the same percentages of recycled aggregate were near 2400 C and 2700 C [186]. The depth of penetration of alkali-activated concrete after 120 days was 21.5 mm for natural aggregate and 20.9 mm for recycled aggregate [171]. A further reduction could be achieved by adding ultrafine slag, due to the formation of a denser microstructure [187]. In this case, the addition of ultrafine slag to geopolymeric concrete with recycled aggregate can achieve a reduction in chloride ion penetration close to 55% (7107 C for the reference sample with 50% of recycled aggregate, and 3100 C for the same percentage of recycled aggregate but with the addition of 30% of ultrafine slag [187]).

Table 22. Values of chloride ion penetration (CIP) found in recent papers for pastes and mortars with CDW as precursors and aggregates.

		Precursor	CDW Precursor %	Aggregate	CDW Aggregate %	Activators	Mol.	CIP (mm)
Nuaklong [146]	2016	FA	0	Cw NS	65	$NaSiO_3$ NaOH	8	45
Nuaklong [146]	2016	FA	0	Cw NS	65	$NaSiO_3$ NaOH	12	35

Table 22. *Cont.*

		Precursor	CDW Precursor %	Aggregate	CDW Aggregate %	Activators	Mol.	CIP (mm)
Nuaklong [146]	2016	FA	0	Cw NS	65	$NaSiO_3$ NaOH	16	21
Liu [99]	2023	Cw MTK	75	NS	0	$NaSiO_3$ NaOH		16–25
Liu [135]	2024	Cw MTK	100	NS	0	$NaSiO_3$ NaOH		14
Liu [98]	2022	Cw concrete	100	NS	-	$NaSiO_3$ NaOH	1.4	22
Liu [98]	2022	Cw mortar	100	NS	-	$NaSiO_3$ NaOH	1.4	20
Liu [98]	2022	Cw paste	100	NS	-	$NaSiO_3$ NaOH	1.4	8
Shaikh [177]	2016	FA	0	Cw Rcb NS	50	$NaSiO_3$ NaOH	8	25.5

FA = fly ash; MTK = metakaolin; Cw = concrete waste; Rcb = red clay brick; Mol. = molarity; NS = natural sand; CIP = chloride ion penetration.

8.6. Acid Attack

Alkali-activated concrete with natural aggregate is less sensitive to sulfuric acid attack than OPC concrete. Alkali-activated mortars with recycled concrete aggregate are more susceptible to acid attack due to the reaction between the acid present in the environment and the calcium compounds present in the old adhered mortar surrounding the aggregates [151]. In alkali-activated materials, the dissolution of silicates happens with a leaching process of non-framework alkaline ions and the removal of Al species via hydrolysis of Si-O-Al bonds. The effect of an acid attack is to increase the Al-OH, Si-OH group, H_4SiO_4 ions, and dimers in the solution. This process also causes a mass loss of the sample, particularly when GGBS was used as a precursor, due to the higher amount of Ca-rich gel in its products [184].

The acid attack of H_2SO_4 solution for alkali-activated mortars obtained with only recycled bricks as precursor showed lower weight loss and minimal compressive strength loss compared to traditional bricks; the main decay process is composed of the dissolution of the framework of alumino-silicate and the formation of gypsum. The acid solution creates sulfates, which break down into gypsum that later reacts with C-A-S-H, forming ettringite [183] and breaking down zeolitic compounds [83]. Acid attack also reduces the compressive strength of the composites, since it creates micro-cracks and voids in the geopolymer matrix, weakening the sample. Among the different kinds of acid attack (sodium chloride, sodium sulfate, sodium sulfate combined with magnesium sulfate, and sulfuric acid), sodium sulfate appeared to be the most aggressive for composites made with fly ash and GGBS due to the leaching of sodium hydroxide. During a sulfuric acid attack, a yellow layer appears on the surface of alkali-activated concrete. This product is mainly SO_2 coming from the reaction between Fe_2O_3 and H_2SO_4 that gives $Fe_2(SO_4)_3$ with three molecules of water. Comparing composites with an alkali-activated binder to those with a traditional OPC binder, sulfuric acid attack is more detrimental to OPC-based concrete. This effect can be measured by a decrease in compressive strength of 26% for OPC-based concrete, and only −11% and −7% for fly ash and GGBS, respectively [183]. In particular, OPC concrete, although it has a lower absorption rate, shows inferior durability when exposed to acid attack.

8.7. Efflorescence Formation

For alkali-activated materials, during curing, it is possible to observe the formation of efflorescence. Sodium plays an important role in the formation of this patina, due to its higher concentration compared to other cations. The unreacted alkali ions (mainly Na^+) coming from the activating solution migrate on the surface through pores and here reacting with atmospheric CO_2, they can form a white salt (efflorescence) composed of

sodium carbonate (Na_2CO_3, $Na_2CO_3 \cdot 7H_2O$, and $Na_2CO_3 \cdot 10H_2O$). These salts were found in many studies [60,65,176,181]. The efflorescence formation can also cause a decrease in strength owing to the decay of the alkali-activated matrix and to the leaching of alkalis and gels [65,183,184].

The addition of metakaolin in the mixture (rich in Al) decreases the amount of excessive alkalis through Al species introduction and N-A-S-H gel formation; instead, the addition of GGBS (rich in Ca) increases the C-A-S-H gel formation, reducing the migration of alkalis. Both the additions reduce the formation of efflorescence, but the addition of metakaolin gives better performance, since GGBS shows internal efflorescence formation with cracks due to higher pressure of crystallization [91,184].

Unfortunately, even a reduction in the molarity of the solution and the inclusion of Ca and Si-based precursors do not seem to completely solve the problem [65], but avoiding the use of Na_2SiO_3 seems to reduce the efflorescence formation too [60]. This decay process also depends on the availability of alkali metal cations in the system. SiO_2 present in Na_2SiO_3 reacts with free alkalis as Na^+ ions, forming weaker $Na(H_2O)^{n+}$ bonds that can easily be broken in a humid environment. If the lateral surface of the sample is covered with a plastic film, binders activated with sodium hydroxide have less efflorescence than those with sodium silicate due to the more compact pore structure achieved with the last one. If the lateral surface is exposed to air, the products activated with sodium hydroxide show efflorescence formation mainly on the bottom of the sample; instead, the ones with sodium silicate have a greater amount of efflorescence than NaOH samples, mainly placed on the top of the sample. This can be explained by considering the sub-efflorescence present at the drying front in the middle of the sample. Since samples made with sodium silicate have higher capillary absorption capacity, moisture is moved upper as the drying line in the sample [181].

9. Discussion

Comparing the results present in the literature highlighted in Tables 10–12, Figure 6A–D, and Tables 18 and 19, it is possible to observe a great variability in the results, with a large range in compressive strength values. This variability is caused by multiple factors that affect the properties of the final product, including the percentage of recycled aggregate (Figure 6A), the fineness of CDW powder (Figure 6B), its chemical composition, silicate modulus (Figure 6C) and molarity of alkaline activators, liquid-to-solid ratio (L/S), curing temperature (Figure 6D) and curing age. The compressive strength has a linear proportion with the percentage of brick waste, driven by an increase in the surface area and higher silica and alumina reactivity that improve the gel formation [188,189]. Instead, concrete waste reduces the mechanical strength. Sometimes, in the literature, it is also possible to find that these parameters affect the geopolymeric product (e.g., for alkali dosage [68,69,76], for SiO_2/Al_2O_3 and Na_2O/SiO_2 molar ratio [50]) differently. For some parameters, such as curing temperature and heat treatment duration, there is a general agreement on their positive effect on improving the compressive strength, as there is also for a smaller precursor particle size. In Table 23 [18,49,64,66,131,143,144,149,190–195], the main parameters and their role in the mechanical strength and durability properties are reported. Tile and brick wastes are good precursors compared to concrete waste. Ceramic waste contains a higher amount of aluminosilicates than concrete waste. This implies that higher NaOH concentrations are needed to break the bonds of the available material during the activation process [190]. Regarding the effect of particle size of the raw CDW material on the mechanical properties, the higher surface area of finer fractions improves and accelerates geopolymerization. The SiO_2/Al_2O_3 and Na_2O/SiO_2 molar ratios depend on the chemical composition of CDW, and their influence depends on the type of precursor used. The silicate modulus and the

molarity of the solution increase the strength only if they are near the optimum value. The increase in alkaline solution improves the polymerization process (dissolution, coagulation, and condensation), creating a higher amount of N-A-S-H gel. For this reason, higher Na_2O concentration assures a higher amount of available Na^+ ions after the dissolution and is free to bond with Si^{4+} and Al^{3+} ions during the last two phases of the process of polymerization. The ability of silicates to bind gel structure is constrained when Na_2O concentration is higher than its optimum value [194]. Compressive strength increases mainly with a reduction in liquid-to-solid ratio and higher curing temperatures. Strength development occurs with a high degree of depolymerization of Si-O-Si and Si-O-Al bonds under the action of OH^-. A reduction in the liquid-to-solid ratio increases the concentration of OH^-. Higher temperature and longer time for thermal process provide more energy to break the chemical bonds, and a higher amount of reactive Si and Al monomers usable for polycondensation reaction [191]. The low influence of curing age on the final strength development is due to the fact that for alkali-activated materials, the development of compressive strength takes place in the first curing stage. Among CDW aggregates, concrete waste gives higher compressive strength thanks to its lower porosity and open absorption. Anyway, the use of CDW as aggregate reduces the mechanical properties compared to natural aggregate due to the presence of residual paste, microcracks in the ITZ, and porosity. The irregular shape of CDW aggregates creates larger voids and weaker interparticle interlock, creating a lower packing density and mechanical performance. An optimum water-to-binder ratio for CDW aggregate was found to be around 0.34, beyond which the excess of water can negatively affect matrix viscosity and disrupt geopolymerization [195]. The use of fine aggregate (<0.25 mm) can increase the water content to assure a suitable workability with a consequent increase in porosity and decrease in compressive strength (−15/17% [143]). The removal of fine fraction for brick waste seems to be detrimental due to the residual reactivity that might contribute to geopolymerization. Instead, the use of intermediate aggregate size (0.25–0.5 mm) for concrete waste has a beneficial effect.

A detailed survey for each country of the quantities of CDW and aluminosilicate waste suitable for alkaline activation is the first step for the development of a new sustainable economy based on AAM. A study of this kind was recently conducted for Italy by Ricciotti in [196]. The possibility of sorting and selecting the waste is another aspect to take into consideration to ensure a good quality of CDW. To achieve this goal, the involvement of industries and institutions is necessary. Finding the correct mix proportion tailored for the CDW at disposal is a complex process where a lot of experiments and tests should be performed. This problem could be solved by the creation of a database with the results present in the literature analyzed with artificial intelligence (AI) that can help the scientist in finding the perfect recipe, reducing the amount of tested samples and time spent in the research [191]. The algorithms collect the data considering 8 parameters: silicate modulus, percentage of Na_2O of alkaline activators, SiO_2/Al_2O_3 ratio, Na_2O/SiO_2 ratio, liquid-to-solid ratio, pretreatment temperature, heat treatment time, and temperature. These data are analyzed, and the final prediction is the result of different base learners (ensemble learning models) according to the relevant rules. Ensemble learning is composed of bagging and boosting base learners. All the data are divided into a training set (used to create the machine learning model) and a testing set (used to validate the model, calculating the error R). A recent study also used a new machine learning framework (T-BoostNet) designed for superior accuracy based on 1117 recipes [197]. This model integrates Transformer-based feature extraction with the regression capabilities of XGBoost. The most influential parameters that affect the mechanical properties are ranked with Shapley Additive explanations (SHAP) to optimize mix-design. This model is actually based on fly ash-based recipes. The possibility of integrating it with the use of CDW could be an interesting

development for new eco-friendly concrete. A possible protocol that provides for the use of these technologies to correctly formulate the optimal recipe is proposed here in Figure 7. Since the formulation of CDW-based mortars or concretes requires specific skills and specialized instruments to characterize the CDW and test the samples, this process cannot be carried out by many companies in the construction industry. Therefore, the real application of CDW often remains merely theoretical. The role of institutions in this sector should be strengthened to create a sustainable cycle in which all the companies wishing to participate in CDW recycling are supported by a standardized procedure and a national laboratory capable of identifying tailored recipes for each CDW. This is necessary, given the high variability of CDW, which is the main cause of differences in compressive strength and durability performance. The dialogue between industry and researchers should be promoted by institutions with new agencies and benefits. In this way, many countries could achieve the goal of reducing CDW landfilling and creating a new economy with new, highly skilled jobs. The recent development of the 3D printing technique makes the study of the rheological behavior and the fresh state properties of AAM with CDW important to formulate new recipes suitable for this apparatus. A first survey was recently performed by Mahmoodi and Kul in [198,199]. To develop this new sector in a sustainable way, the role of institutions is necessary. It is becoming increasingly important to develop national and international legislation regulating the use of these new eco-friendly concretes in the construction industry.

Table 23. Role of the main parameters in the development of mechanical strength and durability.

Parameter	Value	Optimal Value Author	Year	Influence on Strength and Durability
Type of CDW precursor	brick-tiles	Komnitsas [49]	2015	+ brick-tiles − concrete
		Cantero [64]	2024	
		Retamal-Rojas [190]	2025	
Particle size dimension of precursor	<140 µm	Komnitsas [49]	2015	–
		Alhawat [18]	2022	
Silicate modulus	1.4%	Shen [191]	2022	+ near the optimal value − for higher/lower value
Molarity of alkaline activator	9 M	Gorhan [192]	2014	+ near the optimal value − for higher/lower value
		Ouda [193]	2020	
Na_2O%/precursor	10–13%	Neves [194]	2025	+ near the optimal value − for higher/lower value
SiO_2/Al_2O_3 ratio	7–12	Shen [191]	2022	0
		Mahmoodi [131]	2021	
		Kul [66]	2024	
Na_2O/SiO_2 ratio	0.17–0.24	Shen [191]	2022	0
		Mahmoodi [57]	2022	
Liquid/solid ratio	0.3	Shen [191]	2022	–
		Kul [66]	2024	
Treatment temperature	80–100 °C	Shen [191]	2022	+
		Mahmoodi [131]	2021	
Heat treatment time	24 h-48 h	Shen [191]	2022	+
		Kul [66]	2024	
Curing age	28 days	Shen [191]	2022	0
		Retamal-Rojas [190]	2025	
		Neves [194]	2025	

Table 23. *Cont.*

Parameter	Value	Optimal Value Author	Year	Influence on Strength and Durability
Type of recycled aggregate	concrete	Mahmoodi [195]	2025	+ concrete − brick-tiles
		Panizza [143]	2018	
		Sata [149]	2020	
Percentage of replacement for aggregate	always inferior to reference if >20%	Panizza [143]	2018	−
CDW aggregate dimension	0.5–2.0 mm	De Rossi [144]	2019	0

+ = direct proportion between the parameter, strength and durability; − = inverse proportion between the parameter, strength and durability; 0 = scarce effect on strength and durability; CDW = construction and demolition waste.

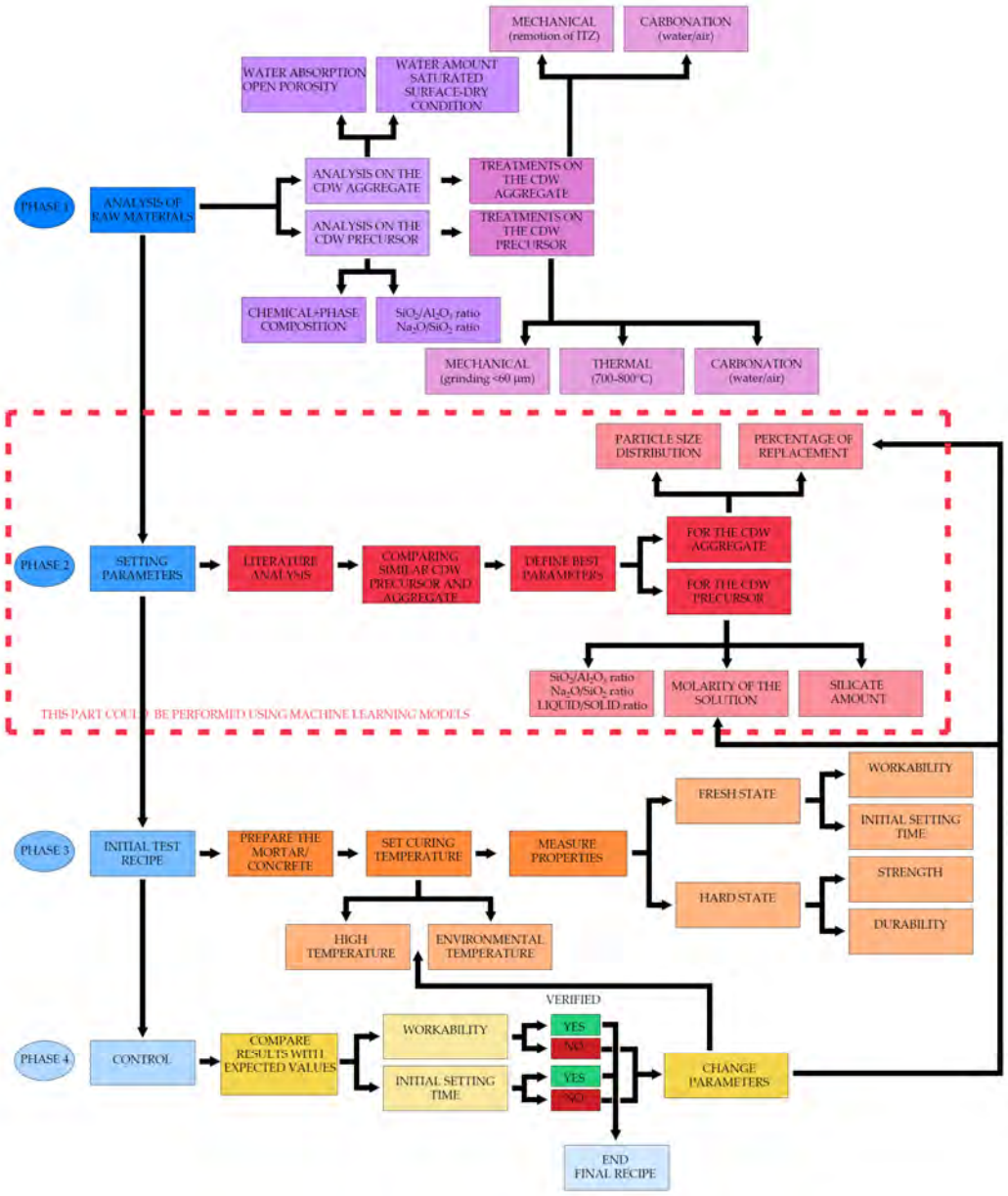

Figure 7. A possible protocol for the correct formulation of a mix-design for CDW-based alkali-activated mortar or concrete.

10. Conclusions

The production of CDW is constantly increasing, particularly in the megalopolises of countries with new emerging economies, where the demand for new buildings is higher.

This makes the reuse of CDW very possible and forces countries to regulate their production and management. The use of CDW as a precursor in the production of alkali-activated material also gives the opportunity to create new jobs in a new sector of the green economy. Based on the research available in the literature on the use of CDW as both precursor and aggregate, the following conclusions can be drawn:

- The main chemical constituents of the CDW are SiO_2, CaO, Al_2O_3, and Fe_2O_3, and their content can vary according to the waste origin.
- CDW can be subjected to mechanical (grinding) and thermal processes (600–900 °C) to improve its reactivity and to decrease its porosity, but the total cost should be calculated since it can make CDW uncompetitive.
- Carbonation can enhance the microstructure of concrete powder, reducing the porosity and increasing the formation of calcium aluminum hydrate products.
- The particle size plays an important role in making CDW a good precursor; the grinding process should be carried out carefully. Fine particles accelerate geopolymerization.
- Curing temperature influences the final properties of geopolymeric products; in particular, an increase in temperature improves the mechanical properties, creating a more compact matrix. High temperature is very important for the activation of low-Ca CDW precursors.
- Increasing the amount of CDW precursors generally decreases the mechanical properties and the workability.
- Mixing different types of CDW can optimize the reuse of CDW, but this heterogeneity can achieve different performances from those expected.
- Alkali-activated concretes can achieve compressive strength values close to traditional OPC concrete only if a previous mix-design is performed, starting from the characteristics of the CDW. In general, well-formulated alkali-activated concrete also has better durability than OPC concrete.
- The use of CDW as aggregate decreases the mechanical properties owing to the presence of cracks and fissures generated during the grinding process and to a higher open porosity compared to natural aggregate.

11. Future Directions

The use of CDW powders as precursors and aggregates in building materials is recognized as an optimal solution for creating a sustainable cycle for reusing construction waste, which is generally sent to landfill, causing significant environmental impact. To improve the use of CDW in alkali-activated materials and develop a new circular economy framework, it is important that members of the construction industry participate actively to propose strategies to create new sustainable business models and job opportunities, taking care of cost efficiency and environmental conservation. Anyway, the use of CDW as a precursor in alkali-activated materials is influenced by several parameters, including reactivity, chemical composition, particle size and dimensions, pre-treatments, SiO_2/Al_2O_3 and Na_2O/SiO_2 molar ratios, and water-to-solid ratio. Concerning their use as recycled aggregate, the main parameters are the nature and origin, the presence of old adhered mortar, chemical composition, open porosity, grinding process, presence of hazardous substances, and pre-treatments. Unfortunately, processes such as crushing, separation, and thermal or chemical treatments are energy-intensive and relatively expensive, increasing the final product costs. This price increase could make alkali-activated materials with CDW less attractive in the market, especially if the end user is already skeptical about using recycled material. For this reason, the management of CDW should be performed according to a proper protocol to improve the quality of the waste, separating from the beginning the different types of materials (concrete, hollow bricks, red clay bricks, tiles, glass, steel,

plastic) and removing the hazardous substances (asbestos as the first one). In this way, the separated waste could be better analyzed and selected according to its better application. After sorting, the waste should be sieved to separate the fine fraction (reusable as precursor) from the coarse fraction (reusable as aggregate). These two procedures (sorting and sieving) are relatively inexpensive, which is why they should always be carried out. The use of concrete waste powder as a precursor should be increased, since brick waste powder is actually more studied and used. In the studies present in the literature, many combinations of fly ash, metakaolin, and blast furnace slag with the addition of different kinds of CDW precursors are present, but the comparison among the results is difficult, owing to the different recipes, activating solution, molarity of the solution, curing temperature, type, and amount of aggregates. Sometimes it is difficult to perform a correct mix-design using CDW as alkali-activated materials, owing to all the different parameters previously described. Shen [191] tested three different machine learning models that, comparing the results in the literature, are able to predict the mechanical properties of alkali-activated mix-design. The creation of a global database with the results achieved in the literature could allow the creation of a software based on artificial intelligence that creates the best recipe according to the characteristics of the CDW at the client's disposal, leading to reduced costs and creating a real sustainable cycle in the construction sector. Further investigations should be conducted on the performance of CDW alkali-activated composite materials to identify the maximum replacement percentage for both the precursor and the aggregate without compromising the stability of structural elements. The growing number of publications on this topic should also raise awareness among legislators in the enactment of new laws regulating the use of this material in buildings and construction.

Supplementary Materials: The following supporting information can be downloaded at: https://www.mdpi.com/article/10.3390/buildings16020309/s1, Table S1. Chemical composition of CDW precursor present in literature. Figure S1. Summary of the percentage of replacement versus compressive strength, considering the mix-designs reported in Tables 10–12. Figure S2. Summary of the fineness versus compressive strength, considering the mix-designs reported in Tables 10–12. Figure S3. Summary of the curing temperature versus compressive strength, considering the mix-designs reported in Tables 10–12.

Author Contributions: Conceptualization, A.S. and S.M.; methodology, L.B.; validation, L.B.; data curation, L.B.; writing—original draft preparation, L.B.; writing—review and editing, L.B., A.S. and S.M.; visualization, L.B.; supervision, A.S. and S.M. All authors have read and agreed to the published version of the manuscript.

Funding: The authors acknowledge the financial support from PRIN2020–Sector PE8, Project code 2020WEFKX5_004. The authors also acknowledge financial support from the PNRR MUR project ECS_00000033_ECOSISTER.

Data Availability Statement: The authors declare the availability of the data reported in this paper.

Conflicts of Interest: The authors declare no conflicts of interest.

Abbreviations

The following abbreviations are used in this manuscript:

AAM	Alkali-Activated Materials
B/A	Binder-to-Aggregate ratio
BET	Brauner–Emmet–Teller instrument
BIM	Building Information Modeling
CDW	Construction and Demolition Waste

C-S-H	Calcium Silicate Hydrate
CIP	Chloride Ion Penetration
DSC	Differential Scanning Calorimetry
EU	Europe
FA	Fly Ash
FTIR	Fourier-Transform Infrared Spectroscopy
GGBS	Ground Granulated Blast-furnace Slag
L/B	Liquid-to-Binder ratio
MIP	Mercury Intrusion Porosimetry
MTK	Metakaolin
OP	Open Porosity
OPC	Ordinary Portland Cement
SEM-EDX	Scanning Electron Microscope Energy Dispersive X-ray spectroscopy
SF	Silica Fume
SO	Sorptivity
TGA	Thermogravimetry
UK	United Kingdom
USA	United States of America
WA	Water Absorption
XRD	X-Ray Diffraction
ρ_g	Bulk Density
σ_c (max) MPa	Maximum Value of Compressive Strength in MPa
σ_c	Compressive Strength Test
σ_f	Flexural Strength Test

References

1. WEF, World Economic Forum, High-Emitting Sectors: Challenges and Opportunities for Low-Carbon Suppliers. Insight Report. 2024. Available online: https://www.weforum.org/publications/high-emitting-sectors-challenges-and-opportunities-for-low-carbon-suppliers/ (accessed on 20 November 2025).
2. Khaiyum, M.Z.; Sarker, S.; Kabir, G. Evaluation of Carbon Emission Factors in the Cement Industry: An Emerging Economy Context. *Sustainability* **2023**, *15*, 15407. [CrossRef]
3. Nikolakopoulos, A.; Steriotis, T.; Charalambopoulou, G.; Karagiannakis, G.; Dimitrakis, D.; Michalis, V.; Katsiotis, M. Reducing carbon emissions in cement production through solarization of the calcination process and thermochemical energy storage. *Comput. Chem. Eng.* **2024**, *180*, 108506. [CrossRef]
4. IEA, International Energy Agency, Direct Emission Intensity of Cement Production in the Net Zero Scenario, 2015–2030. Available online: https://www.iea.org/data-and-statistics/charts/direct-emissions-intensity-of-cement-production-in-the-net-zero-scenario-2015-2030-2 (accessed on 20 November 2025).
5. Tiseo, I. Global CO_2 Emissions from Cement Manufacturing 1970–2023. Available online: https://www.statista.com/statistics/276480/world-carbon-dioxide-emissions-by-sector/?srsltid=AfmBOoq85-xnhQ2vqW_AFLJixsevKApycPhtaasYQAvIA0sauE0Zf8sM (accessed on 20 November 2025).
6. Andrew, R.M. Global CO_2 emissions from cement production, 1928–2018. *Earth Syst. Sci. Data* **2019**, *11*, 1675–1710. [CrossRef]
7. Marmier, A. *Decarbonisation Options for the Cement Industry, EUR 31378 EN*; Publications Office of the European Union: Luxembourg, 2023; ISBN 978-92-76-61599-6. [CrossRef]
8. Our World in Data, Annual CO_2 Emission from Cement. Data Source: Global Carbon Budget. 2024. Available online: https://ourworldindata.org/grapher/annual-co2-cement (accessed on 20 November 2025).
9. Chen, C.; Habert, G.; Bouzidi, Y.; Jullien, A. Environmental impact of cement production: Detail of the different processes and cement plant variability evaluation. *J. Clean. Prod.* **2010**, *18*, 478–485. [CrossRef]
10. Elahi, M.A.; Hossain, M.; Karim, R.; Zain, M.F.M.; Shearer, C. A review on alkali-activated binders: Materials composition and fresh properties of concrete. *Constr. Build. Mater.* **2020**, *260*, 119788. [CrossRef]
11. Velardo, P.; Sáez del Bosque, I.F.; Sánchez de Rojas, M.I.; De Belie, N.; Medina, C. Effect of incorporating biomass bottom ash and construction and demolition waste powder on the physical-mechanical properties and micro-structure of ternary-blended mortars. *Constr. Build. Mater.* **2024**, *432*, 136628. [CrossRef]
12. Huntzinger, D.N.; Eatmon, T.D. A life-cycle assessment of Portland cement manufacturing: Comparing the traditional process with alternative technologies. *J. Clean. Prod.* **2009**, *17*, 668–675. [CrossRef]
13. Luo, J.; Huang, R.; Wang, J.; Zhang, Y. Carbon sequestration by preparing recycled cement, recycled aggregates, and recycled concrete from construction and demolition (C&D) wastes. *Materials* **2024**, *17*, 5020. [CrossRef]
14. Eurostat, Waste Statistics, Statistics Explained Data Expected in September 2024. Available online: https://www.ec.europa.eu/eurostat/statistics-explained/index.php?title=Waste_statistics#Source_data_for_tables_and_graphs (accessed on 20 November 2025).

15. Soldati, L.; Bacciocchi, M.; Tarantino, A.M. Mechanical characterization of sustainable mortars with recycled aggregates from construction and demolition wastes: An experimental investigation. *Materials* **2024**, *17*, 5409. [CrossRef]
16. Zhang, M.; Li, W.; Wang, Z.; Liu, H. Urbanization and production: Heterogeneous effects on construction and demolition waste. *Habitat Int.* **2023**, *134*, 102778. [CrossRef]
17. An, R.; Guo, Y. Estimating construction and demolition waste in the building sector in China: Towards the end of the century. *Waste Manag.* **2024**, *190*, 285–295. [CrossRef]
18. Alhawat, M.; Ashour, A.; Yildirim, G.; Aldemir, A.; Sahmaran, M. Properties of geopolymers sourced from construction and demolition waste: A review. *J. Build. Eng.* **2022**, *50*, 104104. [CrossRef]
19. Pawluczuk, E.; Kalinowska-Wichrowska, K.; Jiménez, J.R.; Fernández-Rodríguez, J.M.; Suescum-Morales, D. Geopolymer concrete with treated recycled aggregates: Macro and microstructural behavior. *J. Build. Engin.* **2021**, *44*, 103317. [CrossRef]
20. Khan, S.A.; Kul, A.; Şahin, O.; Şahmaran, M.; Al-Ghamdi, S.G.; Koç, M. Energy-environmental performance assessment and cleaner energy solutions for a novel Construction and Demolition Waste-based geopolymer binder production process. *Energy Rep.* **2022**, *8*, 14464–14475. [CrossRef]
21. Wang, L.; Zhu, Z.; Xie, X.; Wu, J. Research trends in the treatment and recycling of construction and demolition waste based on literature data-driven visualization. *J. Envir. Manag.* **2024**, *371*, 123018. [CrossRef] [PubMed]
22. Moschen-Schimek, J.; Kasper, T.; Huber-Humer, M. Critical review of the recovery rates of construction and demolition waste in the European Union—An analysis of influencing factors in selected EU countries. *Waste Manag.* **2023**, *167*, 150–164. [CrossRef]
23. Eurostat, Country Factsheets on Construction and Demolition Waste Management. Available online: https://environment.ec.europa.eu/topics/waste-and-recycling/construction-and-demolition-waste_en (accessed on 20 November 2025).
24. Ilcan, H.; Sahin, O.; Kul, A.; Yildirim, G.; Şahmaran, M. Rheological properties and compressive strength of construction and demolition waste-based geopolymer mortars for 3D-Printing. *Constr. Build. Mater.* **2022**, *328*, 127114. [CrossRef]
25. Villaquirán-Caicedo, M.A.; de Gutiérrez, R.M. Comparison of different activators for alkaline activation of construction and demolition wastes. *Constr. Build. Mater.* **2021**, *281*, 122599. [CrossRef]
26. Xiao, R.; Zhang, Y.; Jiang, X.; Polaczyk, P.; Ma, Y.; Huang, B. Alkali-activated slag supplemented with waste glass powder: Laboratory characterization, thermodynamic modelling and sustainability analysis. *J. Clean. Prod.* **2021**, *286*, 125554. [CrossRef]
27. Ma, W.; Hao, J.L. Enhancing a circular economy for construction and demolition waste management in China: A stakeholder engagement and key strategy approach. *J. Clean. Prod.* **2024**, *450*, 141763. [CrossRef]
28. Farooq, F.; Xin, J.; Javed, M.F.; Akbar, A.; Shah, M.I.; Aslam, F.; Alyousef, R. Geopolymer concrete as sustainable material: A state of the art review. *Constr. Build. Mater.* **2021**, *306*, 124762. [CrossRef]
29. Jimenéz, J.R.; Ayuso, J.; Agrela, F.; López, M.; Galvín, A.P. Utilization of unbound recycled aggregates from selected CDW in unpaved rural roads. *Resour. Conserv. Recycl.* **2012**, *58*, 88–97. [CrossRef]
30. Otasowie, K.; Aigbavboa, C.; Oke, A.; Adekunle, P.; Ayorinde, E. Diverse approaches to construction and demolition waste reuse: A case of South Africa. *Eng. Proc.* **2024**, *76*, 2. [CrossRef]
31. Lee, S.; Chang, H.; Lee, J. Construction and demolition waste management and its impacts on the environment and human health: Moving forward sustainability enhancement. *Sustain. Cities Soc.* **2024**, *115*, 105855. [CrossRef]
32. Komnitsas, K. Potential of geopolymer technology towards green buildings and sustainable cities. *Procedia Eng.* **2011**, *21*, 1023–1032. [CrossRef]
33. Tam, V.W.Y.; Soomro, M.; Evangelista, A.C.J. A review of recycled aggregate in concrete applications (2000–2017). *Constr. Build. Mater.* **2018**, *172*, 272–292. [CrossRef]
34. Communication from the Commission to the Council, the European Parliament, the European Economic and Social Committee and The Committee of the Regions—Taking Sustainable Use of Resources Forward—A Thematic Strategy on the Prevention and Recycling of Waste {SEC(2005) 1681} {SEC(2005) 1682}, Document 52005DC0666. Available online: https://eur-lex.europa.eu/legal-content/EN/TXT/?uri=celex:52005DC0666 (accessed on 20 November 2025).
35. Directive (EU) 2008/98/EC of the European Parliament and of the Council of 19 November 2008 on Waste and Repealing Certain Directives. Available online: https://eur-lex.europa.eu/legal-content/EN/TXT/PDF/?uri=CELEX:02008L0098-20180705 (accessed on 20 November 2025).
36. Directive (EU) 2018/851 of the European Parliament and of the Council of 30 May 2018 Amending Directive 2008/98/EC on Waste (Text with EEA Relevance), Document 32018L0851. Available online: https://eur-lex.europa.eu/eli/dir/2018/851/oj/eng (accessed on 20 November 2025).
37. Yi, Y.; Liu, J.; Lavagnolo, M.C.; Manzardo, A. Evaluating the carbon emission reduction in construction and demolition waste management in China. *Energy Build.* **2024**, *324*, 114932. [CrossRef]
38. Cudecka-Purina, N.; Kuzmina, J.; Butkevics, J.; Olena, A.; Ivanov, O.; Atstaja, D. A comprehensive review on construction and demolition waste management practices and assessment of this waste flow for future valorization via energy recovery and industrial symbiosis. *Energies* **2024**, *17*, 5506. [CrossRef]

39. Saad, M.; Ruparathna, R.; Biswas, N.; Tam, E. Developing a reclamation framework to promote circularity in demolition projects. *Recycling* **2024**, *9*, 114. [CrossRef]
40. Martin, H.; Chebrolu, D.; Chadee, A.; Brooks, T. Too good to waste: Examining circular economy opportunities, barriers, and indicators for sustainable construction and demolition management. *Sust. Prod. Consump.* **2024**, *48*, 460–480. [CrossRef]
41. Caro, D.; Lodato, C.; Damgaard, A.; Cristóbal, J.; Foster, G.; Flachenecker, F.; Tonini, D. Environmental and socio-economic effects of construction and demolition waste recycling in the European Union. *Sci. Total Environ.* **2024**, *98*, 168295. [CrossRef]
42. Lins, E.J.M.; Palha, R.P.; Sobral, M.d.C.M.; Araújo, A.G.d.; Marques, É.A.T. Application of building information modelling in construction and demolition waste management: Systematic review and future trends supported by a conceptual framework. *Sustainability* **2024**, *16*, 9425. [CrossRef]
43. Awad, R.; Budayan, C.; Gurgun, A.P. Construction and demolition waste generation prediction by using artificial neural networks and metaheuristic algorithms. *Buildings* **2024**, *14*, 3695. [CrossRef]
44. Nguyen, H.P.; Mueller, A.; Nguyen, V.T.; Nguyen, C.T. Development and characterization of lightweight aggregate recycled from construction and demolition waste mixed with other industrial by-products. *Constr. Build. Mater.* **2021**, *313*, 125472. [CrossRef]
45. Communication from the Commission to the European Parliament, the European Council, The Council, the European Economic and Social Committee and The Committee of the Regions, The European Green Deal, Document 52019DC0640. Available online: https://eur-lex.europa.eu/legal-content/EN/TXT/?uri=celex:52019DC0640 (accessed on 20 November 2025).
46. Xu, H.; van Deventer, J.S.J. The geopolymerization of alumino-silicate minerals. *Int. J. Miner. Process.* **2000**, *59*, 247–266. [CrossRef]
47. Leonelli, C.; Palomo, A. Chemistry and materials science of alkali-activated materials. Alkali-activated materials. In *Environmental Technology Applications*; Woodhead Publishing Series in Civil and Structural Engeneering; Woodhead Publishing: Cambridge, UK, 2022; pp. 13–40. [CrossRef]
48. Kaliyavaradhan, S.K.; Ling, T.C.; Mo, K.H. Valorization of waste powders from cement-concrete life cycle: A pathway to circular future. *J. Clean. Prod.* **2020**, *268*, 122358. [CrossRef]
49. Komnitsas, K.; Zaharaki, D.; Vlachou, A.; Bartzas, G.; Galetakis, M. Effect of synthesis parameters on the quality of construction and demolition wastes (CDW) geopolymers. *Adv. Powder Technol.* **2015**, *26*, 368–376. [CrossRef]
50. Vásquez, A.; Cárdenas, V.; Robayo, R.A.; de Gutiérrez, R.M. Geopolymer based on concrete demolition waste. *Adv. Powder Technol.* **2016**, *27*, 1173–1179. [CrossRef]
51. Zaharaki, D.; Galetakis, M.; Komnitsas, K. Valorization of construction and demolition (C&D) and industrial wastes through alkali activation. *Constr. Build. Mater.* **2016**, *121*, 686–693. [CrossRef]
52. Robayo-Salazar, R.A.; Rivera, J.F.; de Gutiérrez, R.M. Alkali-activated building materials made with recycled construction and demolition wastes. *Constr. Build. Mater.* **2017**, *149*, 130–138. [CrossRef]
53. Ren, P.; Li, B.; Yu, J.G.; Ling, T.C. Utilization of recycled concrete fines and powders to produce alkali-activated slag concrete clocks. *J. Clean. Prod.* **2020**, *267*, 122115. [CrossRef]
54. Akduman, Ş.; Kocaer, O.; Aldemir, A.; Şahmaran, M.; Yildirim, G.; Almahmood, H.; Ashour, A. Experimental investigations on the structural behaviour of reinforced geopolymer beams produced from recycled construction materials. *J. Build. Eng.* **2021**, *41*, 102776. [CrossRef]
55. Huo, W.; Zhu, Z.; Chen, W.; Zhang, J.; Kang, Z.; Pu, S.; Wan, Y. Effect of synthesis parameters on the development of unconfined compressive strength of recycled waste concrete powder-based geopolymers. *Constr. Build. Mater.* **2021**, *292*, 123264. [CrossRef]
56. Liang, G.; Liu, T.; Li, H.; Wu, K. Shrinkage mitigation, strength enhancement and microstructure improvement of alkali-activated slag/fly-ash binders by ultrafine waste concrete powder. *Compos. Part B* **2022**, *231*, 109570. [CrossRef]
57. Mahmoodi, O.; Siad, H.; Lachemi, M.; Dadsetan, S.; Sahmaran, M. Optimized application of ternary brick, ceramic and concrete wastes in sustainable high strength geopolymers. *J. Clean. Prod.* **2022**, *338*, 130650. [CrossRef]
58. Wang, H.; Wang, L.; Shen, W.; Cao, K.; Sun, L.; Wang, P.; Cui, L. Compressive strength, hydration and pore structure of alkali-activated slag mortars integrating with recycled concrete powder as binders. *J. Civil. Eng.* **2022**, *26*, 795–805. [CrossRef]
59. Boros, A.; Erdei, G.; Korim, T. Development of alkali activated inorganic foams based on construction and demolition wastes for thermal insulation applications. *Materials* **2023**, *16*, 4065. [CrossRef] [PubMed]
60. Ozcelikci, E.; Kul, A.; Gunal, M.F.; Ozel, B.F.; Yildirim, G.; Ashour, A.; Sahmaran, M. A comprehensive study on the compressive strength, durability-related parameters and microstructure of geopolymer mortars based on mixed construction and demolition waste. *J. Clean. Prod.* **2023**, *396*, 136522. [CrossRef]
61. Sasui, S.; Kim, G.; Nam, J.; Alam, S.F.; Eu, H.; Lee, Y.; Ahmad, M. Alkali activation of waste concrete powder: Effects of alkali type and concentration. *Ceram. Int.* **2023**, *49*, 16260–16271. [CrossRef]
62. Wan, X.; Li, H.; Che, X.; Xu, P.; Li, C.; Yu, Q. A study on the application of recycled concrete powder in alkali-activated cementitious system. *Processes* **2023**, *11*, 203. [CrossRef]
63. Zhang, B.; Feng, Y.; Xie, J.; Dai, J.; Chen, W.; Xue, Z.; Li, L.; Li, Y.; Li, J. Effects of pretreated recycled powder substitution on mechanical properties and microstructures of alkali-activated cement. *Constr. Build. Mater.* **2023**, *406*, 133360. [CrossRef]

64. Cantero, B.; Neves, R.; Sequeira, L.; de Brito, J.; Bravo, M. Optimisation of the performance of alkali-activated mortars using CDW binders from different sources. *Constr. Build. Mat.* **2024**, *442*, 137677. [CrossRef]
65. Ilcan, H.; Demirbaş, A.O.; Ulugöl, H.; Şahmaran, M. Low-alkali activated construction and demolition waste-based geopolymers. *Constr. Build. Mater.* **2024**, *411*, 134546. [CrossRef]
66. Kul, A.; Ozcelikci, E.; Ozel, B.F.; Ilcan, H.; Sahin, O.; Gunal, M.F.; Yildirim, G.; Sahmaran, M. Optimizing mechanical performance of geopolymers produced from construction and demolition waste: A comparative study of materials from different origins. *Constr. Build. Mater.* **2024**, *426*, 136171. [CrossRef]
67. Sasui, S.; Kim, G.; van Riessen, A.; Alam, S.; Nam, J.; Ishak, S.; Eu, H. Influence of elevated temperature on waste concrete powder and its application in alkali activated materials. *J. Clean. Prod.* **2024**, *434*, 140423. [CrossRef]
68. Reig, L.; Tashima, M.M.; Borrachero, M.V.; Monzó, J.; Cheeseman, C.R.; Payá, J. Properties and microstructure of alkali-activated red clay brick waste. *Constr. Build. Mater.* **2013**, *43*, 98–106. [CrossRef]
69. Robayo, R.A.; Mulford, A.; Munera, J.; de Gutiérrez, R.M. Alternative cements based on alkali-activated red clay brick waste. *Constr. Build. Mater.* **2016**, *128*, 163–169. [CrossRef]
70. Fořt, J.; Vejmelková, E.; Konakova, D.; Alblova, N.; Cachova, M.; Keppert, M.; Rovnaníková, P.; Cerný, R. Application of waste brick powder in alkali activated aluminosilicates: Functional and environmental aspects. *J. Clean. Prod.* **2018**, *194*, 714–725. [CrossRef]
71. Tuyan, M.; Andiç-Çakir, Ö.; Ramyar, K. Effect of alkali activator concentration and curing condition on strength and microstructure of waste clay brick powder-based geopolymer. *Compos. Part B* **2018**, *135*, 242–252. [CrossRef]
72. Hwang, C.L.; Yehualaw, M.D.; Vo, D.H.; Huynh, T.P. Development of high-strength alkali-activated pastes containing high volumes of waste brick and ceramic powders. *Constr. Build. Mater.* **2019**, *218*, 519–529. [CrossRef]
73. Kioupis, D.; Skaropoulou, A.; Tsivilis, S.; Kakali, G. Valorization of brick and glass CDWs for the development of geopolymers containing more than 80% of wastes. *Minerals* **2020**, *10*, 672. [CrossRef]
74. Wong, C.L.; Mo, K.H.; Alengaram, U.J.; Yap, S.P. Mechanical strength and permeation properties of high calcium fly ash-based geopolymer containing recycled brick powder. *J. Build. Engin.* **2020**, *32*, 101655. [CrossRef]
75. Migunthanna, J.; Rajeev, P.; Sanjavan, J. Investigation of waste clay brick as partial replacement of geopolymer binders for rigid pavement application. *Constr. Build. Mater.* **2021**, *305*, 124787. [CrossRef]
76. Ulugöl, H.; Kul, A.; Yildirim, G.; Sahmaran, M.; Aldemir, A.; Figueira, D.; Ashour, A. Mechanical and microstructural characterization of geopolymers from assorted construction and demolition waste-based masonry and glass. *J. Clean. Prod.* **2021**, *280*, 124358. [CrossRef]
77. Aldemir, A.; Akduman, S.; Kocaer, O.; Aktepe, R.; Şahmaran, M.; Yildirim, G.; Almahmood, H.; Ashour, A. Shear behavior of reinforced construction and demolition waste-based geopolymer concrete beams. *J. Build. Eng.* **2022**, *47*, 103861. [CrossRef]
78. Liang, G.; Luo, L.; Yao, W. Reusing waste brick powder as partial mineral precursor in eco-friendly binders: Reaction kinetics, microstructure and life-cycle assessment. *Resour. Conserv. Recycl.* **2022**, *185*, 106523. [CrossRef]
79. Giannopoulou, I.; Robert, P.M.; Sakkas, K.M.; Petrou, M.F.; Nicolaides, D. High temperature performance of geopolymers based on construction and demolition waste. *J. Build. Engin.* **2023**, *72*, 106575. [CrossRef]
80. Ilcan, H.; Sahin, O.; Unsal, Z.; Ozcelikci, E.; Kul, A.; Demiral, N.C.; Ekinci, M.O.; Şahmaran, M. Effect of industrial waste-based precursors on the fresh, hardened and environmental performance of construction and demolition wastes-based geopolymers. *Constr. Build. Mater.* **2023**, *394*, 132265. [CrossRef]
81. Kul, A.; Ozel, B.F.; Ozcelikci, E.; Gunal, M.F.; Ulugol, H.; Yildirim, G.; Sahmaran, M. Characterization and life cycle assessment of geopolymer mortars with masonry units and recycled concrete aggregates assorted from construction and demolition waste. *J. Build. Eng.* **2023**, *78*, 107546. [CrossRef]
82. de Castro Carvalho, I.; de Oliveira, G.T.; Kirchheim, A.P.; da Costa, H.N.; Bezerra Cabral, A.E. Utilization of red ceramic waste in the production of binary eco-friendly alkali-activated binder: Fresh and hardened state investigation. *Case Stud. Constr. Mat.* **2024**, *21*, e03681. [CrossRef]
83. Maaze, M.R.; Shrivastava, S. Development and performance evaluation of recycled brick waste-based geopolymer brick for improved physcio-mechanical, brick-bond and durability properties. *J. Build. Eng.* **2024**, *97*, 110701. [CrossRef]
84. Rakhimova, N.R.; Rakhimov, R.Z. Alkali-activated cements and mortars based on blast furnace slag and red clay brick waste. *Mater. Des.* **2015**, *85*, 324–331. [CrossRef]
85. Samadi, M.; Huseien, G.F.; Mohammadhosseini, H.; Lee, H.S.; Lim, N.H.A.S.; Tahir, M.M.; Alyousef, R. Waste ceramic as low cost and eco-friendly materials in the production of sustainable mortars. *J. Clean. Prod.* **2020**, *266*, 121825. [CrossRef]
86. Erol, F.; Al-Mashhadani, M.M.; Aygörmez, Y.; Nis, A. Effect of ceramic waste powder content and sodium hydroxide molarity on the residual mechanical strength of alkali-activated mortars. *Mater. Chem. Phys.* **2023**, *309*, 128403. [CrossRef]
87. Bassani, M.; Tefa, L.; Coppola, B.; Palmero, P. Alkali-activation of aggregate fines from construction and demolition waste: Valorisation in view of road pavement subbase applications. *J. Clean. Prod.* **2019**, *234*, 71–84. [CrossRef]

88. Robayo-Salazar, R.A.; Valencia-Saavedra, W.; de Gutiérrez, R.M. Construction and Demolition Waste (CDW) Recycling—As both binder and aggregates in Alkali-Activated Materials: A novel re-use concept. *Sustainability* **2020**, *12*, 5775. [CrossRef]
89. Moreno-Maroto, J.M.; Delgado-Plana, P.; Cabezas-Rodríguez, R.; de Gutiérrez, R.M.; Eliche-Quesada, D.; Pérez-Villarejo, L.; Galán-Arboledas, R.J.; Bueno, S. Alkaline activation of high-crystalline low-Al_2O_3 Construction and Demolition Wastes to obtain geopolymers. *J. Clea. Prod.* **2022**, *330*, 129770. [CrossRef]
90. Tan, J.; Cizer, Ö.; De Vlieger, J.; Dan, H.; Li, J. Impacts of milling duration on construction and demolition waste (CDW) based precursor and resulting geopolymer: Reactivity, geopolymerization and sustainability. *Resour. Conserv. Recycl.* **2022**, *184*, 106433. [CrossRef]
91. Tan, J.; Cizer, Ö.; Vandevyvere, B.; De Vlieger, J.; Dan, H.; Li, J. Efflorescence mitigation in construction and demolition waste (CDW) based geopolymer. *J. Build. Engin.* **2022**, *58*, 105001. [CrossRef]
92. Valencia-Saavedra, W.; Robayo-Salazar, R.A.; Mejía de Gutiérrez, R. Hybrid cements and construction elements based on alkaline activation with sodium sulfates from fly ash and construction and demolition waste. *Materials* **2023**, *16*, 6272. [CrossRef]
93. Roy, A.; Sadiqul Islam, G.M. Geopolymer using different size fractions of recycled brick-based mixed demolition waste. *Clean. Mater.* **2024**, *11*, 100224. [CrossRef]
94. Tefa, L.; Bianco, I.; Bassani, M. Stabilising CDW recycled aggregates with alternatives to Portland cement. *Constr. Build. Mater.* **2025**, *471*, 140705. [CrossRef]
95. Liu, M.; Wang, C.; Wu, H.; Yang, D.; Ma, Z. Reusing recycled powder as eco-friendly binder for sustainable GGBS-based geopolymer considering the effects of recycled powder type and replacement rate. *J. Clean. Prod.* **2022**, *364*, 132656. [CrossRef]
96. Cardoza, A.; Colorado, H.A. Alkali-activated cement manufactured by the alkaline activation of demolition and construction waste using brick and concrete wastes. *Open Ceram.* **2023**, *16*, 100438. [CrossRef]
97. Tang, Q.; Ma, Z.; Wu, H.; Wang, W. The utilization of eco-friendly recycled powder from concrete and brick waste in new concrete: A critical review. *Cem. Concr. Compos.* **2020**, *114*, 103807. [CrossRef]
98. Liu, M.; Wu, H.; Yao, P.; Wang, C.; Ma, Z. Microstructure and macro properties of sustainable alkali-activated fly ash mortar with various construction waste fines as binder replacement up to 100%. *Cem. Conc. Comp.* **2022**, *134*, 104733. [CrossRef]
99. Liu, M.; Hu, R.; Zhang, Y.; Wang, C.; Ma, Z. Effect of ground concrete waste as green binder on the micro-macro properties of eco-friendly metakaolin-based geopolymer mortar. *J. Build. Engin.* **2023**, *68*, 106191. [CrossRef]
100. Tan, J.; Cai, J.; Li, J. Recycling of unseparated construction and demolition waste (UCDW) through geopolymer technology. *Constr. Build. Mater.* **2022**, *341*, 127771. [CrossRef]
101. Gu, F.; Xie, J.; Vuye, C.; Wu, Y.; Zhang, J. Synthesis of geopolymer using alkaline activation of building-related construction and demolition wastes. *J. Clean. Prod.* **2023**, *420*, 138335. [CrossRef]
102. Xiao, J.; Ma, Z.; Tongbo, S.; Akbarnezhad, A.; Duan, Z. Mechanical properties of concrete mixed with recycled powder produced from construction and demolition waste. *J. Clean. Prod.* **2018**, *188*, 720–731. [CrossRef]
103. Kaptan, K.; Cunha, S.; Aguiar, J. A Review of the utilization of recycled powder from concrete waste as a cement partial replacement in cement-based materials: Fundamental properties and activation methods. *Appl. Sci.* **2024**, *14*, 9775. [CrossRef]
104. Xi, X.; Zheng, Y.; Zhuo, J.; Zhang, P.; Golewski, G.L. Influence of water glass modulus and alkali content on the properties of alkali-activated thermally activated recycled cement. *Constr. Build. Mater.* **2024**, *452*, 138867. [CrossRef]
105. Pommer, V.; Vejmelková, E.; Černý, R.; Keppert, M. Alkali-activated waste ceramics: Importance of precursor particle size distribution. *Ceram. Int.* **2021**, *47*, 31574–31582. [CrossRef]
106. Bu, C.; Tan, B.; Wu, Q.; Qiao, Y.; Sun, Y.; Yu, L.; Yang, Q. Activation method and reuse of waste concrete powder—A review. *Sustainability* **2023**, *15*, 5451. [CrossRef]
107. Zhang, D.; Zhang, S.; Huang, B.; Yang, Q.; Li, J. Comparison of mechanical, chemical, and thermal activation methods on the utilisation of recycled concrete powder from construction and demolition waste. *J. Build. Eng.* **2022**, *61*, 105295. [CrossRef]
108. Xu, J.; Kang, A.; Wu, Z.; Gong, Y.; Xiao, P. The effect of mechanical-thermal synergistic activation on the mechanical properties and microstructure of recycled powder geopolymer. *J. Clean. Prod.* **2021**, *327*, 129477. [CrossRef]
109. Wu, H.; Yang, D.; Ma, Z. Micro-structure, mechanical and transport properties of cementitious materials with high-volume waste concrete powder and thermal modification. *Constr. Build. Mater.* **2021**, *313*, 125477. [CrossRef]
110. Wu, H.; Xu, J.; Yang, D.; Ma, Z. Utilizing thermal activation treatment to improve the properties of waste cementitious powder and its newmade cementitious materials. *J. Clean. Prod.* **2021**, *322*, 129074. [CrossRef]
111. Vashistha, P.; Park, S.; Pyo, S. A review on sustainable fabrication of futuristic cementitious binders based on application of waste concrete powder, steel slag and coal bottom ash. *Int. J. Concr. Struct. Mater.* **2022**, *16*, 51. [CrossRef]
112. Mahmoodi, O.; Siad, H.; Lachemi, M.; Dadsetan, S.; Sahmaran, M. Development of normal and very high strength geopolymer binders based on concrete waste at ambient environment. *J. Clean. Prod.* **2021**, *279*, 123436. [CrossRef]
113. Ahmari, S.; Ren, X.; Toufigh, V.; Zhang, L. Production of geopolymeric binder from blended waste concrete powder and fly ash. *Constr. Build. Mater.* **2012**, *35*, 718–729. [CrossRef]

114. Capasso, I.; D'Angelo, G.; Fumo, M.; del Rio Merino, M.; Caputo, D.; Liguori, B. Valorisation of tuff and brick wastes by alkali activation for historical building remediation. *Materials* **2023**, *16*, 6619. [CrossRef]
115. Borrachero, M.V.; Payá, J.; Brito, S.; Segura, Y.P.; Soriano, L.; Tashima, M.M.; Monzó, J.M. Reusing construction and demolition waste to prepare alkali-activated cement. *Materials* **2022**, *15*, 3437. [CrossRef] [PubMed]
116. Moraes, J.C.B.; Tashima, M.M.; Akasaki, J.L.; Monzó, J.; Borrachero, M.V.; Soriano, L.; Payá, J. Effect of sugar cane straw ash (SCSA) as solid precursor and the alkaline activator composition on alkali-activated binders based on blast furnace slag (BFS). *Constr. Build. Mater.* **2017**, *144*, 214–224. [CrossRef]
117. Yang, X.; Zhang, Y.; Lin, C. Microstructure analysis and effects of single and mixed activator on setting time and strength of coal-gangue based geopolymers. *Gels* **2022**, *8*, 195. [CrossRef]
118. Robayo-Salazar, R.; Valencia-Saavedra, W.; Mejía de Gutiérrez, R. Reuse of powders and recycled aggregates from mixed construction and demolition waste in Alkali-Activated materials and precast concrete units. *Sustainability* **2022**, *14*, 9685. [CrossRef]
119. Robayo-Salazar, R.A.; Mejía-Arcila, J.M.; de Gutiérrez, R.M. Eco-efficient alkali-activated cement based on red clay brick wastes suitable for the manufacturing of building materials. *J. Clean. Prod.* **2017**, *166*, 242–252. [CrossRef]
120. Komnitsas, K.; Zaharaki, D. Geopolymerization: A review and prospects for the minerals industry. *Miner. Eng.* **2017**, *20*, 1261–1277. [CrossRef]
121. Kravchenko, E.; Lazorenko, G.; Jiang, X.; Leng, Z. Alkali-activated materials made of construction and demolition waste as precursors: A review. *Sustain. Mater. Technol.* **2024**, *39*, e00829. [CrossRef]
122. Patil, S.; Joshi, D.; Mangla, D.; Savvidis, I. Recent development in geopolymer concrete: A review. *Mater. Today Proc.* 2023, *in press*. [CrossRef]
123. Bassani, M.; Tefa, L.; Russo, A.; Palermo, P. Alkali-activation of recycled construction and demolition waste aggregate with no added binder. *Constr. Build. Mater.* **2019**, *205*, 398–413. [CrossRef]
124. Duxson, P.; Provis, J.L.; Lukey, G.C.; Mallicoat, S.W.; Kriven, W.M.; van Deventer, J.S.J. Understanding the relationship between geopolymer composition, microstructure and mechanical properties. *Colloids Surf. A Physicochem. Eng. Asp.* **2005**, *269*, 47–58. [CrossRef]
125. Allahverdi, A. Use of construction and demolition waste (CDW) for alkali-activated or geopolymer cements. In *Handbook of Recycled Concrete and Demolition Waste*; Elsevier: Amsterdam, The Netherlands, 2013; pp. 439–475. [CrossRef]
126. Yaseri, S.; Hajiaghaei, G.; Mohammadi, F.; Mahdikhani, M.; Farokhzad, R. The role of synthesis parameters on the workability, setting and strength properties of binary based geopolymer paste. *Constr. Build. Mater.* **2017**, *157*, 534–545. [CrossRef]
127. Fořt, J.; Vejmelková, E.; Keppert, M.; Rovnaníková, P.; Bezdička, P.; Černý, R. Alkaline activation of low-reactivity ceramics: Peculiarities induced by the precursors' dual character. *Cem. Conc. Comp.* **2020**, *105*, 103440. [CrossRef]
128. Tefa, L.; Bassani, M.; Coppola, B.; Palmero, P. Strength development and environmental assessment of alkali-activated construction and demolition waste fines as stabilizer for recycled road materials. *Constr. Build. Mater.* **2021**, *289*, 123017. [CrossRef]
129. Sharma, A.; Singh, P.; Kapoor, K. Utilization of recycled fine powder as an activator in fly ash based geopolymer mortar. *Constr. Build. Mater.* **2022**, *323*, 126581. [CrossRef]
130. Ye, T.; Xiao, J.; Duan, Z.; Li, S. Geopolymers made of recycled brick and concrete powder—A critical review. *Constr. Build. Mater.* **2022**, *220*, 127232. [CrossRef]
131. Mahmoodi, O.; Siad, H.; Lachemi, M.; Sahmaran, M. Synthesis and optimization of binary systems of brick and concrete wastes geopolymers at ambient environment. *Constr. Build. Mater.* **2021**, *276*, 122217. [CrossRef]
132. Servadei, F.; Natali Murri, A.; Papa, E.; Medri, V.; Landi, E. Thermal behavior of construction and demolition waste-based geopolymer. *Constr. Build. Mater.* **2024**, *452*, 138969. [CrossRef]
133. De Masi, R.F.; Ruggiero, S.; Russo, A.; Vanoli, G.P. Geopolymer-based insulated wall incorporating construction and demolition waste: Experimental assessment of thermo-physical behavior. *Energy Build.* **2024**, *322*, 114743. [CrossRef]
134. Wang, X.; Yurong, Y.; Tong, X.; Gong, Y. Investigation of mineral admixtures on mechanical properties of alkali-activated recycled concrete powders cement. *Buildings* **2022**, *12*, 1234. [CrossRef]
135. Liu, M.; Zhang, Y.; Wang, C.; Ma, Z. Reusing thermoactivated waste paste/concrete powder for sustainable alkali-activated materials: Effects of thermoactivated temperature. *Constr. Build. Mat.* **2024**, *437*, 136973. [CrossRef]
136. Elhadi, K.M.; Raza, A.; Ghazouani, N.; Yaqub, M.; Mabrouk, A. Material characterization of high-ductility geopolymer composites developed with industrial and construction & demolition wastes. *Mater. Lett.* **2025**, *382*, 137961. [CrossRef]
137. Reig, L.; Sanz, M.A.; Borrachero, M.V.; Monzó, J.; Soriano, L.; Payá, J. Compressive strength and microstructure of alkali-activated mortars with high ceramic waste content. *Ceram. Int.* **2017**, *43*, 13622–13634. [CrossRef]
138. Ding, Y.; Dai, J.G.; Shi, C.J. Mechanical properties of alkali-activated concrete: A state-of-the-art review. *Constr. Build. Mater.* **2016**, *127*, 68–79. [CrossRef]
139. Aydin, S.; Baradan, B. The effect of fiber properties on high performance alkali-activated slag/silica fume mortars. *Compos. Part B* **2013**, *45*, 63–69. [CrossRef]

140. Vilaplana, J.L.; Baeza, F.J.; Galao, O.; Alcocel, E.G.; Zornoza, E.; Garcés, P. Mechanical properties of alkali activated blast furnace slag pastes reinforced with carbon fibers. *Constr. Build. Mater.* **2016**, *116*, 63–71. [CrossRef]
141. Amran, Y.H.M.; Alyousef, R.; Alabduljabbar, H.; El-Zeadani, M. Clean production and properties of geopolymer concrete; A review. *J. Clean. Prod.* **2020**, *251*, 119679. [CrossRef]
142. Bui, N.K.; Satomi, T.; Takahashi, H. Mechanical properties of concrete containing 100% treated coarse recycled aggregate. *Constr. Build. Mater.* **2018**, *163*, 496–507. [CrossRef]
143. Panizza, M.; Natali, M.; Garbin, E.; Tamburini, S.; Secco, M. Assessment of geopolymers with Construction and Demolition Waste (CDW) aggregates as a building material. *Constr. Build. Mater.* **2018**, *181*, 119–133. [CrossRef]
144. De Rossi, A.; Ribeiro, M.J.; Labrincha, J.A.; Novais, R.M.; Hotza, D.; Moreira, R.F.P.M. Effect of the particle size range of construction and demolition waste on the fresh and hardened-state properties of fly ash-based geopolymer mortars with total replacement of sand. *Process Saf. Environ. Prot.* **2019**, *129*, 130–137. [CrossRef]
145. Zhu, P.; Hua, M.; Liu, H.; Wang, X.; Chen, C. Interfacial evaluation of geopolymer mortar prepared with recycled geopolymer fine aggregates. *Constr. Build. Mater.* **2020**, *259*, 119849. [CrossRef]
146. Nuaklong, P.; Sata, V.; Chindaprasirt, P. Influence of recycled aggregate on fly ash geopolymer concrete properties. *J. Clean. Prod.* **2016**, *112*, 2300–2307. [CrossRef]
147. El-Seidy, E.; Chougan, M.; Al-Noaimat, Y.A.; Al-Kheetan, M.J.; Ghaffar, S.H. The impact of waste brick and geo-cement aggregates as sand replacement on the mechanical and durability properties of alkali–activated mortar composites. *Results Eng.* **2024**, *21*, 101797. [CrossRef]
148. Volpintesta, F.; Ossoli, E.; Reggiani, A.; Stabile, P.; Santulli, C.; Paris, E. Geopolymers-based application for the up-cycling utilization of construction and demolition waste from the 2016 central Italy earthquakes. *Mater. Lett.* **2023**, *336*, 133849. [CrossRef]
149. Sata, V.; Wongsa, A.; Chindaprasirt, P. Properties of previous geopolymer concrete using recycled aggregates. *Constr. Build. Mater.* **2013**, *43*, 33–39. [CrossRef]
150. Nuaklong, P.; Sata, V.; Chindaprasirt, P. Properties of metakaolin-high calcium fly ash geopolymer concrete containing recycled aggregate from crushed concrete specimens. *Constr. Build. Mater.* **2018**, *161*, 365–373. [CrossRef]
151. Nuaklong, P.; Wongsa, A.; Sata, V.; Boonserm, K.; Sanjayan, J.; Chindaprasirt, P. Properties of high-calcium and low-calcium fly ash combination geopolymer mortar containing recycled aggregate. *Heliyon* **2019**, *5*, e02513. [CrossRef]
152. Xie, J.; Wang, J.; Rao, R.; Wang, C.; Fang, C. Effects of combined usage of GGBS and fly ash on workability and mechanical properties of alkali activated geopolymer concrete with recycled aggregate. *Compos. Part B* **2019**, *164*, 179–190. [CrossRef]
153. Wang, J.; Xie, J.; Wang, C.; Zhao, J.; Liu, F.; Fang, C. Study on the optimum initial curing condition for fly-ash and GGBS based geopolymer recycled aggregate concrete. *Constr. Build. Mater.* **2020**, *247*, 118540. [CrossRef]
154. Ojha, A.; Gupta, L. Comparative study on mechanical properties of conventional and geo-polymer concrete with recycled coarse aggregate. *Mater. Today Proc.* **2020**, *28*, 1403–1406. [CrossRef]
155. Kursula, K.; Perumal, P.; Ohenoja, K.; Illikainen, M. Production of artificial aggregates by granulation and carbonation of recycled concrete fines. *J. Mat. Cycles Waste Manag.* **2022**, *24*, 2141–2150. [CrossRef]
156. Thomas, C.; de Brito, J.; Cimentada, A.; Sainz-Aja, J. Macro and micro properties of multi-recycled aggregate concrete. *J. Clean. Prod.* **2020**, *245*, 118843. [CrossRef]
157. Al-Bayati, H.K.A.; Das, P.K.; Tighe, S.L.; Baaj, H. Evaluation of various treatment methods for enhancing the physical and morphological properties of coarse recycled concrete aggregate. *Constr. Build. Mater.* **2016**, *112*, 284–298. [CrossRef]
158. Shahidan, S.; Azim, M.; Azmi, M.; Kupusamy, K.; Zuki, S.S.M.Z.; Ali, N. Utilizing construction and demolition (C&D) waste as recycled aggregates (RA) in concrete. *Procedia Eng.* **2017**, *174*, 1028–1035. [CrossRef]
159. Xie, J.; Li, J.; Zhang, B.; Chen, W.; Zhong, H.; Yang, J.; Yu, T.; Feng, Y. Effects of pretreated recycled fine aggregates on the mechanical properties and microstructure of alkali-activated mortar. *Case Stud. Constr. Mater.* **2024**, *20*, e02819. [CrossRef]
160. Tam, V.W.Y.; Soomro, M.; Evangelista, A.C.J. Quality improvement of recycled concrete aggregate by removal of residual mortar: A comprehensive review of approaches adopted. *Constr. Build. Mater.* **2021**, *288*, 123066. [CrossRef]
161. Saravanakumar, P.; Abhiram, K.; Manoj, B. Properties of treated recycled aggregates and its influence on concrete strength characteristics. *Constr. Build. Mater.* **2016**, *111*, 611–617. [CrossRef]
162. Ibrahim, M.; Alimi, W.; Assaggaf, R.; Salami, B.A.; Oladapo, E.A. An overview of factors influencing the properties of concrete incorporating construction and demolition wastes. *Constr. Build. Mater.* **2023**, *367*, 130307. [CrossRef]
163. Wang, R.; Yu, N.; Li, Y. Methods for improving the microstructure of recycled concrete aggregate: A review. *Constr. Build. Mater.* **2020**, *242*, 118164. [CrossRef]
164. Tang, W.; Khavarian, M.; Yousefi, A.; Chan, R.W.K.; Cui, H. Influence of surface treatment of recycled aggregates on mechanical properties and bond strength of self-compacting concrete. *Sustainability* **2019**, *11*, 4182. [CrossRef]
165. Mistri, A.; Bhattacharyya, S.K.; Dhami, N.; Mukherjee, A.; Barai, S.V. A review on different treatment methods for enhancing the properties of recycled aggregates for sustainable construction materials. *Constr. Build. Mater.* **2020**, *233*, 117894. [CrossRef]

166. Rahman, S.S.; Khattak, M.J. Roller compacted geopolymer concrete using recycled concrete aggregate. *Constr. Build. Mater.* **2021**, *283*, 122624. [CrossRef]
167. Zhang, T.; Chen, M.; Wang, Y.; Zhang, M. Roles of carbonated recycled fines and aggregates in hydration, microstructure and mechanical properties of concrete: A critical review. *Cem. Con. Comp.* **2023**, *138*, 104994. [CrossRef]
168. Gomes, I.G.; Farinha, C.B.; Veiga, R.; de Brito, J.; Faria, P.; Bastos, D. CO_2 sequestration by construction and demolition waste aggregates and effect on mortars and concrete performance—An overview. *Renew. Sustain. Energy Rev.* **2021**, *152*, 111668. [CrossRef]
169. Wang, J.; Zhang, J.; Cao, D.; Dang, H.; Ding, B. Comparison of recycled aggregate treatment methods on the performance for recycled concrete. *Constr. Build. Mater.* **2020**, *234*, 117366. [CrossRef]
170. Raman, J.V.M.; Ramasamy, V. Various treatment techniques involved to enhance the recycled coarse aggregate in concrete: A review. *Mater. Today Proc.* **2021**, *45*, 6356–6363. [CrossRef]
171. Thomas, B.S.; Yang, J.; Bahurudeen, A.; Chinnu, S.N.; Abdalla, J.A.; Hawileh, R.A.; Hamada, H.M. Geopolymer concrete incorporating recycled aggregates: A comprehensive review. *Clean. Mater.* **2022**, *3*, 100056. [CrossRef]
172. Ren, X.; Zhang, L. Experimental study of interfacial transition zones between geopolymer binder and recycled aggregate. *Constr. Build. Mater.* **2018**, *167*, 749–756. [CrossRef]
173. Singh, B.; Ishwarya, G.; Gupta, M.; Bhattacharyya, S.K. Geopolymer concrete: A review of some recent developments. *Constr. Build. Mater.* **2015**, *85*, 78–90. [CrossRef]
174. Kirthika, S.K.; Singh, S.K. Durability studies on recycled fine aggregate concrete. *Constr. Build. Mater.* **2020**, *250*, 118850. [CrossRef]
175. Panizza, M.; Natali, M.; Garbin, E.; Ducman, V.; Tamburini, S. Optimization and mechanical-physical characterization of geopolymers with Construction and Demolition Waste (CDW) aggregates for construction products. *Constr. Build. Mater.* **2020**, *264*, 120158. [CrossRef]
176. Manzi, S.; Baldazzi, L.; Saccani, A. Formulating Geopolymer Mortars through Construction and DemolitionWaste (CDW) Recycling: A Comprehensive Case Study. *Materials* **2023**, *16*, 7304. [CrossRef]
177. Shaikh, F.U.A. Mechanical and durability properties of fly ash geopolymer concrete containing recycled coarse aggregates. *Int. J. Sustain. Built Environ.* **2016**, *5*, 277–287. [CrossRef]
178. Akbarnezhad, A.; Huan, M.; Mesgari, S.; Castel, A. Recycling of geopolymer concrete. *Constr. Build. Mater.* **2015**, *101*, 152–158. [CrossRef]
179. Kurda, R.; de Brito, J.; Silvestre, J.D. Influence of recycled aggregates and high contents of fly ash on concrete fresh properties. *Cem. Concr. Comp.* **2017**, *84*, 198–213. [CrossRef]
180. Kazmi, S.M.S.; Munir, M.J.; Wu, Y.F.; Patnaikuni, I.; Zhou, Y.; Xing, F. Effect of recycled aggregate treatment techniques on the durability of concrete: A comparative evaluation. *Constr. Build. Mat.* **2020**, *264*, 120284. [CrossRef]
181. Zhou, S.; Zhou, S.; Zhang, J.; Tan, X.; Chan, D. Relationship between moisture transportation, efflorescence and structure degradation in fly ash/slag geopolymer. *Materials* **2020**, *13*, 5550. [CrossRef]
182. Zhang, Z.; Provis, J.L.; Reid, A.; Wang, H. Fly ash based geopolymers: The relationship between composition, pore structure and efflorescence. *Cem. Concr. Res.* **2014**, *64*, 30–41. [CrossRef]
183. Albitar, M.; Ali, M.S.M.; Visinti, P.; Drechsler, M. Durability evaluation of geopolymer and conventional concretes. *Constr. Build. Mater.* **2017**, *136*, 374–385. [CrossRef]
184. Tan, J.; Dan, H.; Ma, Z. Metakaolin based geopolymer mortar as concrete repairs: Bond strength and degradation when subjected to aggressive environments. *Ceram. Int.* **2022**, *48*, 23559–23570. [CrossRef]
185. Joseph, B.; Mathew, G. Influence of aggregate content on the behavior of fly ash based geopolymer concrete. *Sci. Iran.* **2012**, *19*, 1188–1194. [CrossRef]
186. Sata, V.; Chindaprasirt, P. Use of construction and demolition waste (CDW) for alkali-activated or geopolymer concrete. In *Advances in Construction and Demolition Waste Recycling*; Woodhead Publishing: Cambridge, UK, 2020; pp. 385–403.
187. Saloni; Parveen; Lim, Y.Y.; Pham, T.M. Effective utilization of ultrafine slag to improve mechanical and durability properties of recycled aggregates geopolymer concrete. *Clean. Eng. Technol.* **2021**, *5*, 100330. [CrossRef]
188. Javed, I.; Saeed, H.; Ekinci, A. Transforming construction waste into high-performance alkali-activated paste with microstructural and predictive p modelling insights. *Buildings* **2025**, *15*, 3830. [CrossRef]
189. Capasso, I.; D'Angelo, G.; del Rio Merino, M.; Campanile, A.; Caputo, D.; Liguori, B. CDW-based geopolymers: Pro and cons of using unselected waste. *Polymers* **2025**, *17*, 570. [CrossRef]
190. Retamal-Rojas, M.; Aponte, D.; Valencia-Saavedra, W.; Robayo-Salazar, R.; Barra-Bizinotto, M. Hybrid binders through alkaline activation of fine construction and demolition waste. *Materials* **2025**, *18*, 3227. [CrossRef]
191. Shen, J.; Li, Y.; Lin, H.; Li, H.; Lv, J.; Feng, S.; Ci, J. Prediction of compressive strength of alkali-activated construction demolition waste geopolymers using ensemble machine learning. *Constr. Build. Mater.* **2022**, *360*, 129600. [CrossRef]
192. Görhan, G.; Kürklü, G. The influence of the NaOH solution on the properties of the fly ash-based geopolymer mortar cured at different temperatures. *Compos. Part B* **2014**, *58*, 371–377. [CrossRef]

193. Ouda, A.S.; Gharieb, M. Development the properties of brick geopolymer pastes using concrete waste incorporation dolomite aggregate. *J. Build. Eng.* **2020**, *27*, 100919. [CrossRef]
194. Neves, R.; de Brito, J.; Bravo, M. Performance of concrete produced with binders obtained through alkali-activation of different construction and demolition waste. *Constr. Build. Mater.* **2025**, *473*, 141060. [CrossRef]
195. Mahmoodi, O.; Siad, H.; Lachemi, M.; Sahmaran, M. Design optimization and interfacial characterization of geopolymer mixtures upcycling construction and demolition waste-based binders and aggregates using response surface methodology. *Mater. Today Commun.* **2025**, *49*, 114351. [CrossRef]
196. Ricciotti, L.; Lucariello, D.; Perrotta, V.; Apicella, A.; Aversa, R. Sustainable alkali-activated and geopolymer materials: What is the future for Italy? *Recycling* **2025**, *10*, 140. [CrossRef]
197. Hassan, A.; Saleh, R.A.A.; Al-Sameai, H.; de Moura, J.; Alomayri, T.; Zhang, C. Novel hybrid machine learning framework for high-fidelity prediction of fly ash-based geopolymer concrete strength. *Compos. Struct.* **2026**, *378*, 119906. [CrossRef]
198. Mahmoodi, O.; Siad, H.; Lachemi, M.; Sahmaran, M. Recent advances in CDW-based geopolymers: A review of mechanical performance, structural application, 3D printing, durability and sustainability. *J. Environ. Manag.* **2025**, *391*, 126358. [CrossRef]
199. Kul, A.; Kocaer, O.; Aldemir, A.; Yildirim, G.; Lucas, S.S. 3D printable one-part alkali-activated mortar derived from brick masonry wastes. *Case Stud. Constr. Mater.* **2024**, *21*, e04081. [CrossRef]